

# Bedford Institute of Oceanography

---

## l'Institut océanographique de Bedford

Dartmouth/Nova Scotia/Canada

INTEGRATION OF PASSIVE RANGING LORAN-C, SATELLITE NAVIGATION,

DFO - Library / MPO - Bibliothèque

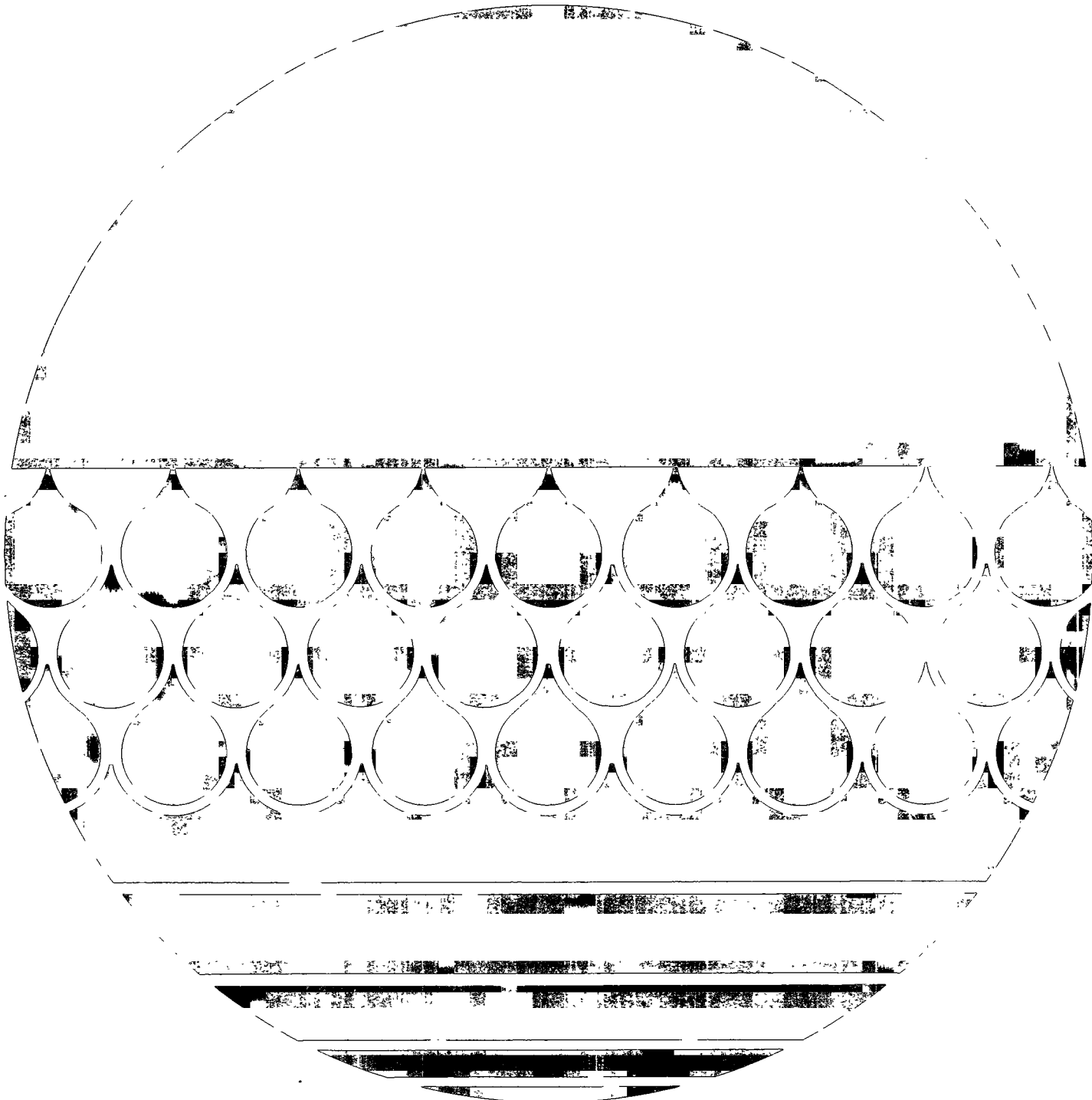


10034802

SHIP'S LOG, AND SHIP'S GYROCOMPASS

S. GRANT

REPORT SERIES/BI-R-76-8/SEPTEMBER 1976



The Bedford Institute of Oceanography is a Government of Canada establishment whose staff undertake scientific research and surveys in the marine environment. It consists of three main units: (1) the Atlantic Oceanographic Laboratory, which is part of Fisheries and Marine Service, Department of the Environment, (2) the Marine Ecology Laboratory, also of Fisheries and Marine Service, Department of the Environment, and (3) the Atlantic Geoscience Centre of the Geological Survey of Canada, Department of Energy, Mines and Resources.

L'Institut océanographique de Bedford est un établissement du gouvernement du Canada, dont le personnel entreprend des travaux de recherche scientifique et des études se rapportant au milieu marin. Il comprend trois services principaux: (1) le Laboratoire océanographique de l'Atlantique, qui fait partie du Service des pêches et des sciences de la mer du ministère de l'Environnement, (2) le Laboratoire d'écologie marine, qui relève également du Service des pêches et des sciences de la mer du ministère de l'Environnement, et (3) le Centre géoscientifique de l'Atlantique de la Commission géologique du Canada, ministère de l'Énergie, des Mines et des Ressources.

BEDFORD INSTITUTE OF OCEANOGRAPHY

Dartmouth, Nova Scotia  
Canada

INTEGRATION OF PASSIVE RANGING LORAN-C, SATELLITE  
NAVIGATION, SHIP'S LOG, AND SHIP'S GYROCOMPASS<sup>1</sup>

by

S. Grant

Hydrography Division  
Atlantic Oceanographic Laboratory  
Ocean and Aquatic Sciences  
Department of the Environment

September 1976

REPORT SERIES

BI-R-76-8

<sup>1</sup> This report is an unaltered printing of the author's M.Sc. thesis, which was submitted to the Department of Surveying Engineering, University of New Brunswick, Fredericton, N.B., in February 1976.

## ABSTRACT

The integration of rho-rho Loran-C, the Transit Doppler satellite system, ship's log, and ship's gyrocompass is studied. The mathematical framework around which the integration takes place consists of an extended Kalman filter. The Kalman filter equations are derived from basic principles and the relationships between the Kalman filter equations and (a) the least squares estimation algorithms and (b) the recursive digital filtering equations are described. A simple example is used to illustrate the operation of the Kalman filter. The integration of rho-rho Loran-C and Transit is considered first. Essentially, corrections to the Loran-C range measurements are determined from comparisons with Transit via a linear Kalman filter. Test results using both good and bad quality data are described. Ship's coordinates are determined from the Loran-C ranges by a least squares estimation technique. The accuracies of estimates of ship's velocity derived from Loran-C and log and gyrocompass are analyzed. A proposed Kalman filter integration of Loran-C, ship's log, and gyrocompass is described.

## SOMMAIRE

On présente une étude de l'intégration du Loran-C rho-rho, du satellite doppler Transit, du loch de navire, et du gyrocompas. Un filtre Kalman modifié sert de modèle mathématique d'intégration. Les équations du filtre Kalman dérivent de principes fondamentaux; on décrit leurs rapports avec (a) les algorithmes d'estimation des moindres carrés et (b) les équations numériques récursives de filtrage. Un exemple simple illustre le fonctionnement du filtre Kalman. On étudie d'abord l'intégration du Loran-C et du Transit. Pour l'essentiel, la correction des relevés de distance par Loran-C est calculée par comparaisons avec le Transit à l'aide d'un filtre Kalman linéaire. On présente les résultats d'essais sur de bonnes données et des données mauvaises. On détermine les coordonnées du navire d'après les relevés du Loran-C, à l'aide d'une technique d'estimation des moindres carrés. On analyse l'exactitude des estimations de la vitesse du navire fournies par le Loran-C, le loch, et le gyrocompas. On décrit un projet d'intégration de ces appareils par filtre Kalman linéaire.

TABLE OF CONTENTS

	<u>Page</u>
Abstract .....	ii
List of Figures .....	v
List of Tables .....	vii
Acknowledgement .....	viii
1. INTRODUCTION .....	1
1.1 Problem Description .....	1
1.2 Outline of Treatment .....	3
2. DESCRIPTION OF SUBSYSTEMS .....	5
2.1 Ship's Logs .....	5
2.1.1 Ship's Doppler Speed Logs .....	6
2.2 Ship's Gyrocompass .....	6
2.3 Loran-C .....	10
2.3.1 Principles of Operation .....	11
2.3.2 Hyperbolic Fixing and Passive and Active Ranging .....	13
2.4 Navy Navigation Satellite System .....	15
3. OPTIMAL ESTIMATION IN DISCRETE NONLINEAR DYNAMIC SYSTEMS	22
3.1 Kalman Filter .....	22
3.2 Kalman Filter and Sequential Adjustment Equations .	30
3.3 Bayes Filter and Phased Adjustment Equations .....	30
3.4 Variance Factor .....	33
3.5 A Simple View of the Kalman Filter .....	34
3.5.1 State Transition Variance - Q .....	35
3.5.2 The State Variance P and Observation Variance R .....	36
3.5.3 The Relationship Between the Kalman Filter and the Low Pass Digital Filter .....	36
4. INTEGRATION OF RHO-RHO LORAN-C AND TRANSIT .....	38
4.1 Historical Perspective .....	38
4.1.1 System Characteristics .....	41
4.2 Rho-rho Loran-C Corrections .....	42
4.2.1 System Synchronization .....	42
4.2.2 Loran-C Propagation Corrections .....	46
4.3 Mathematical Model for Determining Geographic Coordinates .....	51
4.3.1 Least Squares Fix .....	51
4.4 The Combined System .....	54

Table of Contents continued

Page

4.4.1	Kalman Range Correction Filter .....	55
4.4.2	Observation Covariance Matrix R .....	58
4.4.3	State Transition Covariance Matrix Q .....	61
4.4.4	Test Results .....	64
4.4.5	Determining Initial Values for the State Covariance Matrix and State Vector Elements .....	67
4.5	Test Results and Conclusions .....	69
4.5.1	Nantucket Range Corrections .....	71
4.5.2	Cape Race Range Corrections .....	73
4.5.3	Conclusion and Recommendations .....	75
5.	INTEGRATION OF LORAN-C, SHIP'S LOG, AND SHIP'S GYROCOMPASS	79
5.1	Ship's Velocity from Loran-C and Ship's Log and Gyrocompass .....	80
5.1.1	Ship's Velocity from Rho-rho Loran-C .....	80
5.1.2	Velocity from Ship's Log and Gyrocompass .	85
5.2	Kalman Integration Filter .....	87
5.2.1	Kalman Integration Filter Equations .....	91
6.	CONCLUSIONS AND DISCUSSION .....	96
6.1	Discussion and Results .....	96
6.2	Suggestions for Future Work .....	98
	REFERENCES .....	100
	Appendices	
	Appendix I. Transit Covariance Matrix .....	106
	Appendix II                      Program LORSG .....	115

LIST OF FIGURES

<u>Figures No.</u>		<u>Page</u>
2.1	Pendulous Gyrocompass Precession .....	8
2.2	Latitude Effect on Pendulous Gyrocompass .....	8
2.3	Timing of Transmissions of a Loran-C Chain .....	12
2.4	Loran-C Pulse .....	12
2.5	Hyperbolic Lines of Position .....	14
2.6	Ranging Lines of Position .....	16
2.7	Rho-rho Loran-C Coverage of North Atlantic Ocean ...	17
2.8	Influence of Ship's Speed Error .....	20
4.1	Austron 5000 Rho-rho Loran-C System .....	39
4.2	Canadian Marconi CMA-722 Satellite Navigation System	40
4.3	Rho-rho Loran-C Receiver Timing .....	44
4.4	Rho-rho Loran-C/Transit Clock Drift Control Graph ...	47
4.5	Overwater Phase Lag at 100 kHz .....	50
4.6	Loran-C Range Standard Deviation .....	62
4.7	Kalman Range Correction Model Performance .....	66B
4.8	Change of Slope in Kalman Range Correction Model ...	68B
4.9	Ship's Track: Halifax to Spotted Island .....	70
4.10	Correction to Nantucket Loran-C Range from Kalman Range Correction Filter .....	74
4.11	Correction to Nantucket Loran-C Range from Kalman Range Correction Filter .....	74

List of Figures continued

	<u>Page</u>
4.12 Correction to Cape Race Loran-C Range from Kalman Range Correction Filter .....	76
4.13 Correction to Cape Race Loran-C Range from Kalman Range Correction Filter .....	76
5.1 Histograms of Ship's Courses and Speeds Between One- Minute Loran-C Fixes .....	82
5.2 Histograms of Ship's Courses and Speeds from One- Minute Log/Gyro Readings .....	83
5.3 Histograms of Ship's Courses and Speeds Obtained by Filtering One-Minute Loran-C Velocities .....	84
5.4 Ship's Heading During Course Alteration .....	86
5.5 Direction of Ship's Motion due to Wind Forces .....	88
5.6 Ship's Displacement Vector in the Presence of Wind and Current .....	89

LIST OF TABLES

<u>Table No.</u>		<u>Page</u>
1.1	Error Spectra of Navigation Systems .....	4
4.1	Transit Fix Classification .....	63
4.2	Loran-C Data .....	65
4.3	Statistics of Loran-C Data .....	66A
4.4	Transit/Loran-C Test Data .....	72
5.1	Combined Wind/Current Vector Derived from Vector Difference Between Loran-C and Log/Gyro .....	90

## ACKNOWLEDGEMENT

I thank the Canadian Hydrographic Service and particularly Mr. R.M. Eaton for providing the opportunity to undertake this work.

I have benefited greatly from my association with Mr. R.M. Eaton, Mr. N. Stuijbergen, and Dr. D. Wells of the Bedford Institute of Oceanography Navigation Group. Their friendly and constructive criticism has, on numerous occasions, extricated me from the mire created by my ignorance.

The subject of least squares and the link between least squares and Kalman filtering was introduced to me by Dr. E.J. Krakiwsky. His infectious enthusiasm and infinite patience are responsible for many of the results quoted in Chapter 3.

I am particularly indebted to my supervisor, Dr. P. Vanicek, for his helpful comments throughout this investigation.

The assistance of Mrs. Olive Ross was invaluable. Her extensive knowledge in the area of form and format was as important as her faultless typing.

Above all, I wish to acknowledge the patience and support of my wife, Karen.

## CHAPTER 1

### INTRODUCTION

Navigation is the art of determining and controlling the motion of a vehicle. Navigation is used in surface and subsurface vessels, land vehicles, aircraft, rockets and space vehicles. This study is concerned with the particular problem of determining the position and velocity of a ship at sea.

The mathematical foundation for marine navigation was laid at a time when navigation devices were unreliable and inaccurate. As the quality and diversity of the instruments increased the mathematical techniques were improved and expanded. Any method that could not be mastered by an intelligent seaman was discarded or replaced by an approximation or a rule-of-thumb [Anderson, 1966]. Today, as even more accurate and diverse instruments are being introduced, it is becoming increasingly more difficult to incorporate their results into the mathematical framework that has evolved through the years. The result is that the full potential of many of these new devices is not being realized. The need for a more sophisticated approach involving modern high-speed digital computers is clear.

#### 1.1 Problem Description

This study considers the estimation of a ship's position and velocity from observations obtained from passive ranging Loran-C [Grant, 1973], ship's log [Griswold, 1968], ship's gyrocompass [Savet, 1961], and the U.S. Navy Navigation Satellite System (NNSS) [Stansell, 1968].

Errors in Loran-C ranges vary with both position and time. Some errors are random while others increase linearly with time so that the resulting positioning errors can become unacceptably large after several days at sea (see Table 1.1). However, Loran-C does provide continuous positioning that is relatively quite accurate over periods of several hours. Satellite navigation, on the other hand, provides positions every few hours that have a larger scatter than the Loran-C positions but which do not have any long term trends. Satellite navigation requires an accurate knowledge of the ship's velocity during the satellite pass in order to achieve reasonable accuracies. One of the problems considered by this study is how to use satellite navigation positions to remove the long term error trends in the Loran-C ranges.

Ship's log and gyrocompass represent the classical dead-reckoning navigation system. Characteristic of all dead-reckoning systems is the monotonically increasing magnitude of the positioning error with time due to biases in the velocity determinations. Velocities obtained from passive ranging Loran-C, on the other hand, are generally noisier than velocities from the dead-reckoning systems but do not have the problem of biases. The second problem considered by this study is how to extract a smooth unbiased estimate of ship's velocity from these two sources of information. Another part of this problem involves using the log and gyro information to reduce the influence of the Loran-C measurement noise on the Loran-C positions.

In essence, the objective of this study is to develop a procedure that makes the best use of the strengths of passive ranging

Loran-C, Doppler satellite navigation, and ship's log and gyrocompass while minimizing the influence of their weaknesses. The strengths and weaknesses of these navigation systems are summarized in Table 1.1 in terms of their individual error spectra and the error sources.

## 1.2 Outline of Treatment

In Chapter 2 a general description is given of each of the four basic navigation systems considered in this study. The purpose of this chapter is to familiarize the reader with the basic characteristics. The specific details used in integrating these systems are given in Chapters 4 and 5.

The mathematical framework around which the integration takes place is described in Chapter 3. The relationship between Kalman filtering theory and least squares adjustment techniques of surveying engineering are also pointed out. These techniques are used in Chapter 4.

Sections 4.1, 4.2 and 4.3 describe the techniques that were used for combining Doppler satellite navigation and passive ranging Loran-C prior to the commencement of this study. Section 4.4 describes the integration model and gives the details of how values for the elements of the covariance matrices are derived. In the final section of Chapter 4 the performance of the model under less than ideal conditions is described.

Chapter 5 is addressed to the problem of the integration of

Loran-C, ship's log, and ship's gyrocompass. In Section 5.1 the accuracies of ship's velocities determined from Loran-C and ship's log and gyro are analyzed. In Section 5.2 a Kalman filter is proposed that fully integrates Loran-C, ship's log and ship's gyro.

The goal of Chapter 6 is to assess the results of Chapters 4 and 5, to discuss the alternatives, to draw conclusions and make recommendations.

Table 1.1

## ERROR SPECTRA OF NAVIGATION SYSTEMS

Navigation System	Period	Contribution to Error Spectrum (m)	Source of Error
Loran-C	minutes	10's	measurement noise
	hours	0	-
	days	100's	clock drift
Satellite Navigation	minutes	-	-
	hours	100's	ship's velocity
	days	0	-
Ship's Log and Gyrocompass	minutes	0	-
	hours	1,000's	ocean currents
	days	10,000's	ocean currents

## CHAPTER 2

### DESCRIPTIONS OF SUBSYSTEMS

In this chapter the general characteristics of ship's logs, ship's gyrocompasses, passive ranging Loran-C, and the United States Navy Navigation Satellite System are described. The specific details that make these systems suitable for integration are presented later.

#### 2.1 Ship's Logs

Most ship's logs measure a ship's speed through the water not speed over the sea bed. The observed speed therefore differs from the true speed with respect to the ocean bottom by an amount equal to the component of the ocean current in the direction the ship is moving. This can be a major source of error in systems relying on the ship's log for dead reckoning since ocean currents can attain velocities of 3 m/s or more.

There are four main types of ships' logs in use today: impeller logs, pressure or pitot logs, electromagnetic logs, and Doppler logs [Griswold, 1968]. The order in which the four types of logs are listed corresponds approximately to: (1) the length of time they have been in common use, and (2) increasing accuracy. They all have different accuracies and reliabilities depending on many factors such as: ship's speed and motion, hull shape, location of the sensor on the hull, water temperature and salinity, sea state, etc. All except the Doppler log need periodic calibration and only the Doppler log and a special adaptation of the electromagnetic log can be used in ice. In any

integrated ship's navigation system it would be essential to take into account the characteristics of the particular type of log being used. For this study a Doppler log will be assumed.

#### 2.1.1 Ships' Doppler Speed Logs

Doppler logs operate by transmitting sound obliquely forward into the water either in pulses or continuously and measuring the frequency change in the sound reflected back to the sensor from particles in the water. They can be of the single axis or the dual axis variety. Dual axis logs measure a ship's velocity in both the fore-and-aft and the athwart-ship directions. The single axis log, to be considered here, only measures the ship's motion in the fore-and-aft direction.

Most Doppler logs transmit a beam forward and another aft at depression angles of about  $60^\circ$ . By averaging the two Doppler shift frequencies errors in the speed measurement due to minor changes in the ship's trim are cancelled. Pulsed Doppler logs are more common than continuous wave (CW) logs because they are able to operate in noisier environments or where the bottom or water mass scatterers return weak signals. CW logs, on the other hand, are used where greater accuracy is required.

Doppler logs in general are accurate to about 1% of the vessel's speed of 0.1 knot (0.05 m/s) whichever is larger [Eaton, 1974].

#### 2.2 Ships' Gyrocompass

A gyrocompass is a gyroscope with its spin axis constrained to

be perpendicular to the earth's gravity field [Savet, 1961]. In some gyrocompasses the constraint takes the form of a mass suspended below the gyro wheel with the result that such gyros are often called pendulous gyrocompasses. To understand how a gyrocompass works consider such a gyro on the equator with its spin axis pointing west as in Figure 2.1a. As the earth rotates the gyro continues to point at a fixed point in space. With respect to the gyro the gravity potential surface of the earth tilts (Fig. 2.1b) and the pendulous mass induces a torque that tries to bring the spin axis parallel to the earth's gravity potential surface again. The response of the gyro is to precess at right angles to this righting force (i.e. toward the north) (Fig. 2.1c). The gyro continues to precess until its spin axis is at right angles to the direction of tilt (i.e. parallel to the earth's rotation axis). If no damping is applied the gyro overshoots and continues to precess until it is pointing east. In practice a damping force is used to prevent the gyro from continuously oscillating about the direction of north.

If the gyro is moved away from the equator the mass suspended below the gyro will tend to keep the gyro spin axis parallel to the gravity potential surface of the earth (Fig. 2.2). However, the gyro spin axis is now no longer parallel to the earth's rotation axis. As the earth rotates the gyro precesses and, in the northern hemisphere, settles somewhere east of north. In most marine gyrocompasses this effect is compensated for by the application of a small torque by means of a mass on a beam. The position of the mass is changed with latitude. Newer gyrocompasses accomplish this electronically while

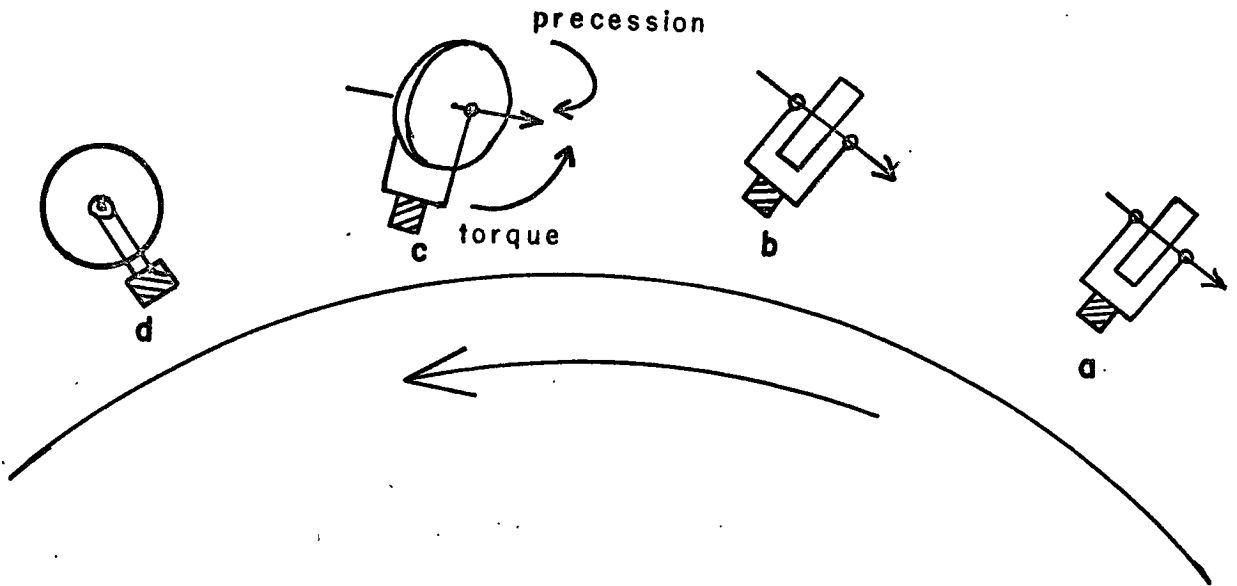


Figure 2.1. Pendulous Gyrocompass Precession

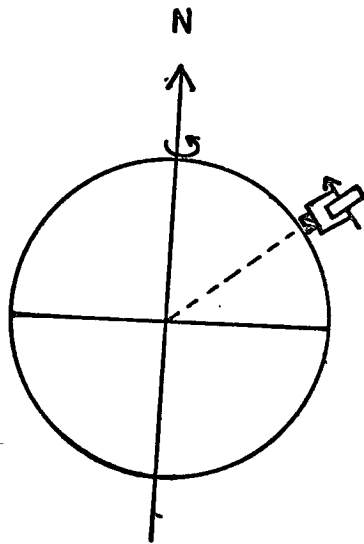


Figure 2.2. Latitude Effect on Pendulous Gyrocompass

some older gyros do not correct for this error at all. In the older gyros the correction is obtained from tables of the following function

$$\alpha = \gamma \tan \phi , \quad (2.1)$$

where  $\phi$  is the latitude and  $\gamma$  is a constant peculiar to the individual gyro. Bowditch [1962] found that  $\gamma$  equalled about  $1.7^\circ$  for Sperry gyrocompasses.

Another source of error results from vehicle motion. With the relatively slow velocities of ships, except in very high latitudes, it is only the north component of a ship's velocity that has any effect on the gyrocompass. The effect of the vessel's motion is to make it appear to the gyro that the earth is actually rotating about an axis slightly different from the true rotational axis. The gyro settles with respect to this 'virtual' axis which, in the northern hemisphere, for a vehicle moving north, is to the west of north by an angle  $\epsilon$  given by

$$\epsilon = \arctan \frac{V \cos \theta}{R_E W_E \cos \phi + V \cos \theta} , \quad (2.2)$$

where  $V$  = ship's speed

$\theta$  = ship's course

$R_E$  = radius of earth

$W_E$  = earth's sidereal rotational velocity [Savet, 1961]

For a ship proceeding north at 15 knots at  $60^\circ\text{N}$  latitude the error is about  $-2^\circ$ . As with the latitude error the vehicle motion error is often corrected by the application of a small torque about the tilt

axis. Older gyros are not compensated for vehicle motion error.

Any change in course or speed usually results in some component of acceleration along the spin axis of the gyrocompass. The pendulous mass is displaced by this acceleration thereby creating a torque about the gyro tilt axis, causing an azimuth precession. This error is known as 'ballistic deflection error' and usually results in a small amplitude damped oscillation in azimuth of the gyro following a change in course or speed. Stuijbergen [1974] reports that at latitude  $74^{\circ}\text{N}$  the error can be as large as  $6\frac{1}{2}^{\circ}$ . However, at lower latitudes and normal ships' speeds this source of error is usually negligible.

For this study it is assumed that errors in ship's course and speed, after the effects of ocean currents and calibration errors have been removed, are random and normally distributed and that readings obtained at one time instant are not correlated with readings at any other instant in time (i.e. white noise assumption).

### 2.3 Loran-C

Loran-C is a long range, 100 kHz, radio navigation system which was conceived during the later part of World War II, was born during the late 1950's, and reached maturity in the late 1960's. In 1970 the U.S. Department of Transportation selected Loran-C to be the primary navigation aid for the U.S. Coastal Confluence Zone. Prior to this time Loran-C stations throughout the world were operated primarily for the U.S. Department of Defence. The increased usage of Loran-C by civilians over the last five years has brought to light a number of operational problems but at the same time has demonstrated that Loran-C

is capable of providing very precise positioning information many hundreds of miles from the farthest transmitter. The United States Department of Transportation decision will mean that existing Loran-C transmitters will be updated and that several new Loran-C transmitters will be brought into operation over the next few years. This program is already underway [Roland, 1973].

### 2.3.1 Principles of Operation

Loran-C transmitters are grouped in chains consisting of one master and several slave or secondary transmitters. At present there are eight chains in operation throughout the world. Starting with the master, each station in a Loran-C chain transmits a series of eight pulses. Figure 2.3 shows the timing of transmissions from a typical Loran-C chain of three stations. The master station transmits a ninth pulse for identification purposes following the group of eight pulses. A typical Loran-C pulse is shown in Figure 2.4. The transmission sequence is repeated at a regular interval called the Group Repetition Period (GRP) which is generally between 0.05 s and 0.1 s. By using a different GRP for each chain all Loran-C stations are able to transmit at the same frequency of 100 kHz with a minimum of mutual interference. In fact, many stations transmit on two different GRP's at the same time.

Prior to about 1969 the slave transmissions were controlled by having them transmit a fixed time interval (coding delay) after reception of the master signal. The result was that when the master signal was noisy or could not be received at the slave station the slave did not know when to transmit. The chain was therefore not usable. This problem was overcome by placing atomic frequency standards at the

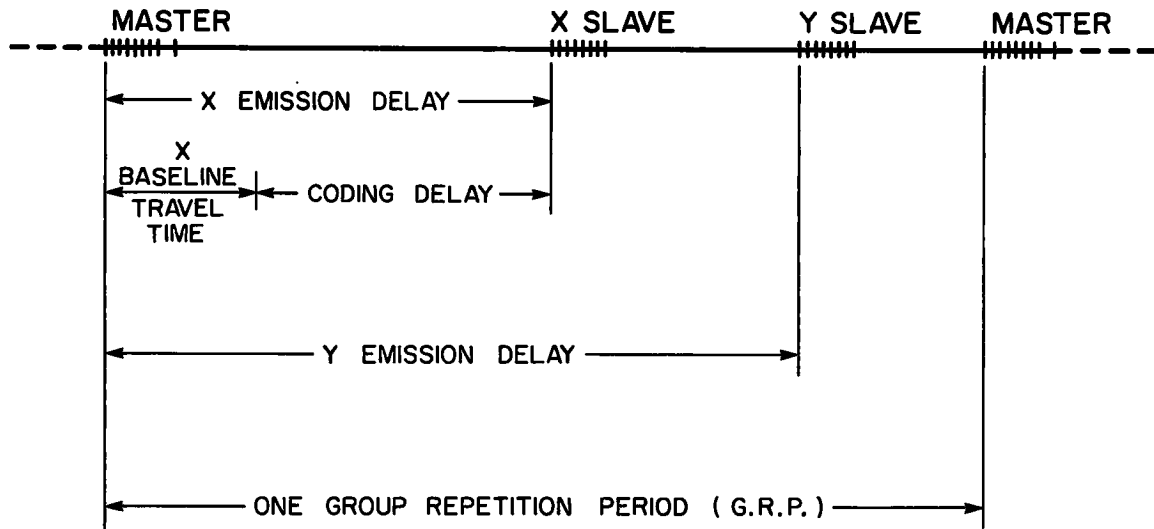


Figure 2.3. Timing of Transmissions of a Loran-C Chain

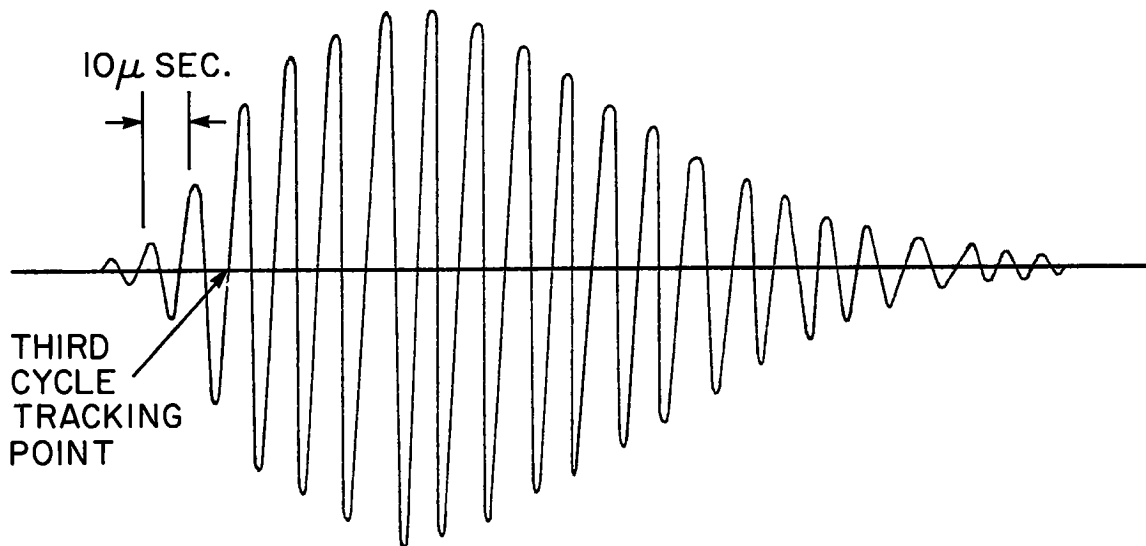


Figure 2.4. Loran-C Pulse

master and each of the slave stations. By counting the cycles of the highly stable frequency generated by the atomic standards the slaves were able to predict the time of arrival of the master signal and consequently could continue to transmit even if the master station was off the air. Since the slave transmitters are no longer 'slaved' to the master signals there has been a tendency over the past few years to refer to them as 'secondary stations' instead of 'slave stations'.

### 2.3.2 Hyperbolic Fixing and Passive and Active Ranging

Loran-C is primarily a hyperbolic navigation aid. That is, a fix (i.e. a set of ship's coordinates) is obtained by measuring the difference of arrival times between the signals from two pairs of fixed shore stations. Each time difference describes a hyperbolic position line on the surface of the earth with the two transmitters at the foci (see Figure 2.5). The receiver's position is determined by the intersection of the two hyperbolae.

The frequency and timing of Loran-C transmissions are precisely controlled by cesium-beam frequency standards (atomic clocks). A receiver that is equipped with a similar atomic clock that is synchronized to the Loran-C transmissions can predict the times of transmission of the shore stations and measure the travel times of the signals to the receiver. By means of a suitable propagation model the ranges to the transmitters over the surface of the earth are derived from the travel times and the receiver's position is found from the intersection of the two range circles. This passive ranging technique is generally known as 'rho-rho' or ' $\rho$ - $\rho$ ' positioning to distinguish it from the case where the ship transmits (i.e. active ranging) and receives retransmitted

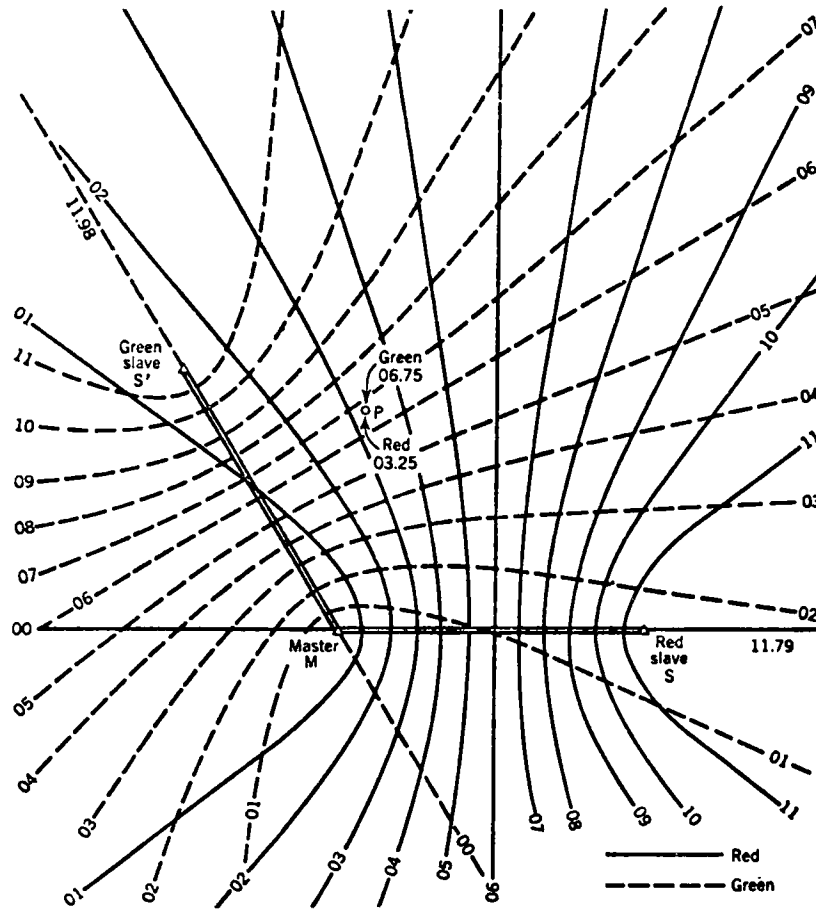


Figure 2.5. Hyperbolic Lines of Position

signals from shore stations (e.g. Decca Lambda) which is known as 'range-range' positioning (see Fig. 2.6). The expression 'rho-rho' is used even when more than two ranges are being measured.

Grant [1973] found that the  $2\sigma$  ranging accuracy of rho-rho Loran-C was 180 m when combined with Doppler satellite navigation and that the system could be used routinely at ranges of 2500 km from the farthest transmitter. Figure 2.7 shows the rho-rho Loran-C coverage of the North Atlantic Ocean.

#### 2.4 Navy Navigation Satellite System

The Navy Navigation Satellite System, Transit Satellite System, or simply Transit, is described in numerous references [Sluiter, 1969; Stansell, 1968; Wells, 1974; and Black *et al.*, 1975]. The Transit System has been in operation since 1964. It now consists of six operational satellites in near-polar orbits at altitudes of about 1100 km. The orbits are nearly circular and the satellites travel at velocities of about 440 km/min. At 45°N latitude there is a pass about every 45 minutes. Normally, about two-thirds of all passes are usable. The satellites can be above the horizon for a maximum of about 18 minutes.

Each satellite transmits on the two harmonically related carrier frequencies of 150 MHz and 400 MHz. Two frequencies are needed to correct for the change in propagation path length from the satellite to the receiver due to ionospheric refraction which is frequency-dependent. Each satellite also transmits information about its position at two-minute intervals. The position data is updated about every 12 hours.

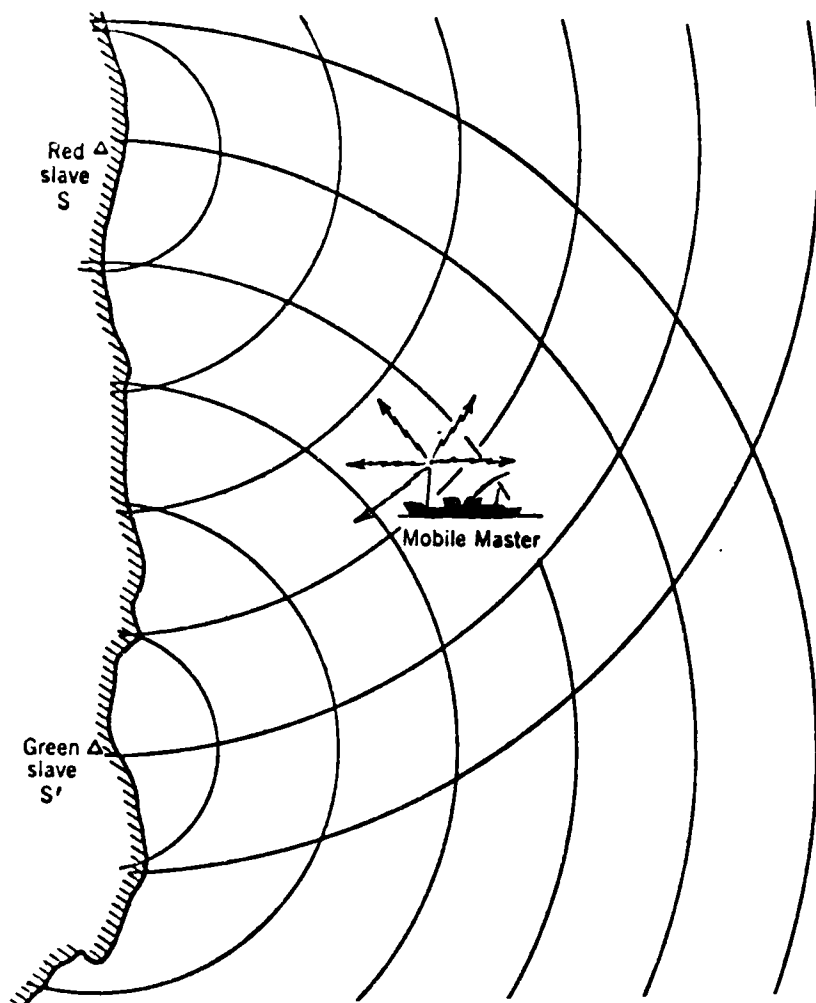


Figure 2.6. Ranging Lines of Position

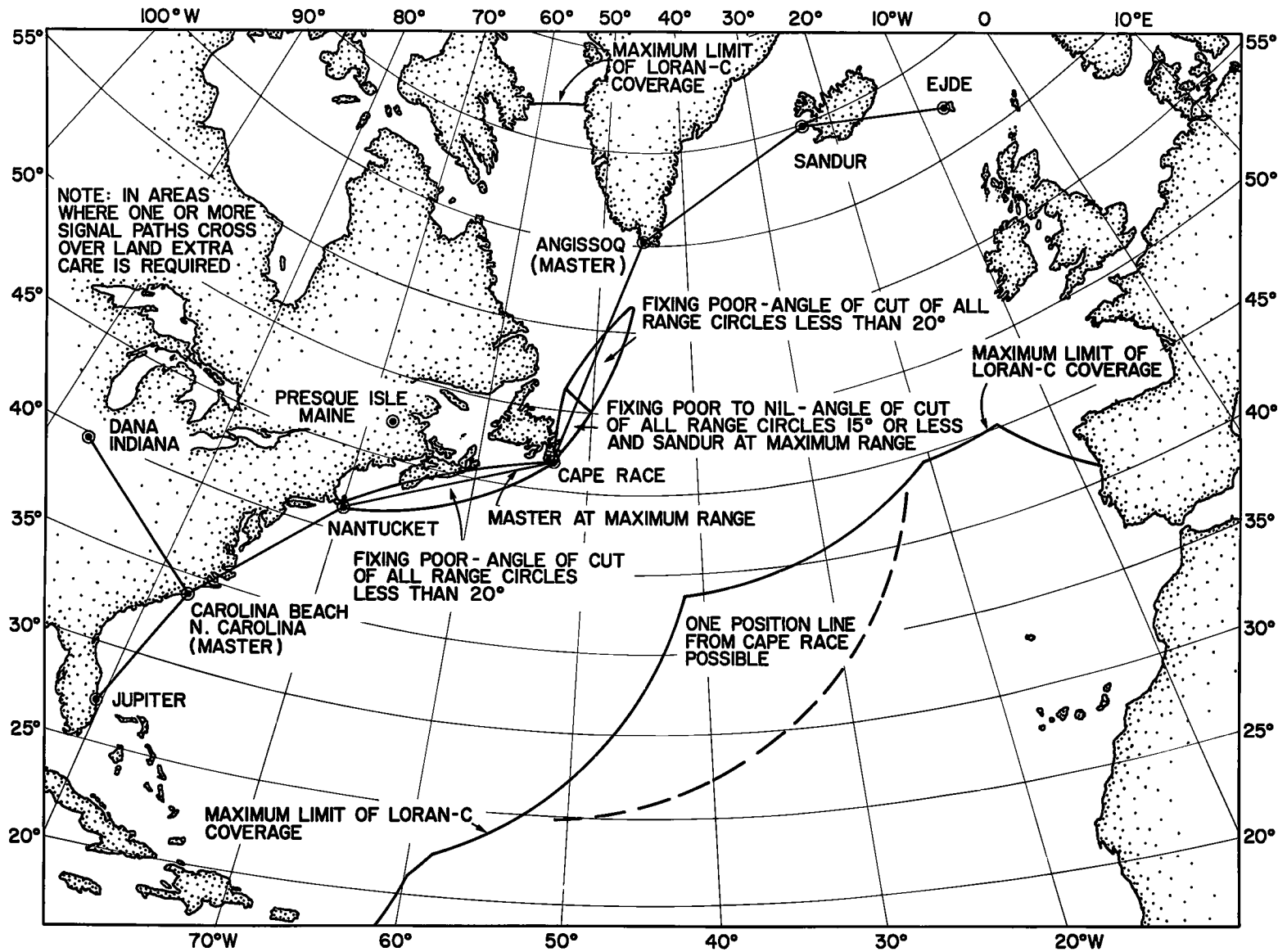


Figure 2.7. Rho-rho Loran-C Coverage of North Atlantic Ocean

The motion of the satellite relative to the receiver causes the frequency of the satellite signal to be shifted due to the Doppler effect. The received frequency  $f_r$  is related to the transmitted frequency  $f_t$  by

$$f_r = f_t \left( 1 - \frac{1}{c} \frac{ds}{dt} \right) \quad (2.3)$$

[Wells, 1974; Gill, 1965] where  $c$  is the velocity of light and  $ds/dt$  is the radial component of the satellite velocity relative to the receiver. Each satellite transmits a series of timing marks which are used by the receiver to start and stop the integration of the beat frequency obtained from  $f_g - f_r$  where  $f_g$  is generated in the receiver. The number of integrated cycle counts  $N$  obtained during any integration interval  $\Delta t$  is related to  $\Delta s$  and  $\Delta f$  by

$$N = \frac{f_g}{c} \Delta s + \Delta f \cdot \Delta t \quad (2.4)$$

where  $\Delta f = f_g - f_t$  and  $\Delta s = s_2 - s_1$ .  $s_1$  and  $s_2$  are the slant ranges from the receiver to the satellite at the start and end of the integration interval.

To obtain a fix from a set of satellite Doppler measurements at sea it is generally assumed that the height of the antenna above a given reference ellipsoid is known and is equal to the geoidal height. Only the two remaining position components latitude  $\phi$  and longitude  $\lambda$  are solved for along with the frequency offset  $\Delta f$  between the satellite and receiver oscillators.

When the receiver is in motion the change in receiver coordinates during the Doppler count interval affects the observed Doppler count  $N$ . The usual solution to this problem is to use the estimated ship's course and speed to correct the observed Doppler counts. Clearly, an error in the estimated course or speed will result in an error in the observed Doppler count which in turn causes an error in the computed receiver coordinates. For ships at sea this problem probably represents the most serious source of error in satellite navigation. Figure 2.8 [Sluiter, 1969] shows the error that can be expected from a one-knot error in the north component of ship's velocity for various elevations.

There are several other sources of error that affect the Doppler count  $N$ . Errors are always present in radio positioning systems due to atmospheric noise and the imperfect measurement process of the receiver. The models for correcting for ionospheric and tropospheric refractions are subject to error, especially at low satellite elevations. The mast of the ship, on which the satellite navigation antenna is mounted, can swing through an arc of 20 to 30 m when the ship rolls. Taken all together, Sluiter [1969] estimates that for a moving vessel the standard deviation of the Doppler measurement is between 25 and 30 counts.

In terms of geographic accuracy high elevation passes will generally give a more accurate latitude than low elevation passes. Low elevation passes are generally poor in both latitude and longitude due to refraction effects. But in general Transit is weaker in longitude than latitude as is evident in Figure 2.8. Since all satellites

# INFLUENCE OF SHIP'S SPEED ERROR ON POSITION OF FIX

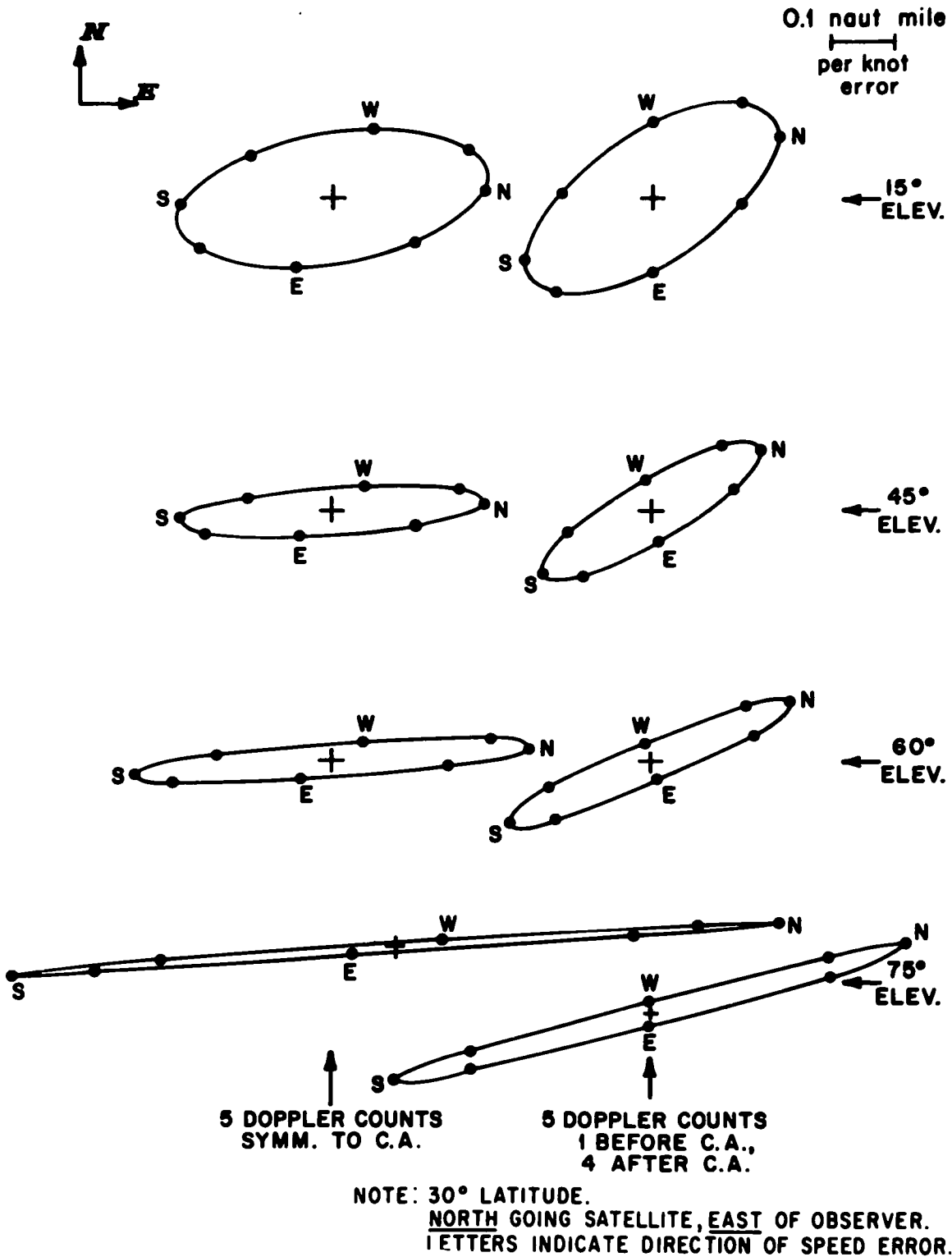


Figure 2.8. Influence of Ship's Speed Error on Position of Fix

pass over the poles the higher the latitude of the receiver the higher will be the average maximum elevation of all the passes. The net result is a weaker longitude determination in high latitudes. Eaton *et al.* [1976] estimate that Transit accuracy varies between 60 and 600 m and that, unlike Loran-C, there is no deterioration in accuracy with time. An analysis of Transit accuracy under various conditions is described in Appendix I. A FOCAL [D.E.C., 1972] program was written to study the influence on the Transit fix of the maximum pass elevation, asymmetry of the Doppler counts about pass centre, and course and speed errors. The results there tend to confirm those of Sluiter (see Fig. 2.8) and Eaton (Table 4.1).

## CHAPTER 3

### OPTIMAL ESTIMATION IN DISCRETE NONLINEAR DYNAMIC SYSTEMS

The problem of estimating a set of parameters or the state of a dynamic system from noisy observations originates from the work of Gauss in the early 1800's. Considerable progress has been made since then. One of the most notable contributions was made by R.E. Kalman in 1960 [Kalman, 1960]. His technique, known as Kalman filtering, has received considerable attention since it was first proposed, particularly by the aerospace industry. Its applicability to the marine navigation problem was first recognized in the late 1960's.

This chapter opens with a derivation of the nonlinear discrete Kalman filter. The relationship between the Kalman filter and the sequential adjustment equations is pointed out in Section 3.2. The Bayes filter [Morrison, 1969] is derived in Section 3.3. and the relationship between the Bayes filter and the phased adjustment equations is described. The variance factor is described in Section 3.4 while in Section 3.5 a simplified Kalman filter is analyzed to gain some insight into its operation.

#### 3.1 Kalman Filter

In Kalman filtering theory there are two models. There is the observation model relating the observed quantities to the unknown parameters and, because the system is changing with time, there is a model of the system dynamics. Either or both of these models can be linear or nonlinear. When they are both linear and continuous they

yield the Kalman filter as it was originally conceived [Kalman, 1960]. Kalman and Bucy [1961] dealt with the linear discrete case. If one set is nonlinear the result is known as the extended Kalman filter. Most practical problems are nonlinear; therefore, in this development, it will be assumed that both sets of model equations are nonlinear.

Let the system dynamics be described by the vector equation

$$X_k = f_k(X_{k-1}) + w_k \quad (3.1)$$

where the time-dependent vector function  $f_k(X_{k-1})$  models the system state at time  $t_k$  from the state  $X_{k-1}$  at time  $t_{k-1}$ . The observation model is described by another vector equation

$$z_k = h_k(X_k) + v_k \quad (3.2)$$

where  $h_k(X_k)$  is a time-dependent vector function which relates the observed quantities  $z_k$  to the elements of the state vector  $X_k$ . Grant and Chamberlain [1974] and Krakiwsky [1975] treat the more general case where the observation vector  $z_k$  and the state vector  $X_k$  are implicitly related.

$w_k$  and  $v_k$  are vectors whose elements are assumed to come from zero mean white noise sequences.  $w_k$  reflects the fact that the dynamics model can only describe the system's motion in the mean sense.  $v_k$  results from observation noise. It is also assumed that there is no correlation between any two of  $w_i$ ,  $v_j$ , and  $X_0$  for all  $i$  and  $j$ .  $X_0$  and its covariance matrix  $P_0$  are assumed to be known and the elements

of  $X_0$  are assumed to come from normally distributed parent populations.  $w_k$  and  $v_k$  do not appear in the Kalman filter equations - only their covariance matrices  $Q_k$  and  $R_k$ .

Essentially the Kalman filter works as follows: from estimates of the state vector  $\hat{X}_{k-1}$  and its covariance matrix  $P_{k-1}$  at time  $t_{k-1}$  predicted estimates of the state vector  $\hat{X}_{k/k-1}$  and the state covariance matrix  $P_{k/k-1}$  are computed for time  $t_k$  using the dynamics model (3.1). The subscript notation is interpreted as follows:  $X_{k/k-1}$  is the estimated state vector (unknown vector) at time  $t_k$  based on observation data up to and including time  $t_{k-1}$ .  $X_{k/k-1}$  is therefore a predicted estimate. A single subscript is used when both subscripts are the same (e.g.  $X_{k-1} = X_{k-1/k-1}$ ). Updated estimates of the state vector  $\hat{X}_k$  and the state covariance matrix  $P_k$  are then computed taking into account both the new observations  $z_k$  and their covariance matrix  $R_k$ , and the predicted estimates of the state vector and its covariance matrix. In the remainder of this section the linearized forms of 3.1 and 3.2 are derived by Taylor's series expansions. By applying the covariance law to the linearized form of 3.1 an equation for the predicted state covariance matrix  $P_{k/k-1}$  is found. Then a set of equations is derived for computing the updated estimates of the state vector and the covariance matrix.

At time  $t_{k-1}$  assume we have estimates of the state vector  $\hat{X}_{k-1}$  and the state covariance matrix  $P_{k-1}$  as a result of  $k-1$  previous iterations of the Kalman filter. During the initial iterations of the filter the influence of  $P_0$ , which was determined by an independent

method, will be greater. Later, however, after many iterations the state covariance matrix will be independent of  $P_0$ . The linearized form of the system dynamics model is obtained by expanding 3.1 in a matrix Taylor's series. The approximation to the true state vector  $X_{k-1}$  used in the expansion is the estimated state vector  $\hat{X}_{k-1}$ .

Retaining only linear terms

$$X_{k/k-1} = f_k(\hat{X}_{k-1}) + F_k \cdot (X_{k-1} - \hat{X}_{k-1}) + w_k \quad (3.3)$$

$$[X_{k/k-1} - f_k(\hat{X}_{k-1})] = F_k \cdot (X_{k-1} - \hat{X}_{k-1}) + w_k$$

$$\delta\hat{X}_{k/k-1} = F_k \cdot \delta\hat{X}_{k-1} + w_k \quad (3.4)$$

where  $F_k$  is the matrix obtained by taking partial derivatives of the elements of  $f_k$  with respect to the state vector elements evaluated at  $\hat{X}_{k-1}$ . The predicted covariance matrix  $P_{k/k-1}$  of the state vector is found from the previous estimate  $P_{k-1}$  by applying the covariance law to 3.4.

$$\begin{aligned} P_{kk-1} &= \begin{bmatrix} F_k & 0 \\ 0 & I \end{bmatrix} \begin{bmatrix} P_{k-1} & 0 \\ 0 & Q_k \end{bmatrix} \begin{bmatrix} F_k & 0 \\ 0 & I \end{bmatrix}^T \\ &= F_k P_{k-1} F_k^T + Q_k \end{aligned} \quad (3.5)$$

where  $Q_k$  is the covariance matrix corresponding to  $w_k$ .

The linearized form of the observation model is obtained by expanding 3.2 in a matrix Taylor's series about the predicted estimate

of the state vector  $\hat{X}_{k/k-1}$ .  $\hat{X}_{k/k-1}$  is obtained from 3.1

$$\hat{X}_{k/k-1} = f_k(\hat{X}_{k-1}) \quad (3.6)$$

where the best estimate of the noise vector, its mean, which was assumed to equal zero, is used. Retaining only linear terms the linearized observation model becomes

$$z_k = h_k(\hat{X}_{k/k-1}) + H_k \cdot (\hat{X}_k - \hat{X}_{k/k-1}) + v_k \quad (3.7)$$

$$[z_k - h_k(\hat{X}_{k/k-1})] = H_k \cdot (\hat{X}_k - \hat{X}_{k/k-1}) + v_k$$

$$\delta z_k = H_k \cdot \delta \hat{X}_k + v_k \quad (3.8)$$

where  $H_k$  is the matrix obtained by taking partial derivatives of the elements of  $h_k$  with respect to the state vector elements evaluated at  $\hat{X}_{k/k-1}$ . According to the method of Lagrange the weighted least squares estimate of  $\hat{X}_k$  is obtained by minimizing the function

$$\hat{v}_k^T R_k^{-1} \hat{v}_k + (\hat{X}_k - \hat{X}_{k/k-1})^T P_{k/k-1}^{-1} (\hat{X}_k - \hat{X}_{k/k-1}) \quad (3.9)$$

subject to the constraint

$$z_k = h_k(\hat{X}_{k/k-1}) + H_k \cdot (\hat{X}_k - \hat{X}_{k/k-1}) + \hat{v}_k \quad (3.10)$$

The variation function is

$$\begin{aligned} \phi = & \hat{v}_k^T R_k^{-1} \hat{v}_k + (\hat{X}_k - \hat{X}_{k/k-1})^T P_{k/k-1}^{-1} (\hat{X}_k - \hat{X}_{k/k-1}) \\ & + 2\hat{K}^T [z_k - h_k(\hat{X}_{k/k-1}) - H_k \cdot (\hat{X}_k - \hat{X}_{k/k-1}) - v_k] \end{aligned} \quad (3.11)$$

where  $\hat{K}$  is the vector of Lagrange multipliers. The derivatives of  $\phi$  with respect to  $\hat{v}_k$  and  $\hat{X}_k$  are set equal to zero to determine the extremum, in this case the minimum.

$$\begin{aligned} \frac{\partial \phi}{\partial \hat{v}_k} = & 2\hat{v}_k^T R_k^{-1} - 2\hat{K}^T = 0 \\ R_k^{-1} \hat{v}_k - \hat{K} = & 0 \end{aligned} \quad (3.12)$$

$$\begin{aligned} \frac{\partial \phi}{\partial \hat{X}_k} = & 2(\hat{X}_k - \hat{X}_{k/k-1})^T P_{k/k-1}^{-1} - 2\hat{K}^T H_k = 0 \\ P_{k/k-1}^{-1} (\hat{X}_k - \hat{X}_{k/k-1}) - H_k^T \hat{K} = & 0 \end{aligned} \quad (3.13)$$

Equations 3.10, 3.12 and 3.13 are the normal equations which, in hypermatrix form, are

$$\begin{bmatrix} R_k^{-1} & 0 & -I \\ 0 & P_{k/k-1}^{-1} & -H_k^T \\ -I & -H_k & 0 \end{bmatrix} \begin{bmatrix} \hat{v}_k \\ (\hat{X}_k - \hat{X}_{k/k-1}) \\ \hat{K} \end{bmatrix} + \begin{bmatrix} 0 \\ 0 \\ z_k - h_k(\hat{X}_{k/k-1}) \end{bmatrix} = 0 \quad (3.14)$$

These equations, when solved for  $\hat{X}_k$ , yield

$$\hat{X}_k = \hat{X}_{k/k-1} + G_k [z_k - h_k(\hat{x}_{k/k-1})] \quad (3.15)$$

where

$$G_k = P_{k/k-1} H_k^T (R_k + H_k P_{k/k-1} H_k^T)^{-1} \quad (3.16)$$

is called the Kalman gain matrix. An expression for the estimated state covariance matrix  $P_k$  is obtained by replacing  $h_k(\hat{X}_{k/k-1})$  by its linear approximation  $h_k(0) + H_k \cdot \hat{X}_{k/k-1}$  and rewriting Equation 3.15 as

$$\hat{X}_k = (I - G_k \cdot H_k) \hat{X}_{k/k-1} + G_k \cdot z_k - G_k \cdot h_k(0) \quad (3.17)$$

where the term  $G_k \cdot h_k(0)$  is a constant. The covariance law is applied to 3.17 to obtain

$$P_k = (I - G_k H_k) P_{k/k-1} (I - G_k H_k)^T + G_k R_k G_k^T \quad (3.18)$$

$$\begin{aligned} &= P_{k/k-1} - G_k H_k P_{k/k-1} + (G_k R_k + G_k H_k P_{k/k-1} H_k^T \\ &\quad - P_{k/k-1} H_k^T) G_k^T \end{aligned} \quad (3.19)$$

But from 3.16

$$G_k (R_k + H_k P_{k/k-1} H_k^T) = P_{k/k-1} H_k^T$$

or

$$G_k R_k + G_k H_k P_{k/k-1} H_k^T - P_{k/k-1} H_k^T = 0$$

Since this is the expression in the brackets of 3.19 the equation for the estimated state covariance becomes simply

$$P_k = P_{k/k-1} - G_k H_k P_{k/k-1} \quad (3.20)$$

Equations 3.6, 3.5, 3.16, 3.15, and 3.20, evaluated in that order, constitute the discrete extended Kalman filter. They are repeated here for easy reference.

$$\hat{X}_{k/k-1} = f_k(\hat{X}_{k-1}) \quad (3.21a)$$

$$P_{k/k-1} = F_k P_{k-1} F_k^T + Q_k \quad (3.21b)$$

$$G_k = P_{k/k-1} H_k^T (R_k + H_k P_{k/k-1} H_k^T)^{-1} \quad (3.21c)$$

$$\hat{X}_k = \hat{X}_{k/k-1} + G_k [z_k - h_k(\hat{X}_{k/k-1})] \quad (3.21d)$$

$$P_k = P_{k/k-1} - G_k H_k P_{k/k-1} = (I - G_k H_k) \cdot P_{k/k-1} \quad (3.21e)$$

When either the dynamic model or the observation model is linear,  $\hat{X}_{k-1}$  and  $\hat{X}_k$  become linear functions of  $\hat{X}_{k-1}$  and  $z_k$  respectively and Equations 3.21a and 3.21d can be written in the simpler linear form

$$\hat{X}_{k/k-1} = F_k \cdot \hat{X}_{k-1} \quad (3.22a)$$

and 
$$\hat{X}_k = \hat{X}_{k/k-1} + G_k(z_k - H_k \cdot \hat{X}_{k/k-1}) \quad (3.22b)$$

### 3.2 Kalman Filter and Sequential Adjustment Equations

When there is no time variability the Kalman filter equations reduce to the sequential least squares adjustment equations. If the state vector  $X_k$  is not changing with time Equations 3.21a and b become identities and the double subscripts are no longer needed. Substituting  $G_k$  into 3.21d and 3.21e the result is

$$\hat{X}_k = \hat{X}_{k-1} + P_{k-1} H_k^T (R_k + H_k P_{k-1} H_k^T)^{-1} [z_k - h_k(\hat{X}_{k-1})] \quad (3.23a)$$

$$P_k = P_{k-1} - P_{k-1} H_k^T (R_k + H_k P_{k-1} H_k^T)^{-1} H_k P_{k-1} \quad (3.23b)$$

which, allowing for differences in notation, are identical to Equations 10.9 and 10.11 of Wells and Krakiwsky [1971]. This result is also derived in Section 10.2 of Wells and Krakiwsky [1971].

### 3.3 Bayes Filter and Phased Adjustment Equations

Given the nonsingular matrices  $R(n \times n)$  and  $P(m \times m)$  and the rectangular matrix  $H(n \times m)$ , Morrison [1969] and Wells [1974] prove the following matrix identities

$$(P^{-1} + H^T R^{-1} H)^{-1} = P - P H^T (R + H P H^T)^{-1} H P \quad (3.24)$$

$$(P^{-1} + H^T R^{-1} H)^{-1} H^T R^{-1} = P H^T (R + H P H^T)^{-1} \quad (3.25)$$

Krakiwsky [1975] uses these identities to prove that the phased adjustment equations are equivalent to the sequential adjustment equations. Morrison [1969] uses them to prove that the Kalman filter is algebraically equivalent to the Bayes filter. The Bayes filter can be derived from the Kalman filter equations as follows.

Substitute 3.21c into 3.21e to get

$$P_k = P_{k/k-1} - P_{k/k-1} H_k^T (R_k + H_k P_k H_k^T)^{-1} H_k P_{k/k-1} \quad (3.26)$$

A comparison of this result with 3.24 reveals that the equations for  $P_k$  can be written

$$P_k = (P_{k/k-1}^{-1} + H_k^T R_k^{-1} H_k)^{-1} \quad (3.27)$$

Comparing Equations 3.25 and 3.21c it is clear that the Kalman gain matrix can be found by

$$G_k = (P_{k/k-1}^{-1} + H_k^T R_k^{-1} H_k)^{-1} H_k^T R_k^{-1} \quad (3.28)$$

But the expression in brackets is  $P_k$ . Therefore

$$G_k = P_k H_k^T R_k^{-1} \quad (3.29)$$

The Bayes filter equations thus are:

$$\hat{X}_{k/k-1} = f_k(\hat{X}_{k-1}) \quad (3.30a)$$

$$P_{k/k-1} = F_{k/k-1} P_{k-1} F_{k/k-1}^T + Q_k \quad (3.30b)$$

$$P_k = (P_{k/k-1}^{-1} + H_k^T R_k^{-1} H_k)^{-1} \quad (3.30c)$$

$$G_k = P_k H_k^T R_k^{-1} \quad (3.30d)$$

$$\hat{X}_k = \hat{X}_{k/k-1} + G_k [z_k - h_k(\hat{X}_{k/k-1})] \quad (3.30e)$$

Dropping the time variability, Equations 3.30 a and b become identities and the double subscripts become single subscripts. Inverting both sides of 3.30c and substituting  $G_k$  into 3.30e the result is

$$P_k^{-1} = P_{k-1}^{-1} + H_k^T R_k^{-1} H_k \quad (3.31a)$$

$$\hat{X}_k = \hat{X}_{k-1} + P_k H_k^T R_k^{-1} [z_k - h_k(\hat{X}_{k-1})] \quad (3.31b)$$

Except for the differences in notation these equations are the same as the phased adjustment equations 4.35 and 4.36 of Krakiwsky [1975].

From a comparison of Equations 3.21 and 3.30 it appears, for the parametric observation equation being dealt with here, that the Bayes filter is more advantageous for problems in which the dimension of the observation vector is larger than the dimension of the state vector since a square matrix the size of the state vector must be inverted. The Kalman

filter, on the other hand, is better for problems involving observation vectors whose dimension is smaller than the state vector since a square matrix the size of the observation vector has to be inverted.

### 3.4 Variance Factor

The state covariance matrix is independent of the observations. Its usefulness as an indicator of the accuracy of the estimated state vector elements is dependent entirely on the previous state covariance matrix  $P_{k-1}$ , the observation covariance matrix  $R_k$ , and the state transition covariance matrix,  $Q_k$ . However, if it is assumed that the state covariance matrix is accurate to within a scale factor the residuals can be used to estimate that scale factor. In adjustment calculus the scale factor is known as the variance factor and is denoted by  $\hat{\sigma}_0^2$ . An estimate of the variance factor is obtained from the following equation:

$$\hat{\sigma}_0^2 = \frac{\hat{v}^T T^{-1} \hat{v}}{df} \quad (3.32)$$

where the estimated residual vector  $\hat{v}$  is obtained from

$$\hat{v} = z_k - h_k(\hat{X}_k) \quad (3.33)$$

$$T = R_k + H_k P_{k/k-1} H_k^T \quad (3.34)$$

and  $df$  = degrees of freedom. The degrees of freedom in this case are equal to the number of observations. Generally, the degrees of freedom are equal to the number of unknowns ( $n$ ) minus the number of observations ( $m$ ) but in this case the predicted state vector elements are pseudo-

observations so that, in effect, there are  $n+m$  observations. Computing the degrees of freedom as the number of observations minus the number of unknowns results in:  $(m+n) - n = m$  degrees of freedom.

An estimated state covariance matrix is therefore obtained from

$$\hat{P}_k = \hat{\sigma}_0^2 P_k \quad (3.35)$$

### 3.5 A Simple View of the Kalman Filter

In this section a very simple Kalman filter is described. The object of this section is to illustrate some of the features of the Kalman filter, using simple one-dimensional models, that are not at all evident in more complex models. The problem we will consider has a one-dimensional state vector and a one-dimensional observation vector and the observation model and the system dynamics model are both identities. An identity observation model means that the observation is itself an estimate of the element in the state vector. An identity dynamics model implies that there is no variation in the state vector element with time apart from fluctuations that result from noise or errors in the dynamics model.

In terms of the Kalman filter Equations 3.21 the above simplifications reduce the three covariance matrices  $P$ ,  $Q$ , and  $R$  to simple variances and  $F = 1$  and  $H = 1$ . Rewriting Equations 3.21 we obtain

$$\hat{X}_{k/k-1} = \hat{X}_{k-1} \quad (3.36a)$$

$$P_{k/k-1} = P_{k-1} + Q_k \quad (3.36b)$$

$$G_k = P_{k/k-1} / (R_k + P_{k/k-1}) \quad (3.36c)$$

$$\hat{X}_k = \hat{X}_{k/k-1} + G_k (z_k - \hat{X}_{k/k-1}) \quad (3.36d)$$

$$P_k = (1 - G_k) P_{k/k-1} \quad (3.36e)$$

An inspection of these equations reveals that they describe a sequential technique for computing a weighted average of a sequence of numbers and its variance with the additional feature that old data is given less weight.

### 3.5.1 State Transition Variance - Q

The primary function of the state transition variance is an indicator of the accuracy of the state transition model. A larger state transition variance indicates that the predicted estimate of the state is less reliable than normal and the predicted state variance is therefore increased by a larger amount. Another interpretation of this characteristic of the state transition variance is in terms of the response of the Kalman filter. A large value of  $Q$  causes the filter to respond more quickly to new data since, as  $Q$  becomes larger,  $P_{k/k-1}$  increases with the result that the gain  $G_k$  tends toward 1. In Equation 3.36d as  $G_k$  tends to 1, less notice is taken of old data and new data predominate.

In some situations  $Q_k$  and  $R_k$  do not change to any great extent with  $k$ . Under these conditions, after many cycles of the Kalman filter, the state variance  $P_k$  settles and fluctuates about an equilibrium (dynamic equilibrium) value that is independent of its starting value. The value at which  $P_k$  settles is determined solely by the values of  $Q_k$

and  $R_k$ . In the dynamic equilibrium condition the level of  $P_k$  tends to be increased by increasing  $Q_k$  and decreased by decreasing  $R_k$ .  $Q_k$  increases the state variance by simple addition. A small  $R_k$  decreases the state variance by tending to increase the gain  $G_k$  so that the term  $(1 - G_k)$  in 3.36e becomes smaller.

### 3.5.2 The State Variance P and Observation Variance R

The filtering function of these equations can be observed by considering what happens when good or bad observations are made and the quality of the observation is known and reflected by the observation variance  $R$ . Let us consider the case of a very good observation. The good observation will have a small observation variance  $R_k$  with the result that in Equation 3.36c the gain  $G_k$  will tend to 1. In 3.36d a gain near 1 means that  $\hat{X}_{k/k-1}$  tends to cancel leaving only the new observation. Therefore when the data are good less notice is taken of the old estimates and more weight is placed on the new data. Furthermore, the state variance  $P_k$  is reduced in 3.36e to reflect the higher quality of the new estimates. By a similar argument it can be seen that less notice is taken of observation data that are known to be of poor quality.

### 3.5.3 The Relationship Between the Kalman Filter and the Low Pass Digital Filter

The simple linear digital filter can be expressed as

$$y(k) = \alpha y(k-1) + (1 - |\alpha|)u(k) \quad (3.37)$$

where  $\alpha$  is a constant in the range  $(-1, +1)$ ,  $y(k)$  and  $y(k-1)$  are

estimates of the quantity being sought for times  $k$  and  $k-1$  respectively, and  $u(k)$  is the current observation. For  $-1 < \alpha < 0$ , Equation 3.37 is a high pass filter while for  $0 < \alpha < 1$  it is a low pass filter. We are interested in the latter case here. Dropping the absolute value sign and letting

$$\alpha = 1 - \gamma$$

Equation 3.37 becomes

$$\begin{aligned} y(k) &= (1-\gamma) y(k-1) + \gamma u(k) \\ &= y(k-1) + \gamma[u(k) - y(k-1)] \end{aligned} \quad (3.38)$$

which is identical in form to Equation 3.36d. It apparently can be concluded from this that the low pass filter is simply an elementary Kalman filter.

## CHAPTER 4

### INTEGRATION OF RHO-RHO LORAN-C AND TRANSIT

In this chapter an integrated navigation system that combines information from rho-rho Loran-C and Transit is described. The equipment used was an Austron Model 5000 rho-rho Loran-C system (Fig. 4.1) and a Canadian Marconi CMA-722 Satellite Navigation system (Fig. 4.2). The configuration as it existed prior to the commencement of this project is described in Sections 4.1 through 4.3. In Section 4.1 the characteristics of the two systems that make them compatible for combined operation are described. Section 4.2 gives the details of the corrections that are applied to the observed Loran-C ranges. Section 4.3 describes the least squares mathematical model used to compute the latitude and longitude from the Loran-C ranges. Improvements that have been prompted by this study are then described in detail.

In the next chapter the accuracies of ship's velocities obtained from Loran-C and ship's log and gyro are analyzed. A Kalman filter that integrates Loran-C, ship's log and ship's gyro is proposed.

#### 4.1 Historical Perspective

In 1972 the Bedford Institute of Oceanography (BIO) purchased an Austron Loran-C system. It consisted of a Loran-C receiver, an atomic frequency standard, and a minicomputer to tie the two together. The computer was also supplied with a limited amount of computer memory for user programs. Machine language programs were written to compute latitude, longitude, course and speed from the Loran-C ranges.

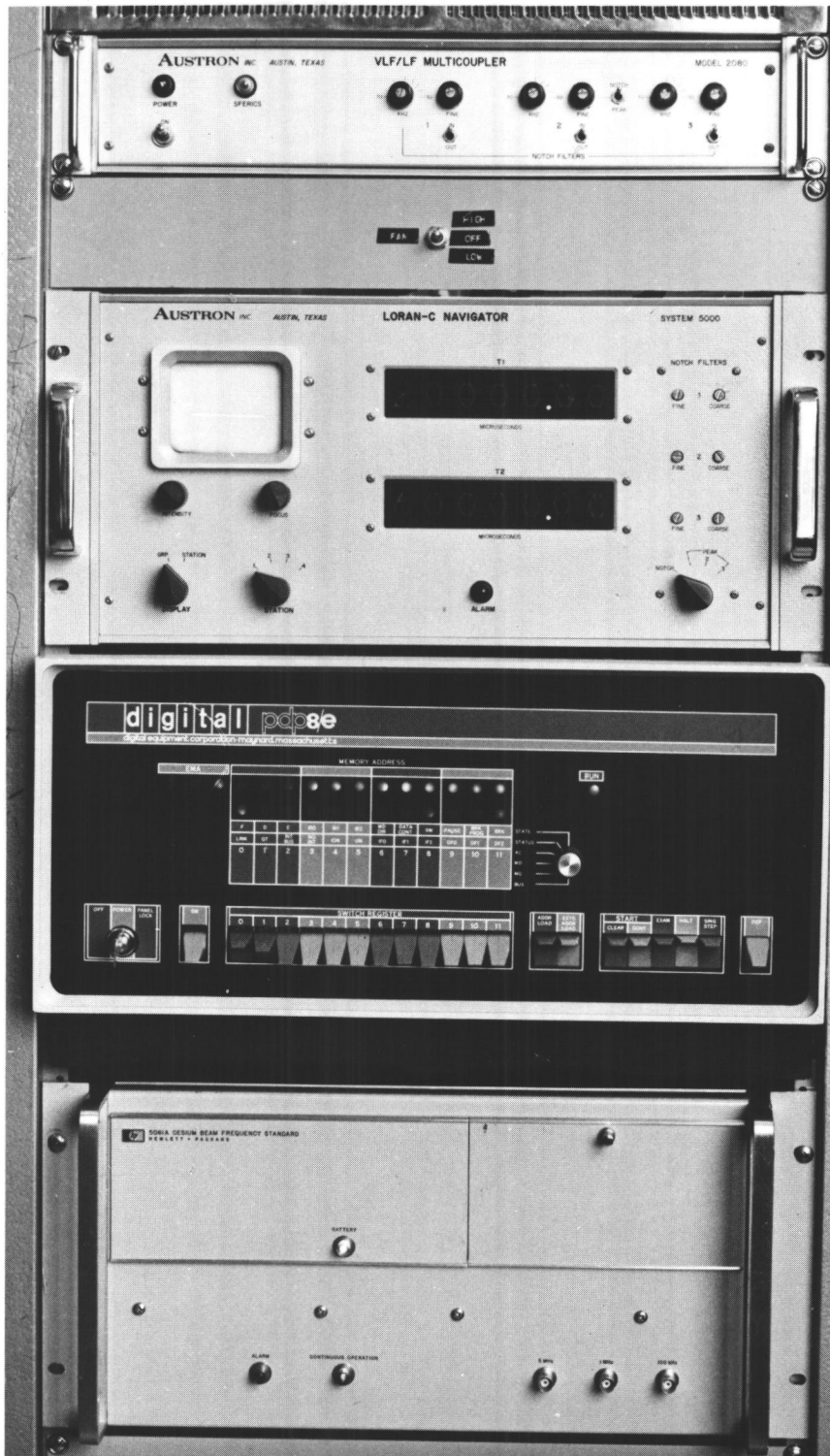


Figure 4.1. Austron 5000 Rho-rho Loran-C System [Grant, 1973]

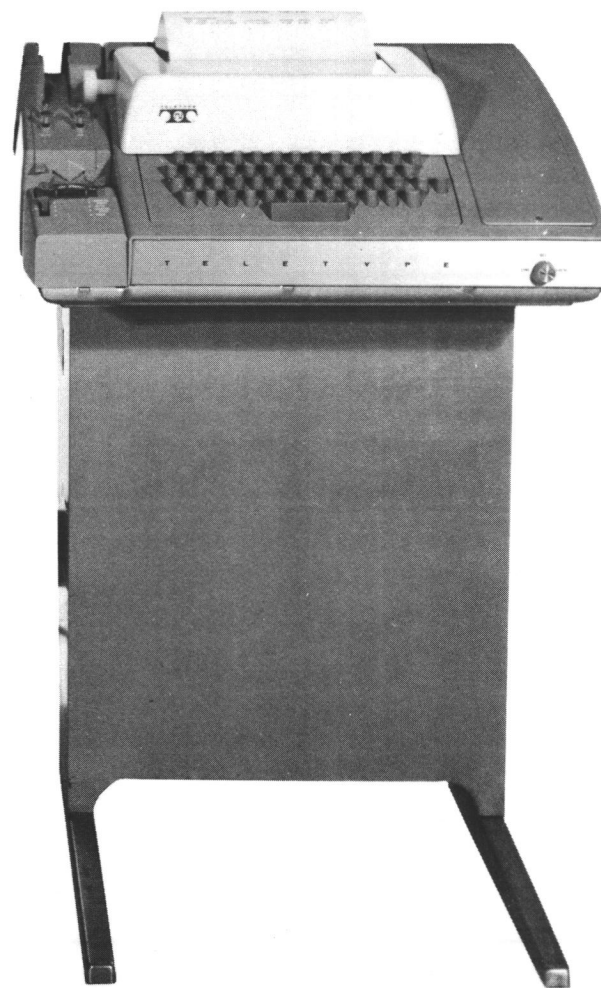
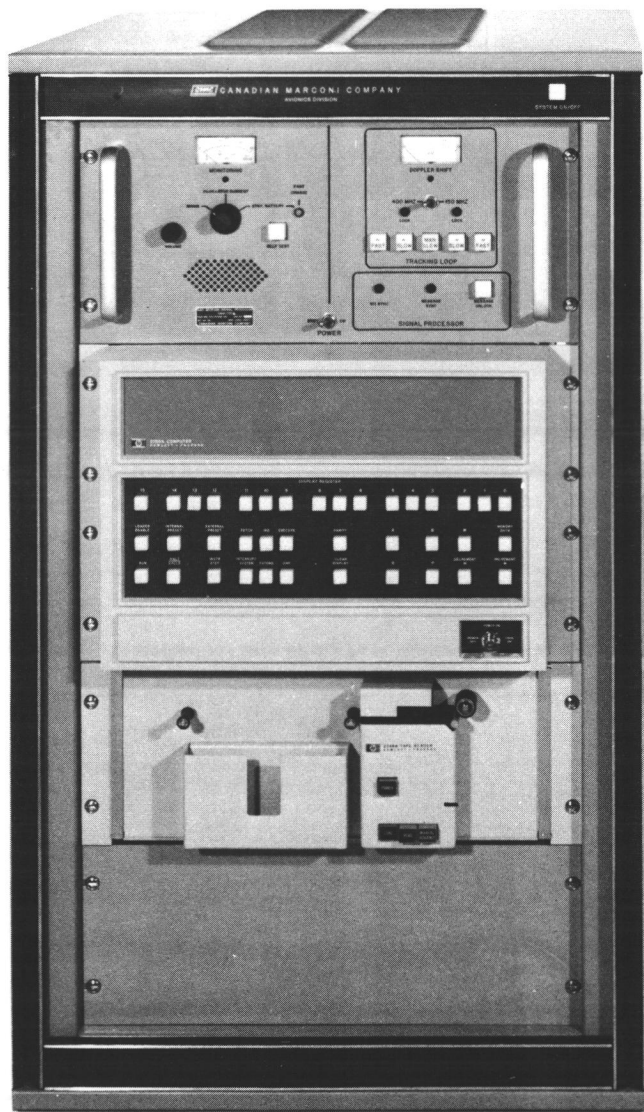


Figure 4.2. Canadian Marconi CMA-722 Satellite Navigation System

Techniques for operating the system alone and, later, with Transit were developed. The status of the system at the commencement of this study is described by Grant [1973]. The essential features are repeated here.

#### 4.1.1 System Characteristics

Rho-rho Loran-C provides virtually continuous measurements of ranges to fixed shore transmitters. The measurements are very stable over periods of several minutes. Ship's velocity obtained from Loran-C averaged over five minutes or more is therefore quite accurate. Velocity derived from Loran-C has the advantage over log and gyro that the velocity is relative to the ocean bottom, not the water mass, and so eliminates the effect of currents. But Loran-C ranges sometimes have biases due to propagation anomalies (e.g. land-path effects) and poor time synchronization. They can also accumulate errors over the long term (e.g. days or weeks) due to the frequency offset between the transmitter and receiver atomic frequency standards. Error growth rates of 15 metres per day are not uncommon.

Transit, on the other hand, provides fixes every 1 to 2 hours that are accurate to 60 to 600 metres and are free of systematic errors [Eaton *et al.*, 1976]. The fix accuracy depends partly on the quality of the vessel's course and speed information used by the Transit but does not deteriorate with time as is the case with rho-rho Loran-C.

Rho-rho Loran-C and Transit appear to complement each other very well. The Loran-C supplies continuous, high resolution positioning and velocity information. The Transit provides periodic checks to control the long period component of Loran-C errors.

## 4.2 Rho-rho Loran-C Corrections

There are two main corrections to Loran-C range measurements: receiver synchronization corrections and radio wave propagation corrections. The receiver synchronization corrections can be separated into timing and frequency synchronization corrections. Receiver synchronization techniques are discussed in the next section.

The propagation of low frequency (LF) radio waves has been studied extensively [e.g. Millington, 1949; Brunavs and Wells, 1971; Jöhler, 1962; Potts and Weider, 1972; Doherty, 1974]. However, errors in propagation prediction are still probably the largest source of error in rho-rho Loran-C range measurements. Corrections to Loran-C ranges due to propagation effects is the subject of Section 4.2.2.

Unpredictable errors due to timing problems at the Loran-C transmitter and propagation disturbances in the coverage area are rare but do occasionally occur. Such errors are usually detected by a sudden otherwise unexplained shift in the ship's position, by an increase in the residuals when more than one range is being measured (see Section 4.3) or from the comparisons with Transit. Weekly notices listing all such timing and propagation disturbances are available from the United States Naval Oceanographic Office, Washington.

### 4.2.1 System Synchronization

One of the first steps in rho-rho Loran-C operation is the selection of the appropriate Group Repetition Period (GRP). Following the entry of the GRP into the Loran-C system computer the system generates timing marks at intervals of the GRP. A signal acquisition

procedure is then carried out during which the receiver tracking circuits are aligned with the incoming pulses. Thereafter, under computer control, the receiver automatically tracks the same point of the received pulses. The pulses are transmitted every GRP and therefore, for a stationary receiver, always arrive at a constant time interval after the generation of the internal timing mark (see Fig. 4.3). Ideally, the internally generated time mark should coincide with the time of transmission of the Loran-C signal, in which case the time interval from the internal time mark to reception of the signal is simply the signal propagation time. Except by accident, this is never the case. In order to relate the time interval measured by the receiver to the signal travel time the interval between the time of transmission and the time of generation of the internal timing mark must be known. The determination of this interval is known as time synchronization.

*Time Synchronization.* The technique of Loran-C time synchronization is simple. The time interval between the internally generated time mark and the time of reception of the Loran-C signal is measured by the receiver. Simultaneously, the receiver position is determined by some independent method and the travel time of the Loran-C signal from the transmitter to the receiver position is computed. The difference between the computed and observed travel times is applied as a time synchronization correction to all further measurements. The accuracy of the synchronization correction essentially depends on (a) the accuracy of the independently determined receiver position, and (b) the accuracy of the propagation prediction model. Loran-C propagation prediction problems are discussed in the next section. If the ship is stationary

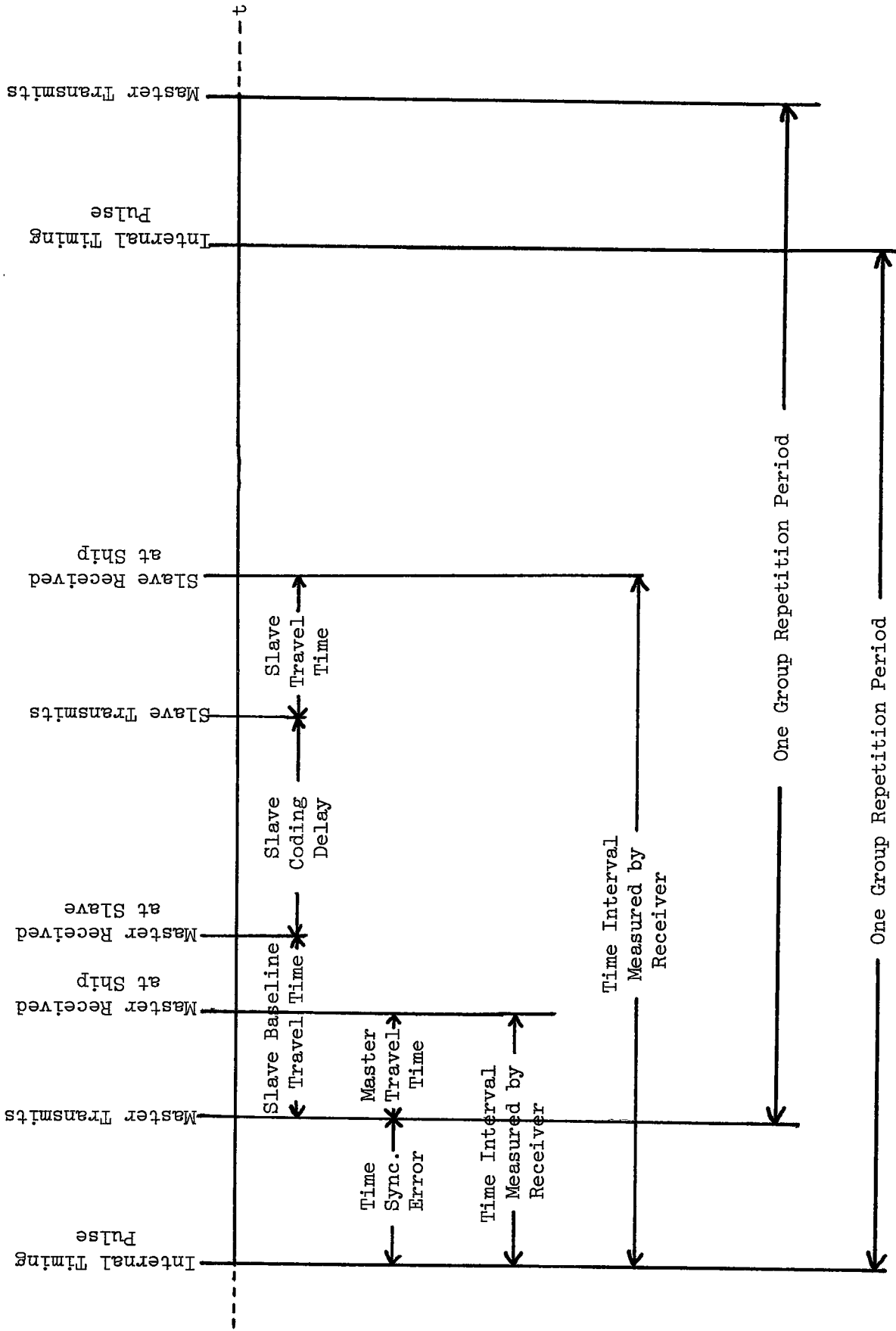


Figure 4.3. Rho-rho Loran-C Receiver Timing

alongside a jetty the receiver position can be determined very precisely by conventional surveying techniques. If the ship is at sea a reference system such as Transit must be used. However, several Loran-C/Transit comparisons are needed because of the limited accuracy of a single Transit fix before the Loran-C system is properly synchronized. For example, assuming a satellite pass every 2 hours with a standard deviation of 200 m about 4 days are required to synchronize the Loran-C system to 0.1  $\mu$ s. Since radio waves travel at about 300 m/ $\mu$ s this represents a ranging error of about 30 m.

*Frequency Synchronization.* Atomic frequency standards are used to measure time intervals (i.e. they are atomic clocks) by having them count cycles of the highly stable frequency. The difference between time intervals measured by two different standards is only a few parts in  $10^{12}$ . This frequency difference results in a cumulative timing error (time drift). In terms of Loran-C operation where such 'clocks' are used, both to control the times of Loran-C transmission and to measure the times of signal reception, a frequency difference of (say) 5 parts in  $10^{12}$  results in an error after one day of 0.43  $\mu$ s. This timing error is equivalent to a range error of about 130 m after the first day, 260 m after the second day, and so on.

Grant [1973] found that by logging Loran-C range readings over a period of a few days with the receiver stationary and plotting them against time, a clock drift rate could be determined that was valid as a correction to future observations to within about 0.05  $\mu$ s/day (15 m/day). This represents a time drift error (or equivalently a frequency synchronization error) of six parts in  $10^{13}$ .

When the ship is at sea, a reference positioning system such as Transit must be used. This is done by comparing the observed Loran-C range with the computed range from the Transit fix. By plotting these differences against time it is theoretically possible to determine the relative clock drift rate to within a few tenths of a microsecond per day after several days of comparisons. However, in practice, the clock drift is not the only source of error and over several days as the ship moves about the coverage area, various of the other errors are apt to creep into the Loran-C ranges. A plot of the differences between Transit and Loran-C will not reflect the variations of the errors due only to clock drift. In practice, the Loran-C range differences for each range are plotted against time on a control graph such as Figure 4.4 and periodic adjustments to both the synchronization and clock drift corrections are entered into the Loran-C computer by the operator to keep the differences between Transit and Loran-C as small as possible.

#### 4.2.2 Loran-C Propagation Corrections

In vacuum radio waves travel at the velocity of light: 299.7925 m/ $\mu$ s. Radio waves that propagate through the earth's atmosphere and over the conducting surface of the earth (i.e. ground waves) travel at slower velocities. The velocities of terrestrial radio waves vary with frequency, distance, atmospheric and geological conditions along the path and many other factors. Actual radio waves therefore always arrive later than those predicted using the velocity of light and, since most radio positioning systems actually measure the phase of the incoming signals, the delaying effect is known as phase lag.

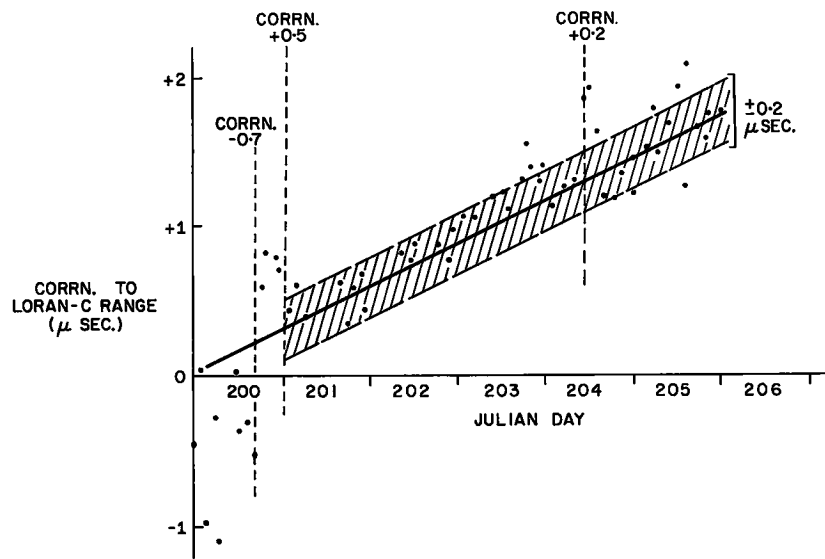


Figure 4.4. Rho-rho Loran-C/Transit Clock Drift Control Graph

The phase lag of the ground wave is usually looked upon as the sum of the phase lags of the primary field (due to the retardation effects of the atmosphere) and the secondary factor (due to the presence of the conducting surface of the earth and the vertical lapse of atmospheric refractivity). In linear units the phase lag caused by the atmosphere is

$$P_{\text{T}'} = N \cdot 10^{-6} \cdot d \quad (4.1)$$

where  $P_{\text{T}'}$  is the theoretical phase lag and  $d$  is the distance to the transmitter and they both are in units of metres. The refractivity  $N$  depends on atmospheric pressure, temperature and humidity. For the average atmosphere the value of  $N = 338$  is often assumed [Brunavs and Wells, 1971]. The secondary factor ( $F$ ) is a complex function of the characteristics of the radiation source, the conductivity, permittivity and roughness of the earth's surface and the vertical lapse of permittivity of the atmosphere. The total theoretical phase lag  $P_{\text{T}}$  is found from

$$P_{\text{T}} = P_{\text{T}'} + F \quad (4.2)$$

The conductivity of the sea surface is nearly homogeneous and constant, while for land areas it changes with both time and place.  $F$  can therefore be predicted much more accurately over sea water than over land. For the practical problem of determining corrections to Loran-C ranges to a vessel at sea it has been assumed that the radio wave propagation paths are all over sea water. In most marine areas this is a reasonable assumption since the transmitters are located near

the coast. For on-line operation over water phase lag corrections are determined by evaluating the following polynomial in distance  $d$

$$P_T = A/d + B + C \cdot d + D \cdot d^2 \quad (4.3)$$

where  $A = 8.853$ ,  
 $B = -0.13511$ ,  
 $C = 8.687 \times 10^{-4}$ ,  
 $D = 1.265 \times 10^{-8}$ .

$P_T$  and  $d$  are in microseconds. The polynomial constants were obtained from a least squares fit to tables compiled by Mr. P. Brunavs, Canadian Hydrographic Service, Ottawa. The algorithm and assumptions are described in Brunavs and Wells [1971]. They estimate that their propagation model computes overwater phase lag to an accuracy of 1:30,000 although it was only tested to 500 km. The polynomial fit was accurate to about 0.1  $\mu$ s. Taken together the overwater phase lag computed from Equation 4.3 is probably accurate to one part in 30,000 at  $1\sigma$ . The overwater phase lag is plotted against distance in Figure 4.5.

In some marine areas there are considerable stretches of land along the path between the ship and the Loran-C transmitter. The effect of the land is to introduce a larger phase lag than would be observed by an all overwater path. If the conductivity of the land is known the approximate overland phase lag can be computed by Millington's method [Millington, 1949] and used to correct the observed ranges. This is the technique the BIO has been using. Unfortunately, it is

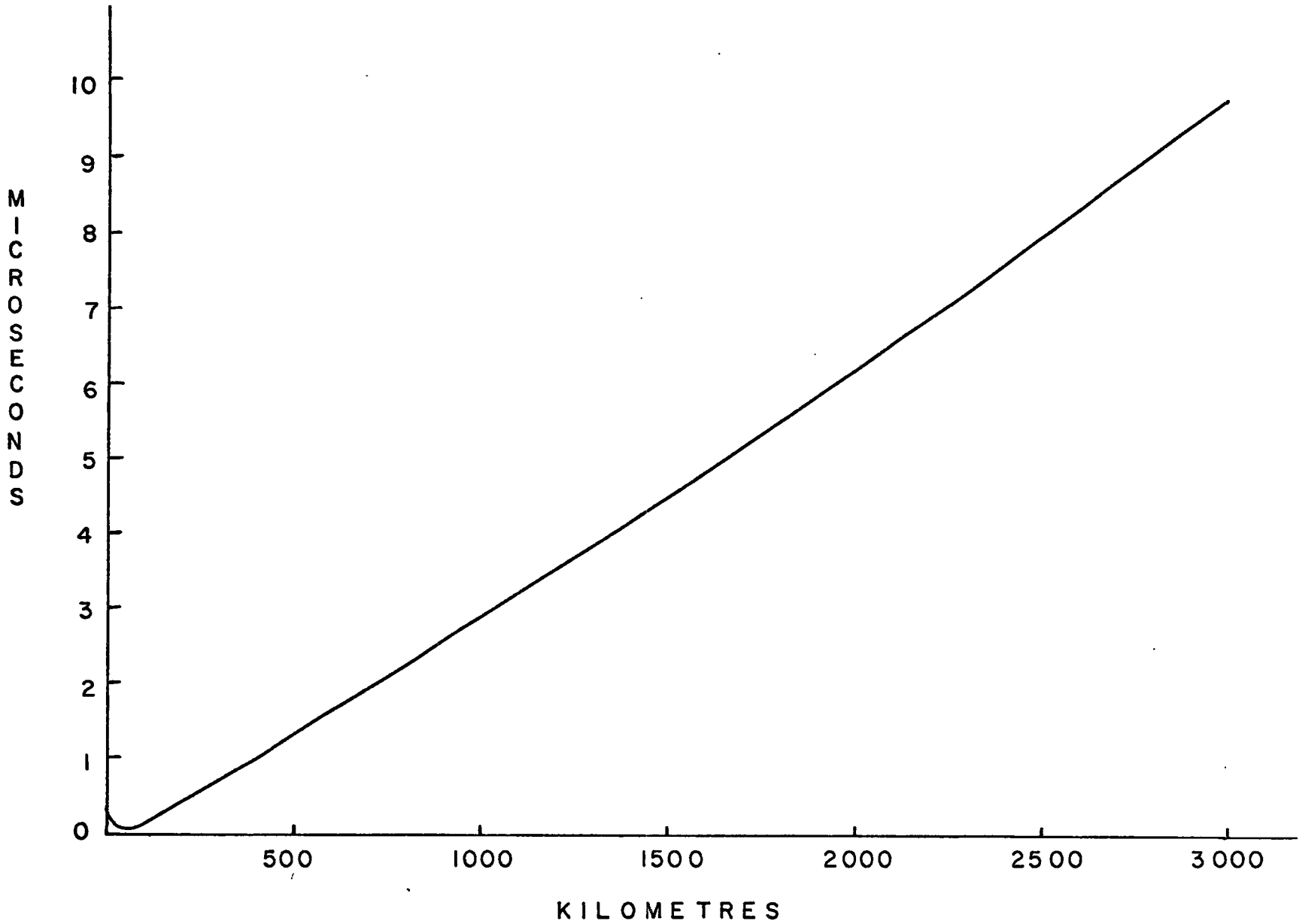


Figure 4.5. Overwater Phase Lag at 100 kHz (1  $\mu$ s = 300 m)

difficult to estimate the correct conductivity of the land masses and the conductivity often changes with time due to seasonal effects. Calibration checks against Transit in the operational area are therefore used to adjust the computed corrections. An analysis [Hagglund, 1973] of a month's Loran-C and Transit data collected in the Labrador Sea in 1972 indicated that the overland phase lag corrections are accurate to about  $0.25 \mu\text{s}$  (75 m). More recent data analyzed later in 1975 has confirmed this result.

#### 4.3 Mathematical Model for Determining Geographic Coordinates

The procedure for using rho-rho Loran-C at sea can be separated into two operations:

- (1) Correcting the Loran-C ranges for clock drift and phase lag, and
- (2) Computing the geographic coordinates and ship's velocity from the corrected Loran-C ranges.

The techniques for determining the corrections have just been described. In the next section this procedure is partly automated via the Kalman filtering approach. In this section the method for computing the geographic coordinates from the corrected Loran-C ranges is described.

##### 4.3.1 Least Squares Fix

The latitude and longitude are computed by the method of least squares. The observation model relating the observed ranges  $z_i$  and the latitude ( $\phi$ ) and longitude ( $\lambda$ ) is

$$h_i(\phi, \lambda) - z_i = 0 \quad (4.4)$$

where 
$$h_i(\phi, \lambda) = a \cdot (u + du) \quad (4.5)$$

$$u = \arccos(\sin\phi \sin\phi_i + \cos\phi \cos\phi_i \cos[\lambda - \lambda_i]) \quad (4.6)$$

$$du = -\frac{f}{4} \left[ \left( \frac{u+3\sin u}{1-\cos u} \right) (\sin\phi - \sin\phi_i)^2 + \left( \frac{u-3\sin u}{1+\cos u} \right) (\sin\phi + \sin\phi_i)^2 \right] \quad (4.7)$$

$a$  is the semi-major axis of the reference ellipsoid,

$f$  is the flattening, and

$\phi_i$  and  $\lambda_i$  are the latitudes and longitudes of the fixed

Loran-C transmitters.

Equation 4.5 is known as the Andoyer-Lambert long-line formula and is derived by Thomas [1965]. It is derived from the equation for the Great Elliptic Arc (i.e. the space curve defined by the intersection of the plane containing the two end points and the centre of the earth and the surface of the reference ellipsoid). The equation for the Great Elliptic Arc length is of the form

$$S = a (u + du + du^2 + \dots)$$

where  $du$  is a function of  $f$ ,  $du^2$  is a function of  $f^2$ , etc. Truncation of the series after  $du$  gives the Andoyer-Lambert long line formula while truncation after  $du^2$  gives the so-called Forsyth-Andoyer-Lambert formula. Both these formulae were compared with the rigorous Helmert formula by Thomas [1965] and were found to be accurate to 45 m and 14 m respectively for lines to 6000 km and for all azimuths. The

Andoyer-Lambert long line formula was chosen over several other formulae (e.g. Puissant, Rudoe, Clarke, Robin, Bessel) because it was compact and therefore more suitable for use in a minicomputer and yet it retained a reasonable level of accuracy even over the long lines (up to 4000 km) encountered with Loran-C.

Estimates of the ship's coordinates are found using the non-linear simultaneous least squares adjustment equations described in Chapter 7 of Wells and Krakiwsky [1971]. They are the same as the phased adjustment Equations 3.31 derived in Chapter 3 under the additional assumptions:

- (a) The ship's coordinates are virtually unknown prior to commencement of the fix calculation so that  $P_{k-1}^{-1}$  is a null matrix, and
- (b) All ranges are taken together so that the subscripts in 3.31 are not needed.

Substituting 3.31a into 3.31b and using the subscript '0' to denote an initial estimate we obtain the simultaneous least squares adjustment equation

$$\hat{X} = X_0 + (H^T R^{-1} H)^{-1} H^T R^{-1} [z - h(\hat{X}_0)] \quad (4.8)$$

where  $\hat{X} = \begin{bmatrix} \hat{\phi} \\ \hat{\lambda} \end{bmatrix}$  and  $X_0 = \begin{bmatrix} \phi_0 \\ \lambda_0 \end{bmatrix}$ .

The elements of the design matrix H are obtained by differentiating the spherical part of Equation 4.5 with respect to  $\phi$  and  $\lambda$  to get:

$$\frac{\partial h_i}{\partial \phi} = H_{i1} = -a \left( \frac{-\cos \phi \sin \phi_i + \sin \phi \cos \phi_i \cos(\lambda - \lambda_i)}{\sin u} \right) \quad (4.9)$$

$$\frac{\partial h_i}{\partial \lambda} = H_{i2} = -a \left( \frac{\cos \phi \cos \phi_i \sin(\lambda - \lambda_i)}{\sin u} \right) \quad (4.10)$$

The problem is iterated until the improvement is less than some limit. In practice, the limit is chosen to be one metre. To avoid tying up the computer in case of an undefined position the calculation is terminated after a maximum of 20 iterations and an error message is typed.

Prior to the commencement of this study the observation covariance matrix  $R$  was set equal to an identity matrix. If a particular range could not be used for some reason the corresponding diagonal element of  $R^{-1}$  was set equal to zero. Occasionally the diagonal elements of  $R^{-1}$  were given values between zero and one if a range reading was noisier than the others.

#### 4.4 The Combined System

In the next two sections an improved technique for using rho-rho Loran-C and Transit together is described. The principles of operation remain essentially the same as described in the preceding section. The main difference is in the method used for determining the corrections to the Loran-C ranges. The graphical procedure described in Section 4.2.1 is replaced by an automatic computer-based procedure that uses a simple linear Kalman filter. The main problem encountered in the development of this technique involved the weighting of the Loran-C and Transit observations and the weighting within the

Kalman filter. The Kalman filter is described in the next section and a discussion of the weighting is left until Section 4.4.2.

#### 4.4.1 Kalman Range Correction Filter

In Section 4.2.1 a procedure was described for manually controlling the corrections to Loran-C ranges from Transit comparisons. It was assumed that the range errors changed linearly with time due to the relative drift between the receiver and transmitter atomic clocks. At each Transit fix the difference between computed and observed Loran-C ranges were plotted on control graphs. For each range the operator would then change the synchronization correction, the rate or both to make the applied correction correspond more closely to the observed error.

The Kalman Range Correction Filter is designed to work in much the same way as the manual method. The correction to each Loran-C range is modelled by the linear equations

$$S_k = S_{k-1} + \alpha_{k-1} \cdot \Delta t + w_{1,k-1} \quad (4.11)$$

$$\alpha_k = \alpha_{k-1} + w_{2,k-1} \quad (4.12)$$

where  $S_k$  is the correction at time  $t_k$ ,  $S_{k-1}$  was the correction at time  $t_{k-1}$ ,  $\alpha_{k-1}$  is the rate of change of the correction with time (i.e. clock drift rate) as determined at time  $t_{k-1}$  and  $\Delta t$  is the time interval  $t_k - t_{k-1}$ .  $w_{1,k-1}$  and  $w_{2,k-1}$  are random noise terms. Equation 4.12 tells us that in the model the rate does not change with time. The

linearized Kalman state prediction model corresponding to Equations 4.11 and 4.12 is

$$\begin{bmatrix} S \\ \alpha \end{bmatrix}_{k/k-1} = \begin{bmatrix} 1 & \Delta t \\ 0 & 1 \end{bmatrix} \begin{bmatrix} S \\ \alpha \end{bmatrix}_{k-1} \quad (4.13)$$

or 
$$\hat{X}_{k/k-1} = F \cdot \hat{X}_{k-1} \quad (4.14)$$

Assuming that the state covariance matrix  $P_{k-1}$  and the state transition covariance matrix  $Q_k$  are known the predicted state covariance matrix  $P_{k/k-1}$  can be obtained using Equation 3.21b.

The observation model is an identity. A direct estimate of the correction  $s_k$  is found at each Transit fix from the differences between the observed Loran-C ranges and the theoretical ranges computed from the Transit fix. This difference is the observed clock drift correction  $z_k$  plus noise. The observation model relating the observation  $z_k$  and the state vector elements  $S$  and  $\alpha$  is

$$z_k = S_k \quad (4.15)$$

or 
$$z_k = [1 \quad 0] \begin{bmatrix} S \\ \alpha \end{bmatrix}_k \quad (4.16)$$

or 
$$z_k = HX_k \quad (4.17)$$

For this model the Kalman filter equations written out in full

are:

$$\begin{bmatrix} S \\ \alpha \end{bmatrix}_{k/k-1} = \begin{bmatrix} 1 & \Delta t \\ 0 & 1 \end{bmatrix} \cdot \begin{bmatrix} S \\ \alpha \end{bmatrix}_{k-1} \quad (4.18a)$$

$$\begin{bmatrix} \sigma_s^2 & \sigma_{s\alpha} \\ \sigma_{\alpha s} & \sigma_\alpha^2 \end{bmatrix}_{k/k-1} = \begin{bmatrix} 1 & \Delta t \\ 0 & 1 \end{bmatrix} \cdot \begin{bmatrix} \sigma_s^2 & \sigma_{s\alpha} \\ \sigma_{\alpha s} & \sigma_\alpha^2 \end{bmatrix}_{k-1} \cdot \begin{bmatrix} 1 & 0 \\ \Delta t & 1 \end{bmatrix} + \begin{bmatrix} \sigma_{q11}^2 & \sigma_{q12} \\ \sigma_{q21} & \sigma_{q22}^2 \end{bmatrix}_k \quad (4.18b)$$

$$\begin{bmatrix} G_1 \\ G_2 \end{bmatrix} = \begin{bmatrix} \sigma_s^2 & \sigma_{s\alpha} \\ \sigma_{\alpha s} & \sigma_\alpha^2 \end{bmatrix}_{k/k-1} \cdot \begin{bmatrix} 1 \\ 0 \end{bmatrix} \left( \sigma_{z_k}^2 + [1 \ 0] \begin{bmatrix} \sigma_s^2 & \sigma_{s\alpha} \\ \sigma_{\alpha s} & \sigma_\alpha^2 \end{bmatrix}_{k/k-1} \cdot \begin{bmatrix} 1 \\ 0 \end{bmatrix} \right)^{-1} \quad (4.18c)$$

$$\begin{bmatrix} S \\ \alpha \end{bmatrix}_k = \begin{bmatrix} S \\ \alpha \end{bmatrix}_{k/k-1} + \begin{bmatrix} G_1 \\ G_2 \end{bmatrix} \cdot [z_k - S_k] \quad (4.18d)$$

$$\begin{bmatrix} \sigma_s^2 & \sigma_{s\alpha} \\ \sigma_{\alpha s} & \sigma_\alpha^2 \end{bmatrix}_k = \begin{bmatrix} \sigma_s^2 & \sigma_{s\alpha} \\ \sigma_{\alpha s} & \sigma_\alpha^2 \end{bmatrix}_{k/k-1} - \begin{bmatrix} G_1 \\ G_2 \end{bmatrix} [1 \ 0] \begin{bmatrix} \sigma_s^2 & \sigma_{s\alpha} \\ \sigma_{\alpha s} & \sigma_\alpha^2 \end{bmatrix}_{k/k-1} \quad (4.18e)$$

When the covariance matrices have been determined the Kalman

Range Correction Filter operates as follows:

- (1) Between Transit fixes the state vector elements (slope and synchronization) are used to compute corrections to the Loran-C ranges;
- (2) At Transit fixes the state vector elements and state covariance matrix are updated using the Kalman filter Equations 4.18.

#### 4.4.2 Observation Covariance Matrix R

Because they are stationary, surveyors on land are usually able to make large numbers of observations over long periods of time and are therefore able to derive accurate estimates of the error statistics of their observation set. Navigators at sea on the other hand are always in motion and the number of observations is restricted to those they can make in a single time instant. Navigators must therefore rely on statistical models to determine the accuracy of their observations.

Ideally, statistical models should be constructed from a data base that spans the whole operational range of the instrument (i.e. the entire coverage area and a full seasonal cycle) and the reference system should be at least an order of magnitude more accurate than the system under study. In most marine applications this is impractical or even impossible to achieve. For example, no reference system is available in the deep ocean areas with which to check Loran-C accuracy and it is completely impractical to attempt to make year-round observations of Loran-C even in the limited areas where more accurate reference systems are available. Another consideration that becomes much more important for the sort of real time application with which this study is concerned is the need to keep the model compact and fast to evaluate.

In the Kalman Range Correction Filter the observation is the difference between the observed Loran-C range and the range computed from the Transit fix. The observation covariance matrix R must therefore reflect the fact that both Loran-C and Transit errors are

contributing. That is

$$\sigma_{z_i}^2 = \sigma_{\text{Loran-C}}^2 + \sigma_{\text{Transit}}^2 \quad (4.19)$$

where  $\sigma_{\text{Loran-C}}^2$  is the variance of the Loran-C range measurement and  $\sigma_{\text{Transit}}^2$  is the variance of the Transit fix in the direction of the Loran-C transmitter. Given the Transit fix covariance matrix

$$\Sigma_{\text{Transit}} = \begin{bmatrix} \sigma_{\phi}^2 & \sigma_{\phi\lambda} \\ \sigma_{\lambda\phi} & \sigma_{\lambda}^2 \end{bmatrix} \quad (4.20)$$

Equation 4.19 can be rewritten as

$$\sigma_{z_i}^2 = \sigma_{\text{Loran-C}}^2 + A \Sigma_{\text{Transit}} A^T \quad (4.21)$$

where

$$A = \begin{bmatrix} \frac{\partial r}{\partial \phi} & \frac{\partial r}{\partial \lambda} \end{bmatrix} \quad (4.22)$$

and the elements of A are found using Equations 4.9 and 4.10.

Grant [1973] listed the sources of Loran-C errors and gave estimates of their magnitudes. These estimates were updated and improved by Bryant *et al.* [1974]. Based on these results a quadratic polynomial in range was derived to compute the range observation standard deviation

$$\sigma_r = A + B \cdot r + C \cdot r^2 \quad (4.23)$$

where  $A = 135.0$

$$B = -0.17 \times 10^{-3}$$

$$C = 0.86 \times 10^{-10}$$

and  $\sigma_r$  and  $r$  are in metres.

The standard deviation curve is plotted against range in Figure 4.6 along with the corresponding weight function obtained from the inverse of the standard deviation squared (i.e. one over variance). This polynomial is included as part of the real time program and is used both for weighting observations during the fix calculation (replacing the identity matrix described in the last paragraph of Section 4.3.1) and for computing  $\sigma_{\text{Loran-C}}^2$  in Equation 4.21.

The Transit covariance matrix is more difficult to obtain because the Transit fix calculation is being carried out in a separate computer using proprietary Canadian Marconi software which does not compute the unknown covariance matrix. In the process of considering this problem a computer program was written in FOCAL (D.E.C. 1972) to accept certain parameters of the satellite pass (e.g. maximum elevation, number of 30 s dopplers before and after pass centre, course and speed covariance matrix) and then compute the covariance matrix equation 4.20 (see Appendix I for program listing and sample outputs). However, operationally this routine would have required a considerable amount of memory in the already limited PDP-8/E in which the programming was being done. Also, it would have been necessary for the operator to enter this information into the PDP-8/E via the teletype thereby increasing the possibility of blunders. The only alternative was to ask the operator to assess each Transit fix and estimate the Transit

fix covariance matrix. The estimation procedure had to be simple so a diagonal Transit covariance matrix was assumed. The operator notes the relevant Transit fix parameters and enters Table 4.1 (which was compiled by Mr. R.M. Eaton, BIO). After he has determined which category the fix falls into the operator enters this information into the Loran-C computer along with the time, latitude and longitude. Program LORSG described in Appendix II also uses this method for determining Transit fix accuracy.

#### 4.4.3 State Transition Covariance Matrix Q

The state transition covariance matrix Q used in the Kalman Range Correction Filter is

$$Q = \Delta t \begin{bmatrix} q_{11} & q_{12} \\ q_{21} & q_{22} \end{bmatrix} = \Delta t \begin{bmatrix} 0.002 & 0 \\ 0 & 0.0001 \end{bmatrix} \quad (4.24)$$

where  $\Delta t$  is the time interval in days since the last Transit fix. The time factor  $\Delta t$  is necessary so that the state covariance matrix does not increase by large jumps when the Transit fixes are closely spaced in time. The diagonal form was chosen for simplicity.

The  $q_{11}$  element of Q was determined from Grant [1973] who found that the clock drift rate was valid as a correction to future observations to within about  $0.05 \mu\text{s/day}$  ( $15 \text{ m/day}$ ). This implies that the synchronization error increases at the rate of  $0.05 \mu\text{s/day}$  or that  $q_{11} = (0.05 \mu\text{s})^2 = 0.002 \mu\text{s}^2$ . The  $q_{22}$  element of Q was chosen arbitrarily to be small but not zero.

The state transition covariance matrix Q is discussed further

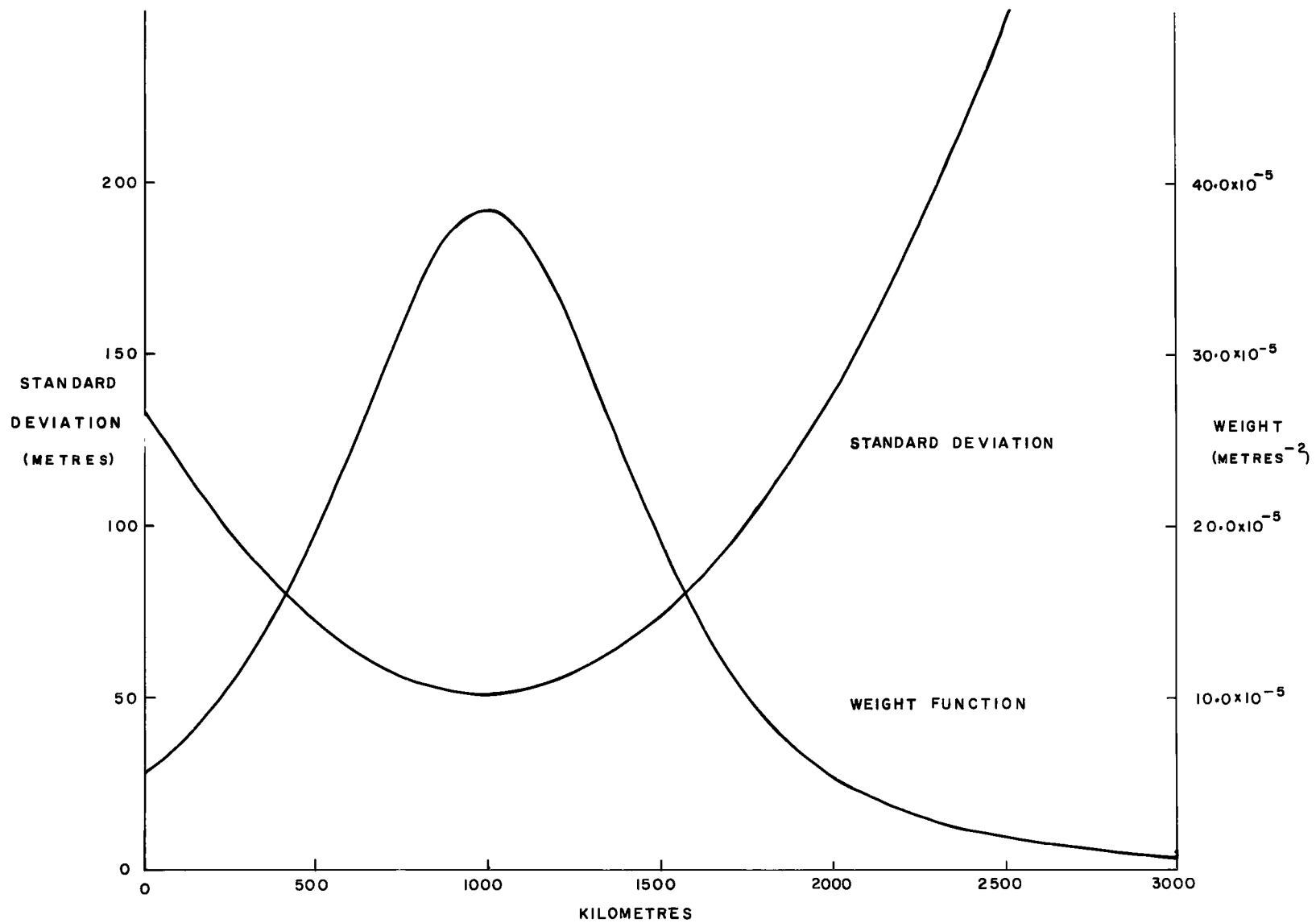


Figure 4.6. Loran-C Range Standard Deviation and Weight Function

Table 4.1

## TRANSIT FIX CLASSIFICATION

(Note: These are arbitrary values,  
not directly supported by evidence.)

Criteria	Good Fix	Fair Fix	Poor Fix
Speed Scatter from mean over successive 5 or 10 min fixes (these scatter figures can be doubled if course near 90° or 270°)	0.2 kt	0.4 kt	0.6 kt
Course Scatter from mean over successive 5 or 10 min fixes (this tolerance can be doubled if course near 0° or 180°)	2°	4°	6°
Maximum Elevation for the pass	20-60°	15-65°	10-70°
Number of 30 s Doppler counts	24	20	16
Balance of Dopplers about pass centre (minimum number of counts on one or other side)	8	6	4
Residual: first determine average residual from previous good passes (this depends on program in use). Call this 'r'	1r	3r	10r
$\sigma_\phi$	100 m	200 m	400 m
$\sigma_\lambda$	120 m	300 m	700 m

NOTE: Fix quality is decided if one criterion puts it in a lower category. All estimates at 1 $\sigma$ .

in Section 4.5.

#### 4.4.4 Test Results

A set of Loran-C/Transit comparisons were processed by the Kalman Range Correction Filter to demonstrate its performance. The data were collected in mid-April 1975 off the coast of Nova Scotia. Only Transit fixes that fell within the first column in Table 4.1 were used to compute the Loran-C range corrections. The data are listed in Table 4.2. There was no land along the propagation path between the ship and the transmitter and no propagation or timing disturbances were observed during the data collection period (U.S.N.O. Time Service Notices, Series 4). These facts show that the data were collected under almost ideal conditions and that the only changes in the Loran-C range corrections should be due to the relative drift between the receiver and transmitter atomic clocks and random noise.

A linear parametric model [e.g. Wells and Krakiwsky, 1971] was used to obtain the linear least squares fit to the data. The computed corrections and residuals are given in Table 4.2 along with the original data. The slope, intercept, estimated variance factor and estimated covariance matrix are given in Table 4.3. All the observed Loran-C corrections were assumed to be of equal quality so an identity weight matrix was used. To the extent that this assumption is correct the variance factor is a measure of the variance of the observed Loran-C corrections.

The Kalman Range Correction Filter was programmed in FOCAL (D.E.C., 1972) for a PDP-8/E computer.

Table 4.2  
LORAN-C DATA

Day	Time	Observed Correction ( $\mu\text{s}$ )	(From Least Squares Fit)	
			Computed Correction ( $\mu\text{s}$ )	Residuals ( $\mu\text{s}$ )
105	0030	0.57	0.15	0.42
105	0200	0.20	0.18	0.03
105	1400	0.63	0.41	0.22
105	1600	0.25	0.45	-0.20
105	1930	0.15	0.52	-0.37
106	0300	0.90	0.66	0.24
106	0450	0.72	0.70	0.02
106	0550	0.45	0.72	-0.27
106	0740	1.05	0.75	0.30
106	1800	1.22	0.95	0.27
106	2030	0.85	1.00	-0.15
106	2220	0.72	1.04	-0.32
106	2240	1.40	1.04	0.36
107	0040	0.65	1.08	-0.43
107	0910	1.25	1.25	0.00
107	1600	1.20	1.38	-0.18
107	2110	1.53	1.48	0.05
107	2300	1.23	1.52	-0.29
108	1320	1.42	1.80	-0.38
108	2300	2.15	1.98	0.17
109	0040	1.95	2.02	-0.07
109	0200	2.35	2.04	0.31
109	2040	2.32	2.40	-0.08
109	2130	2.45	2.42	0.03
109	2210	2.55	2.43	0.12
109	2230	2.20	2.44	-0.24
110	1630	3.15	2.79	0.36

The data in Table 4.2 were processed by the Kalman Range Correction Filter using a state transition covariance matrix  $Q$  given by (4.24) and  $R = 0.07 \mu\text{s}^2$ . The starting values for the state vector elements and the state covariance matrix elements were

$$X_0 = \begin{bmatrix} 0 \\ 0.42 \end{bmatrix}$$

$$P_0 = \begin{bmatrix} 0.01 & 0.0 \\ 0 & 0.001 \end{bmatrix}$$

Table 4.3

## STATISTICS OF LORAN-C DATA

Slope	0.466	$\mu\text{s}/\text{day}$
Intercept	0.137	$\mu\text{s}$
$\hat{\sigma}_0^2$	0.066	
Estimated Covariance Matrix	$\begin{bmatrix} 0.0087 \\ 0.0025 \end{bmatrix}$	$\begin{bmatrix} 0.0025 \\ 0.00097 \end{bmatrix}$

Figure 4.7 illustrates the performance of the Kalman Range Correction Filter. The circles represent the Loran-C and Transit comparisons, the straight line represents the least squares fit through the data, and the solid stepped line is the output of the Kalman Range Correction Filter. The circles can be interpreted as the instantaneous correction that should be applied to the Loran-C range if the Transit

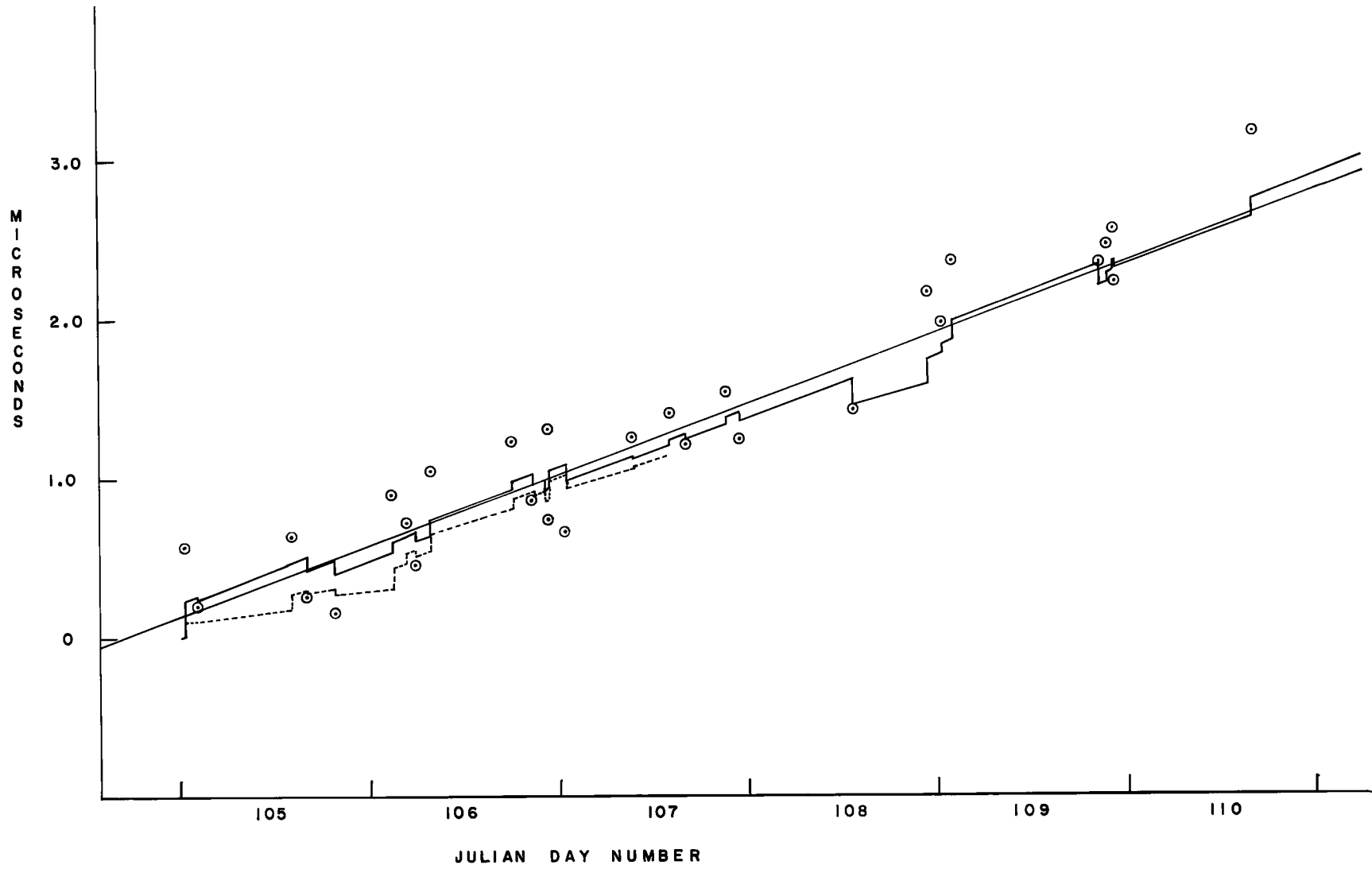


Figure 4.7. Kalman Range Correction Model Performance

fix is errorless. The solid stepped line represents the correction the filter applies. The dashed line represents the correction the filter would apply if it had been given the incorrect starting slope of zero. It eventually merges with the solid stepped line.

#### 4.4.5 Determining Initial Values for the State Covariance Matrix and State Vector Elements

Kalman filters must have reasonable estimates of the starting values for the state vector and state covariance matrix. The procedure for obtaining these starting values for the Kalman Range Correction Filter is described in this section.

Prior to this study estimates of the relative drift rate of the Loran-C receiver atomic clock were obtained by logging Loran-C ranges during a clock rating period for a few days prior to the commencement of the cruise. The drift rate was obtained by plotting the ranges against time and fitting a straight line (usually by eye) to the plotted ranges and noting the slope. Thereafter time-dependent corrections were applied to compensate for the atomic clock drift. As the cruise progressed the corrections were adjusted by the operator who monitored the Loran-C errors on a control graph (Fig. 4.4) compiled from Transit and Loran-C comparisons.

The procedure for obtaining starting values for the Kalman Range Correction Filter is theoretically the same except the straight line fit is done by the method of least squares and an estimated covariance matrix is computed at the same time. As with the previous method there are a number of practical limitations. Often the initial estimates for the state vector elements are disturbed just before

sailing. A common occurrence is a power interruption during the change-over from the shore power supply to the ship's power. The effect is a loss of system timing synchronization. After resynchronizing the system the corresponding element in the state covariance matrix should be increased in value to reflect the fact that the synchronization correction is not as good as that determined during the clock rating period. The frequency synchronization or slope correction should still be valid and so the corresponding element in the state covariance matrix remains unchanged.

Sometimes it is not possible to carry out a clock rating prior to sailing. In this case neither the slope nor the synchronization corrections are known. The only alternative in this case is to use arbitrary guessed values and allow the system to eventually determine the correct estimates from comparisons with Transit.

In situations where the initial estimates of the state vector elements are poor it is important to increase the size of the starting values of the state covariance matrix elements. The system is then able to respond more quickly to the Transit comparisons. This is illustrated by Figure 4.8 where the slope correction determined by the Kalman Range Correction Filter as it processed the data in Table 4.2 is plotted against time for a starting covariance

$$P_0 = \begin{bmatrix} 0.001 & 0 \\ 0 & 0.001 \end{bmatrix} \quad (\text{curve B})$$

and for a starting covariance

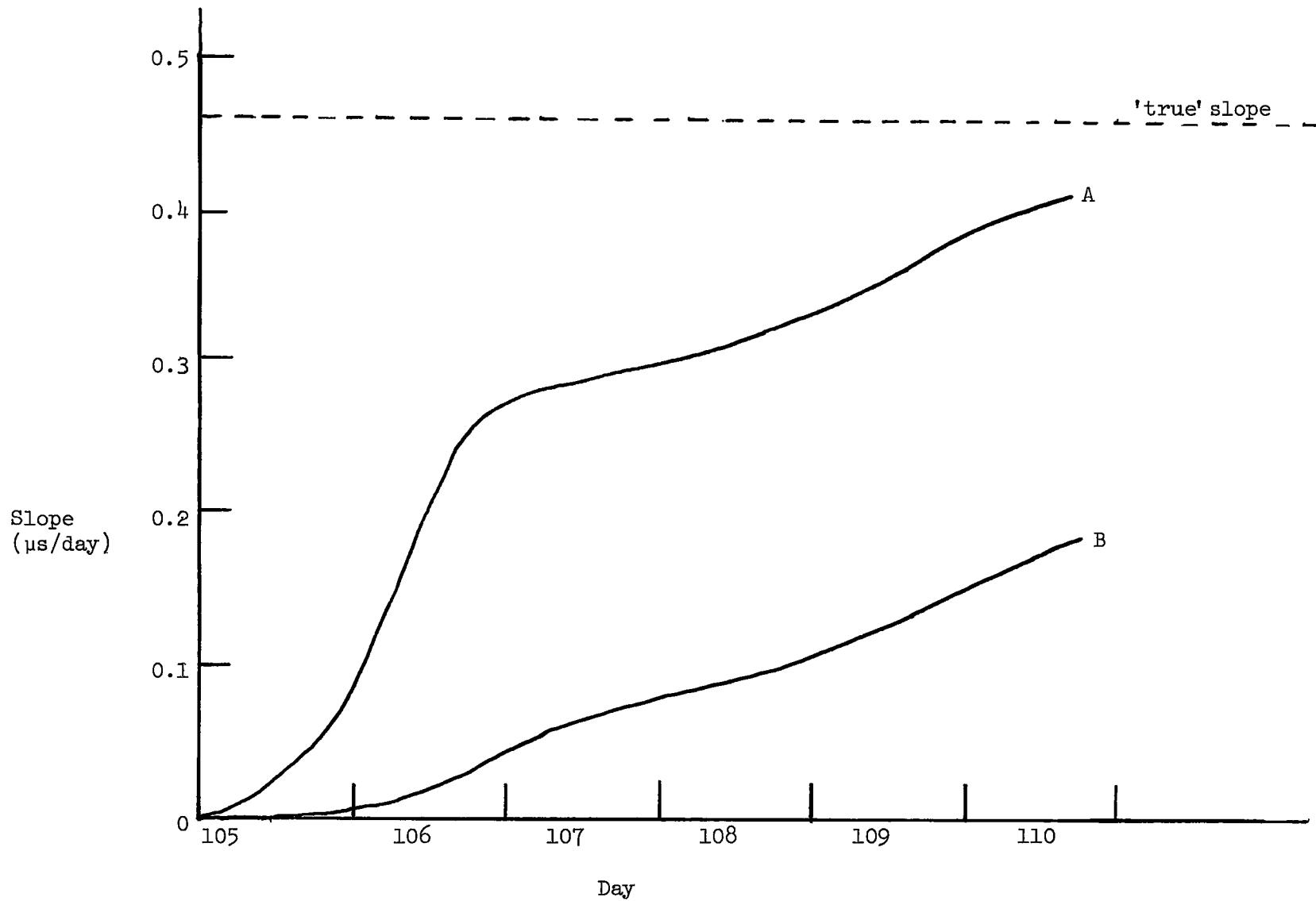


Figure 4.8. Change of slope in Kalman Range Correction Filter. Curves A and B show slope response for high and low starting values for P respectively.

$$P_0 = \begin{bmatrix} 0.1 & 0 \\ 0 & 0.1 \end{bmatrix} \quad (\text{curve A})$$

For comparison the slope determined from the linear least squares fit is also shown.

#### 4.5 Further Test Results and Conclusions

In this section a set of data is analyzed that contains large nonlinear variations due to overland phase lag. In practice the Loran-C ranges are corrected for the additional phase lag due to land path before being used in the fix calculation. Here, however, these effects are ignored in order to test the operation of the Kalman Range Correction Filter under abnormal conditions.

The test data were collected during the spring of 1975 onboard *MV Martin Karlsen* while enroute to the Labrador Sea to carry out routine hydrographic and geophysical surveys. The ship's track is shown in Figure 4.9. Throughout the trip four Loran-C range measurements were recorded once per minute on magnetic tape: one to Nantucket, one to Angissoq, Greenland, and two to Cape Race, Newfoundland. The two range measurements to Cape Race were possible since Cape Race transmits at two different Group Repetition Periods.

In the next two sections the results of the Kalman Range Correction Filter's attempt to correct for the abnormally large overland phase lag errors are discussed for the Nantucket range and one of the Cape Race ranges. In Section 4.5.3 conclusions are drawn and recommendations are made.

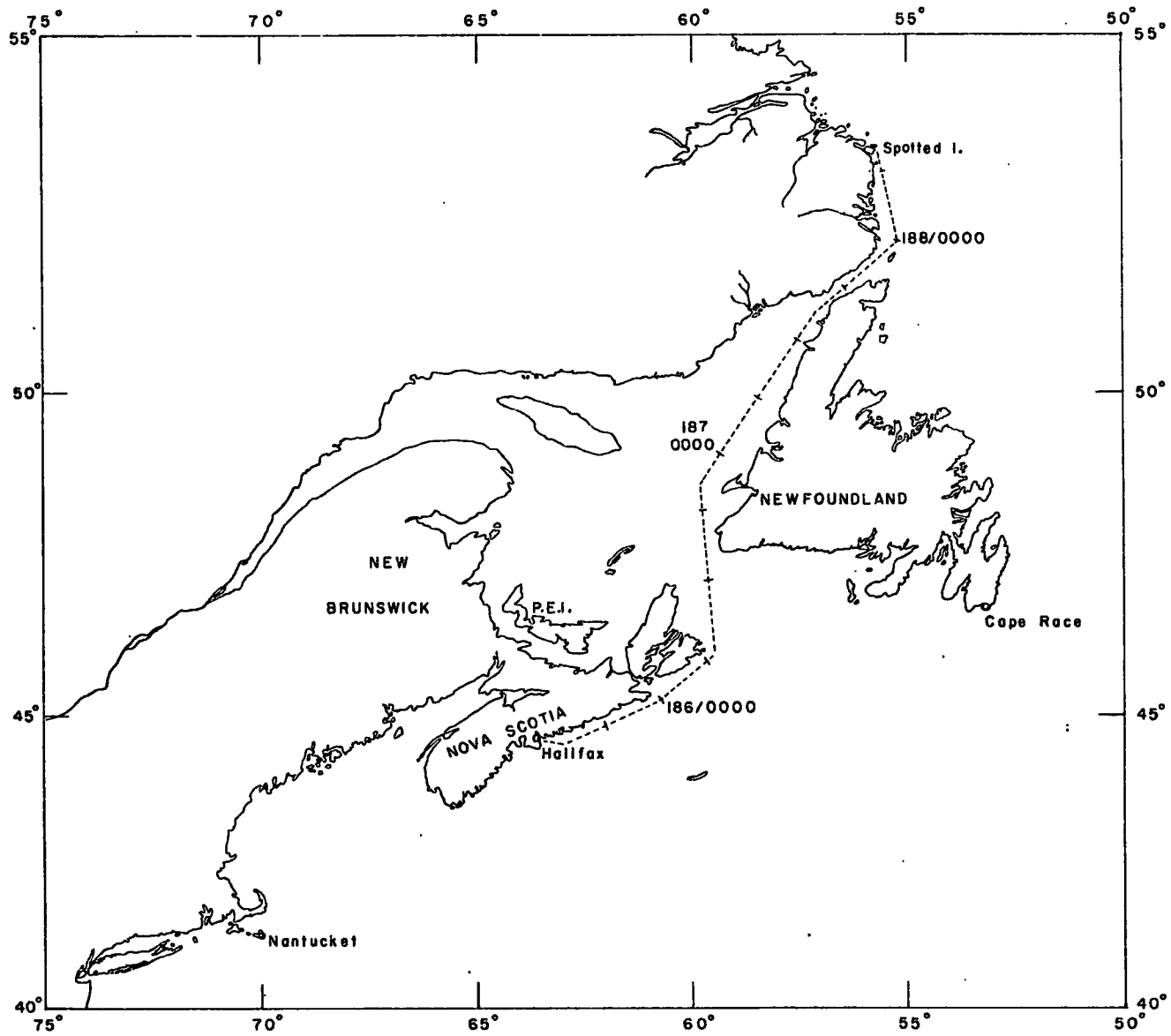


Figure 4.9. Ship's track: Halifax to Spotted Island, July 1975

#### 4.5.1 Nantucket Range Corrections

From the ship's track shown in Figure 4.9 it is evident that the Loran-C signal propagation path from Nantucket to the ship was all over water from the time the ship left Halifax until about 0600 day 186 when the ship altered course to the north to enter Cabot Strait between Nova Scotia and Newfoundland. Almost immediately the signal path had to travel the length of Nova Scotia. As the ship proceeded northward the amount of land path increased and reached a maximum at about noon of day 186. Later that day, as the ship continued on a northerly course, the signal propagation path passed to the north of Cape Breton Island so that the proportion of land path was reduced by about one-third. Thereafter the amount of land path remained practically constant as the ship made her way northward through the Gulf of St. Lawrence.

In Chapter 4 it was mentioned that land along the signal propagation path increases the phase lag so that a larger correction is needed than if the propagation path is all over water. Millington's Method [Millington, 1949, and Chapter 4] was used to compute the theoretical additional overland phase lag for several points along the ship's track and is plotted as a dashed curve in Figure 4.10.

During the passage to Spotted Island fixes were being obtained from Transit at intervals of a few hours. The accuracy of each fix was assessed according to Table 4.1. For each fix the theoretical Loran-C readings were computed assuming no clock drift and no overland phase lag. The differences between the observed and theoretical Loran-C readings were found and are plotted as the small circles in

Table 4.4

## TRANSIT/LORAN-C TEST DATA

Day	Time	Transit Data				Loran-C Corrections	
		Latitude	Longitude	$\sigma_\phi$	$\sigma_\lambda$	Cape Race	Nantucket
185	1610	44 41.197	62 18.533	200	300	0.22	0.08
185	1720	44 46.794	62 02.812	120	150	0.64	-0.34
185	1840	44 52.935	61 44.111	100	120	0.57	-0.40
185	1900	44 54.555	61 39.355	130	200	0.10	0.06
185	2030	45 01.737	61 18.003	150	180	-0.29	0.57
186	0230	45 40.248	60 02.567	120	150	0.65	-0.53
186	0320	45 46.513	59 52.846	120	150	-0.03	0.14
186	0400	45 51.524	59 45.430	100	120	0.47	-0.48
186	0420	45 53.782	59 41.690	120	150	2.02	-1.74
186	0520	46 01.005	59 32.084	100	120	-1.41	0.68
186	0540	46 04.178	59 31.869	150	200	-1.77	0.27
186	0640	46 14.328	59 31.967	100	120	-0.36	-1.49
186	0710	46 19.732	59 31.899	100	150	0.41	-2.29
186	0830	46 34.736	59 31.695	120	150	-0.50	-1.42
186	0900	46 40.408	59 31.915	150	180	0.77	-2.53
186	1040	46 59.046	59 31.699	120	200	0.04	-2.35
186	1550	47 49.551	59 31.036	100	120	-1.03	-1.36
186	1630	47 55.831	59 29.964	200	300	-1.18	-1.74
186	1710	48 02.189	59 28.994	150	200	-1.38	-1.63
186	1740	48 07.006	59 28.189	100	120	-1.81	-1.21
186	2150	48 45.1470	59 12.023	100	150	-2.39	-0.52
186	2330	49 00.045	59 00.553	120	150	-1.61	-0.48
186	0040	49 10.201	58 52.441	100	120	-1.98	-0.47
187	0230	49 25.868	58 39.505	100	120	-2.03	-0.54
187	0600	49 55.224	58 14.496	200	300	-2.47	0.32
187	0950	50 26.872	57 46.265	200	300	-2.93	1.07
187	1430	51 01.807	57 17.020	100	120	-2.64	-0.09
187	1720	51 26.640	56 37.599	100	120	-1.79	-0.79
187	1820	51 33.070	56 21.864	150	200	-2.03	-0.51
187	1840	51 35.237	46 16.935	100	120	-1.97	-0.55
187	1910	51 38.419	56 09.283	100	120	-1.77	0.14
187	2050	51 49.077	55 45.229	100	120	-1.12	-0.52

Figure 4.10. The Transit data and Loran-C comparisons for the Nantucket range and one of the Cape Race ranges are tabulated in Table 4.4. The Transit/Loran-C comparisons clearly show the influence of the overland phase lag.

The Transit/Loran-C data were processed by the Kalman Range Correction Filter using the state transition covariance matrix  $Q$  given in Section 4.4.3. The stepped curve in Figure 4.10 shows the output of the filter. The filter responds to a limited extent to the variations due to overland phase lag, but, what is more important, it does not display any erratic behaviour.

$$Q = \Delta t \begin{bmatrix} 0.02 & 0 \\ 0 & 0.001 \end{bmatrix} \quad (4.25)$$

(i.e. ten times larger than 4.24). The output is plotted in Figure 4.12 and, as expected, shows more response than in Figure 4.10.

#### 4.5.2 Cape Race Range Corrections

The variation in the observed Cape Race Loran-C readings was caused by the signal travelling over Newfoundland when the ship was passing up through the Gulf of St. Lawrence. The theoretical overland phase lag is shown as the dashed curve in Figure 4.12 along with the Transit/Loran-C comparisons (circles).

The observations were processed by the Kalman Range Correction Filter for both values of  $Q$  given by 4.24 and 4.25. The results are shown as the stepped curves in Figures 4.12 and 4.13. As with the Nantucket range the response of the filter was greater for the larger

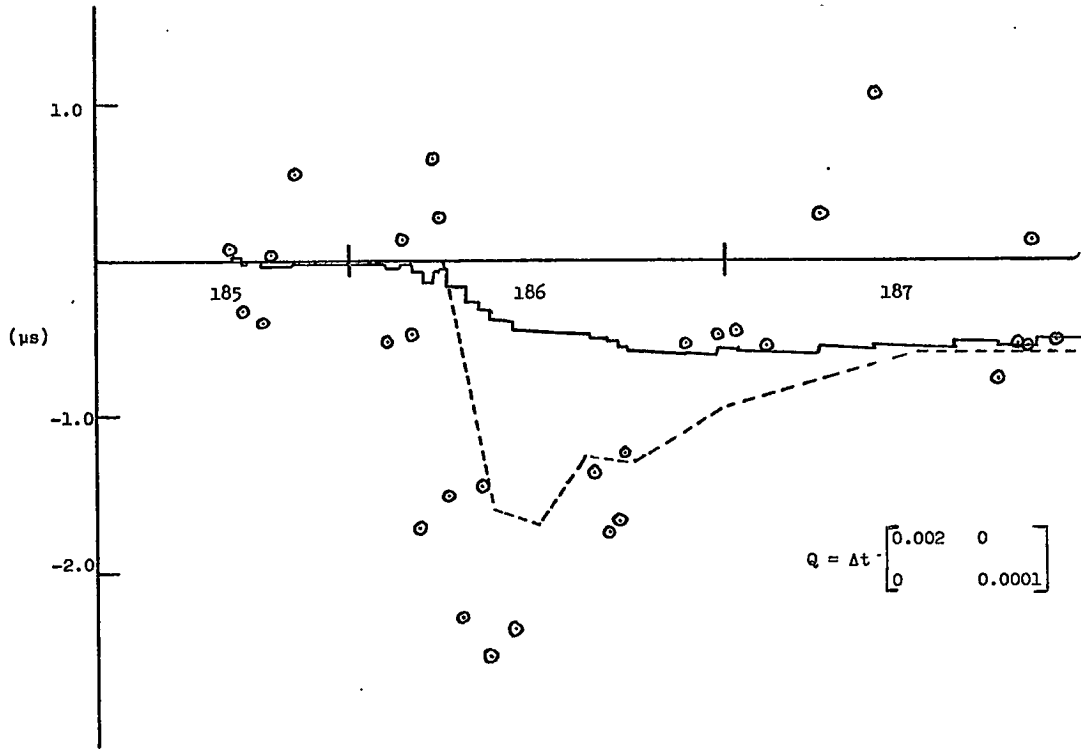


Figure 4.10. Correction to Nantucket Loran-C Range from Kalman Range Correction Filter

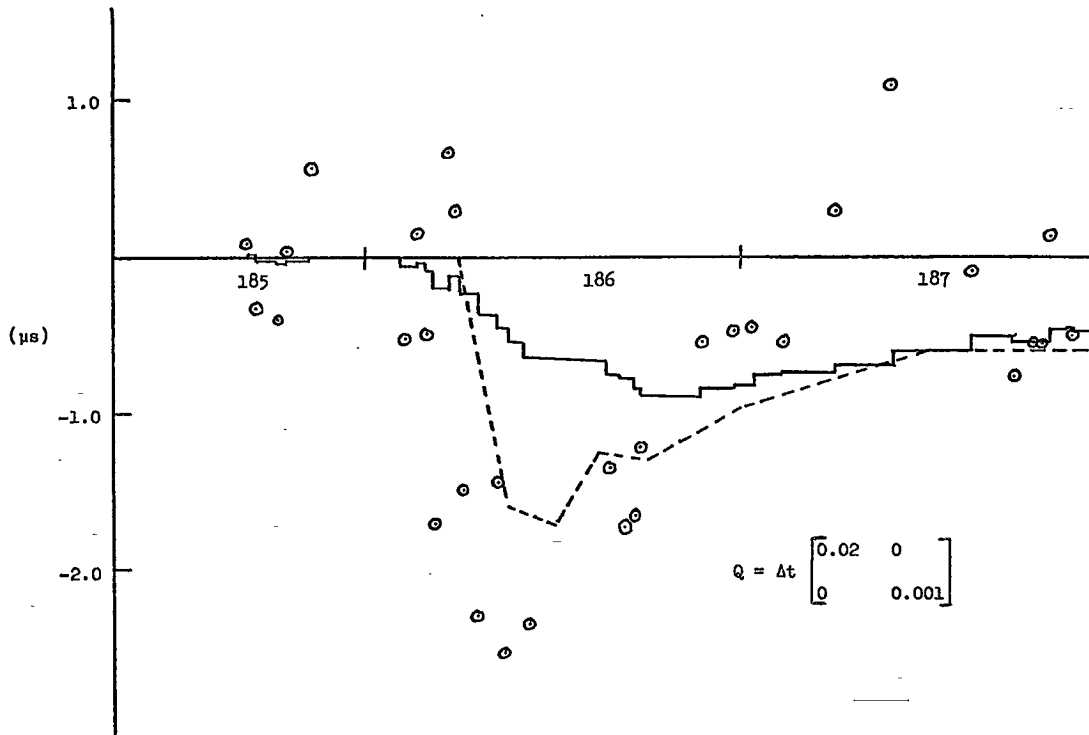


Figure 4.11. Correction to Nantucket Loran-C Range from Kalman Range Correction Filter

values of  $Q$ .

#### 4.5.3 Conclusions and Recommendations

The results just described demonstrate that the Kalman Range Correction Filter remains stable even when the nonlinear variations are much larger than those that would normally be encountered. The fact that the filter did not follow the variations due to overland phase lag even closely is not significant since, during normal operations, most of the errors due to land path are removed. Indeed, it is important that the filter did not follow the short period fluctuations due to noise in the Transit and Loran-C measurements since it was designed to model the long term trends due to clock drift.

From these results it appears that a more realistic estimate for the state transition covariance matrix  $Q$  is probably in the range between the values given by 4.24 and 4.25. These values for the elements of  $Q$  are approximately 1% to 10% of the values for the elements of the state covariance matrix  $P$ . Operationally, it might be better to allow the operator to vary  $Q$  between these two limits in response to the prevailing conditions.

An important aspect of any estimation technique is the problem of robustness (i.e. making the procedure insensitive to gross errors). This is especially important in real time applications. The most common technique for making least squares methods more robust is by selectively editing out observations that are not within some specified limit of the expected value. This is the approach used here to make both the Kalman Range Correction Filter and the Least Squares Fix

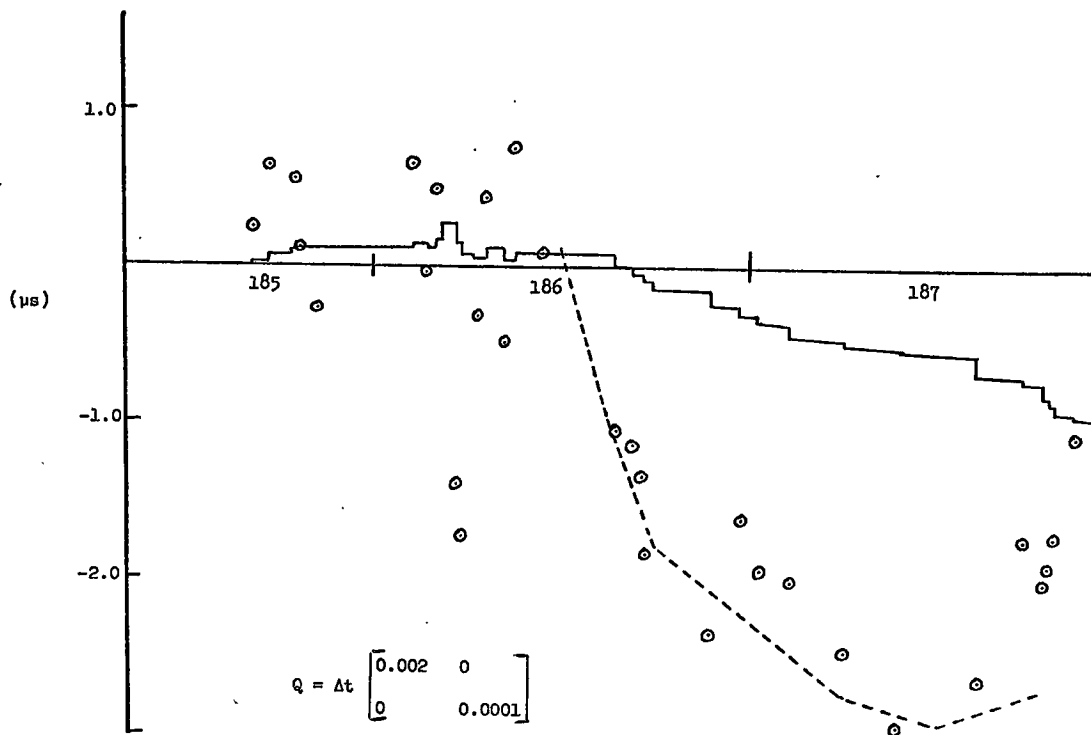


Figure 4.12. Correction to Cape Race Loran-C Range from Kalman Range Correction Filter

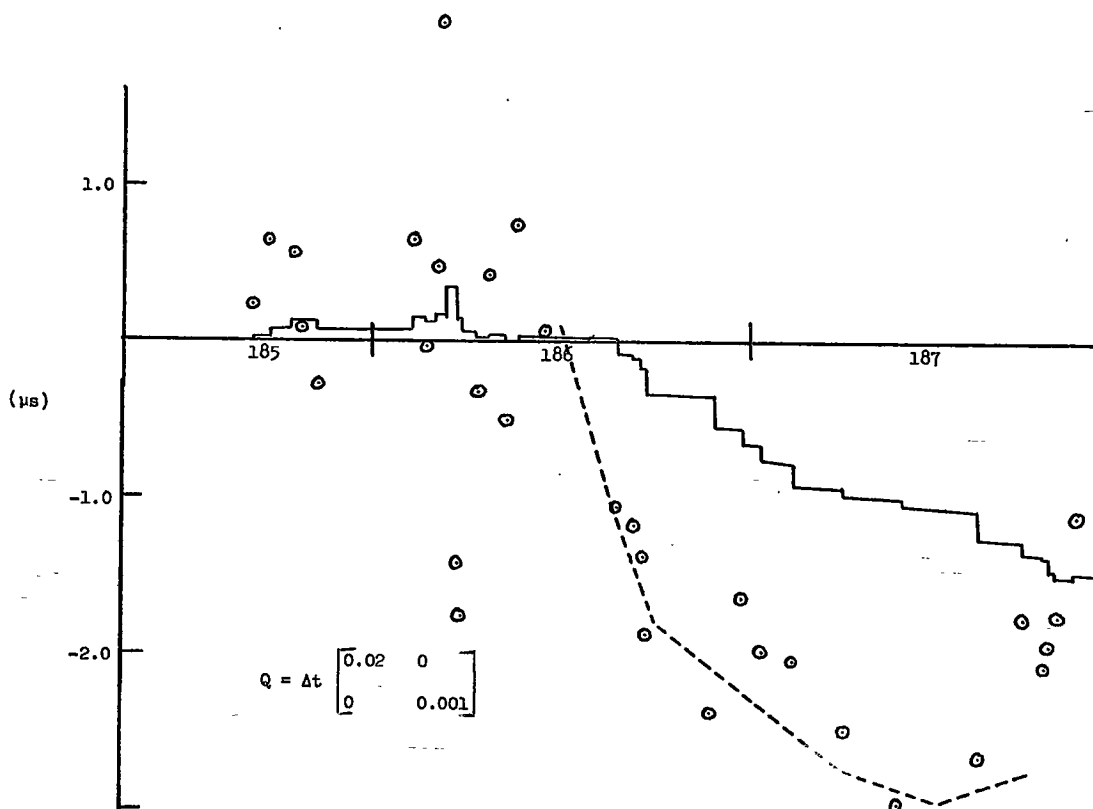


Figure 4.13. Correction to Cape Race Loran-C Range from Kalman Range Correction Filter

more robust.

The initial approximation used in the Least Squares Fix algorithm is the previous fix. Assuming that ships never travel faster than 100 km/hr (54 knots) it is reasonable to expect the next fix to be within  $100 \cdot \Delta t$  km of the previous fix where  $\Delta t$  is the time interval in hours since the last fix. It is also reasonable to expect the elements of the misclosure vector (i.e. the difference between the observed ranges and the ranges corresponding to the approximate position) to be less than  $100 \cdot \Delta t$  km. The approach used in LORSG is to terminate the fix calculation when any element of the misclosure vector is greater than 10 km. A better approach would be to use an expanding limit with time, as described above. A further improvement would be to set only the corresponding row of the design matrix equal to zero so that the offending range would be ignored in the fix calculation. However, with this approach, a check would be necessary to ensure that there are at least two independent range measurements so that a fix could be computed. Another alternative is to use the latest estimate of the ship's course and speed to predict the ship's position at the time of the next fix. The predicted estimate of the ship's position is used as the initial approximation for the fix calculation. A fixed limit is used to test the elements of the misclosure vector. This, in essence, is the procedure used as part of the Kalman Integration Filter described in the next chapter.

In the program LORSG the Kalman Range Correction Filter is made more robust by testing the difference between the observed and

predicted range correction. When the difference is larger than 3  $\mu$ s the observation is ignored.

## CHAPTER 5

### INTEGRATION OF LORAN-C, SHIP'S LOG, AND SHIP'S GYROCOMPASS

In the previous chapter a technique for integrating rho-rho Loran-C and Transit was described which gave continuous, accurate estimates of the ship's position. The key element was a linear Kalman filter that modelled the corrections to the Loran-C ranges from comparisons with Transit. Estimates of the vessel's velocity for use in the Transit fix calculation were assumed to be obtained from Loran-C. In Section 5.1 we consider the problem of determining the ship's velocity. In the absence of ship's log and gyrocompass observations the ship's velocity is found by computing the displacement vector between two Loran-C fixes and dividing by the time interval. Smoothed estimates are obtained by passing the course and speed data through a low pass digital filter. In Section 5.1.2 velocity estimates from ship's log and gyro are discussed. The significance of the fact that the log only measures the ship's velocity component relative to the water mass in the direction of the ship's heading is considered.

In Section 5.2 a different approach to the integration problem is taken. To this point the Kalman filter has only been used to compute corrections to observations which are then used in a simultaneous least squares procedure. In Section 5.2 the Kalman state vector elements consist of the unknown observer latitude and longitude, the observer's velocity components and the ocean current velocity.

### 5.1 Ship's Velocity from Loran-C and Ship's Log and Gyrocompass

Velocity estimates from Loran-C tend to be very noisy but have the advantage that they are relative to the earth's surface. Velocities from ship's log and gyrocompass, on the other hand, are smoother but have offsets due to the influence of winds and ocean currents. By combining these two types of data smoother estimates of the ship's velocity and estimates of the ocean current vector are possible.

#### 5.1.1 Ship's Velocity from Rho-rho Loran-C

Estimates of ship's course and speed are found from two Loran-C fixes ( $\phi_1, \lambda_1$ , and  $\phi_2, \lambda_2$ ) and the time interval  $\Delta t$  between them as follows:

$$\text{Course} = \arctan (\Delta\phi/\Delta\lambda\cos\phi) \quad (5.1)$$

$$\text{Speed} = \sqrt{(\Delta\phi \cdot a)^2 + (\Delta\lambda \cdot a \cdot \cos\phi)^2} \quad (5.2)$$

where

$$\Delta\phi = \phi_2 - \phi_1$$

$$\Delta\lambda = \lambda_2 - \lambda_1$$

$$a = \text{earth's radius}$$

$$\phi = (\phi_2 + \phi_1)/2$$

A plane earth approximation is used because the interval  $\Delta t$  between fixes is usually one minute (and is seldom longer than 10 minutes). At ship's speeds of 27 km/hr the error introduced by this assumption is less than 45 m.

To illustrate the accuracy of the velocity information obtained by this method the Loran-C data described in section 4.4.3 was processed

and courses and speeds between successive one-minute fixes were computed. A period during day 185 was selected when the ship was steering a steady course at a constant speed. Figure 5.1 shows the histograms of the courses and speeds obtained over a typical one-hour period. The means and standard deviations are also given. For comparison, Figure 5.2 shows the histograms of the one-minute ship's log and gyro observations collected during the same period. The Loran-C estimates are clearly inferior by almost an order of magnitude in the ship's course standard deviations. The 5% trimmed estimates are obtained by eliminating the highest 5% and lowest 5% of the observations prior to computing the statistics [Huber, 1972].

To obtain more useful results the Loran-C derived course (C) and speed (S) were separately filtered using a simple recursive low-pass digital filter of the form

$$\hat{C}_k = \hat{C}_{k-1} + K(C_k - \hat{C}_{k-1}) \quad (5.1)$$

$$\hat{S}_k = \hat{S}_{k-1} + K(S_k - \hat{S}_{k-1}) \quad (5.2)$$

where  $K = 1 - e^{-(\Delta t/\beta)}$  (5.3)

$\Delta t$  = time interval between fixes

$\beta$  = time constant

and the caps denote filtered estimates. Figure 5.3 shows histograms of the filtered Loran-C velocity components for  $\beta = 3.3$  minutes and  $\beta = 10$  minutes. However, you never get something for nothing. The smoother estimates of the velocities given by the filter during periods

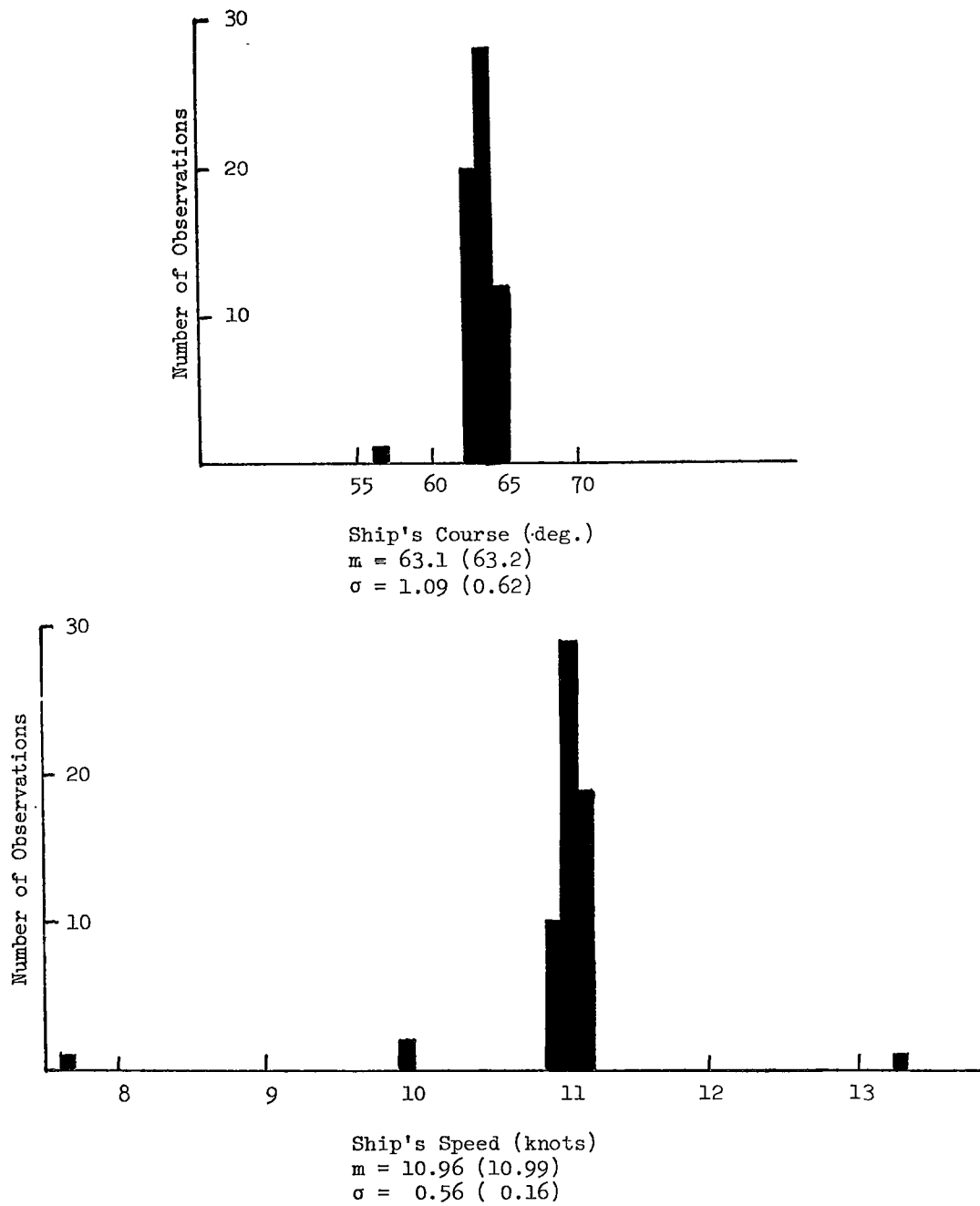
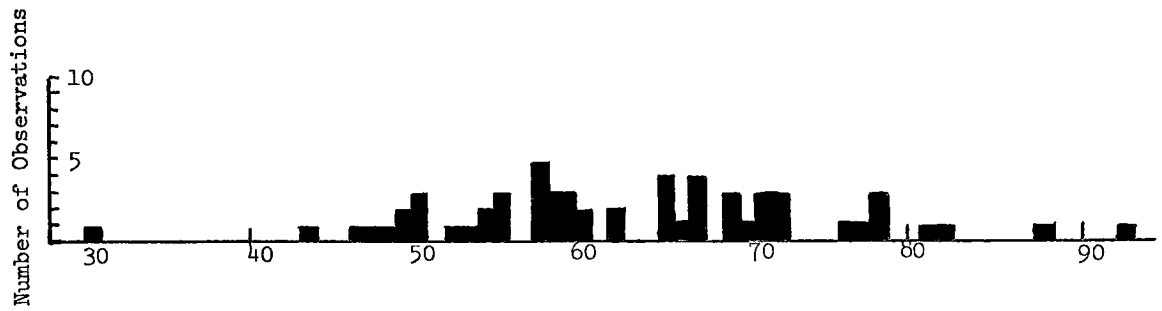
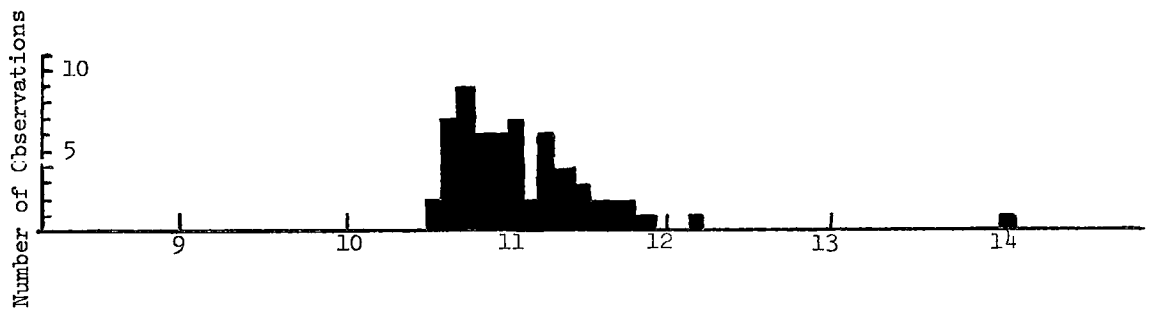


Figure 5.2. Histograms of ship's courses and speeds from one-minute log/gyro readings. (Values in brackets are 5% trimmed estimates.)

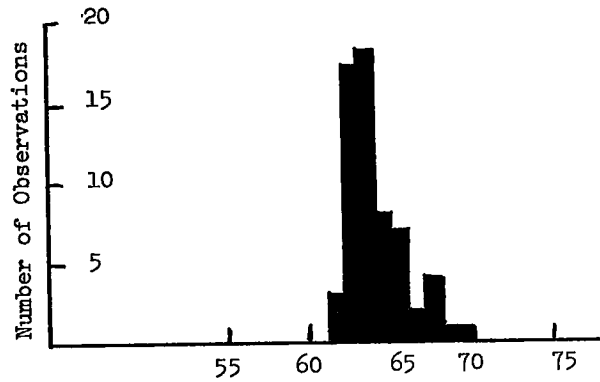


Ship's course (deg.)  
 $m = 63.0$  (62.6)  
 $\sigma = 11.6$  (9.19)

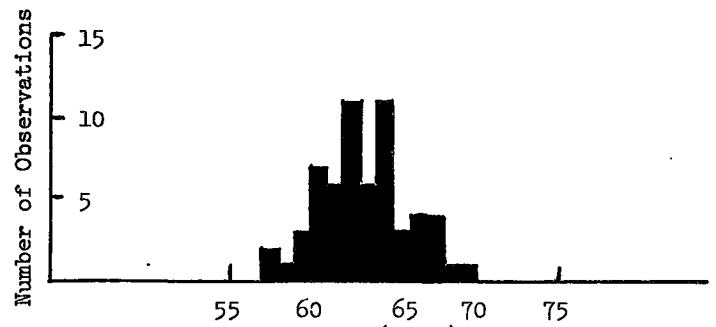


Ship's speed (knots)  
 $m = 11.1$  (11.0)  
 $\sigma = 0.53$  (0.32)

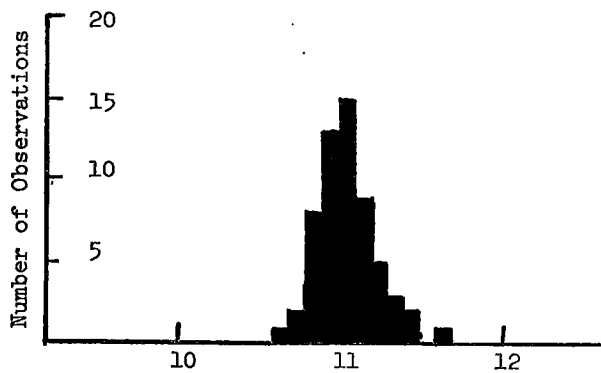
Figure 5.1. Histograms of ship's courses and speeds between one-minute Loran-C fixes. (Values in brackets are 5% trimmed estimates.)



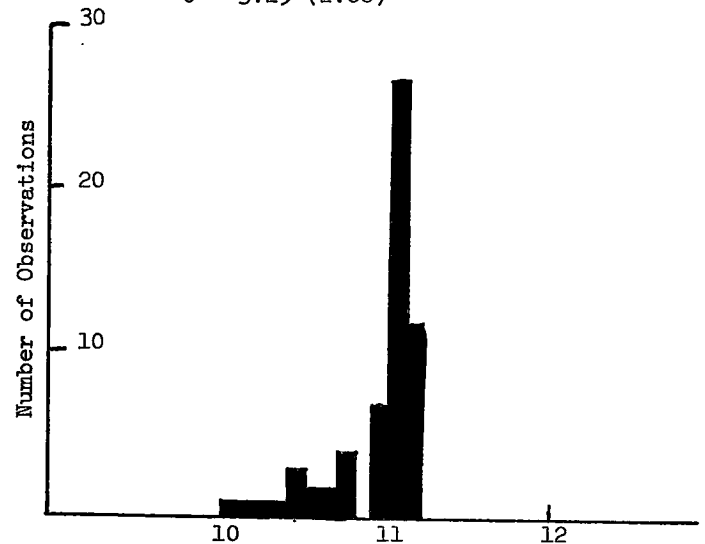
Ship's course (deg.)  
 $m = 63.1$  (63.0)  
 $\sigma = 0.94$  (0.79)



Ship's Course (deg.)  
 $m = 63.0$  (63.0)  
 $\sigma = 3.25$  (2.88)



Ship's speed (knots)  
 $m = 11.0$  (11.)  
 $\sigma = 0.35$  (0.26)



Ship's speed (knots)  
 $m = 11.0$  (11.0)  
 $\sigma = 0.11$  (0.09)

Figure 5.3. Histograms of ship's courses and speeds obtained by filtering one-minute Loran-C velocities. Left side:  $\beta = 3.3$  minutes; Right side:  $\beta = 10$  minutes. (Values in brackets are 5% trimmed estimates.)

when the ship is maintaining a steady course and speed are obtained at the expense of large errors when the ship is maneuvering. This is illustrated by Figure 5.4 which shows the ship's heading as determined by gyrocompass, raw one-minute Loran-C courses, and filtered Loran-C courses during an  $18^\circ$  alteration in course.

#### 5.1.2 Velocity from Ship's Log and Gyrocompass

It is evident from the preceding section that over a given time interval ship's log and gyro are much smoother estimators of ship's velocity than estimates from Loran-C. However, log and gyrocompass observations have biases due to the influence of both wind and ocean currents.

A single axis ship's log only measures the component of ship's velocity in the direction the ship is pointing. Frequently due to wind effects the ship moves through the water at an angle relative to the ship's heading (see Figure 5.5). The displacement vector of the ship after a period of time is therefore the sum of the displacement measured by the ship's log and gyro plus the displacement caused by the wind. The influence of the wind on a ship is a complicated function of the shapes of the hull and superstructure, the relative direction and speed of the wind, and the ship's velocity. If the influence of the wind can be determined, the displacement of the ship with respect to the water mass can be computed by adding the vectors  $\bar{S}$  and  $\bar{W}$  shown in Figure 5.6. If the water mass is moving relative to the surface of the earth the displacement of the ship after some time interval is illustrated by Figure 5.6.

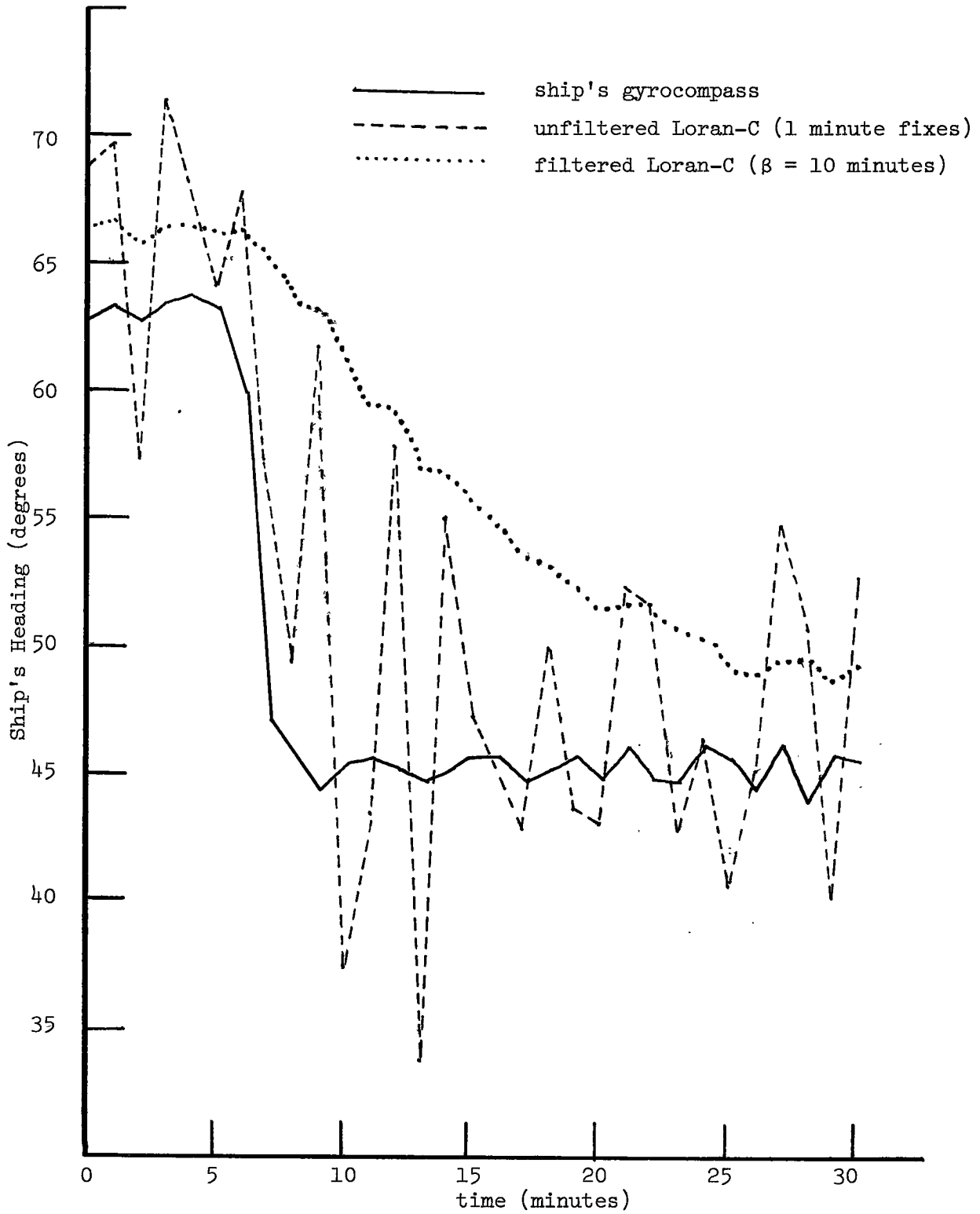


Figure 5.4. Ship's Heading During Course Alteration

An indication of the size and variation of the combined wind/current vector is given by Table 5.1. This table was constructed from the data described in Section 4.4.5 by taking the vector differences between the one-hour mean velocities obtained from Loran-C and ship's log and gyro.

A simple linear Kalman filter similar in form to the Kalman Range Correction Filter could be derived to estimate the wind/current displacement vector.

## 5.2 Kalman Integration Filter

The approach thus far has been to use observations from one sensor with short term noise but no biases or trends to determine corrections to observations from another sensor that is stable over the short term but which may have bias errors and trends. In effect, the Kalman filter has been used as a low-pass filter. The flow of information has been from the sensor with good long term stability to the sensor with poor long term stability, but not *vice versa*. The filter proposed in this section remedies this situation by using the Kalman filter to estimate the unknown ship's position and velocity directly from rho-rho Loran-C and ship's log and gyro observations. The alternative suggested in the last section was to use the Kalman filter to simply estimate corrections to the ship's velocity components.

It is expected that the smoothness of the ship's log and gyro velocity observations will propagate through the filter to make the positions obtained from the filter more stable relative to each other.

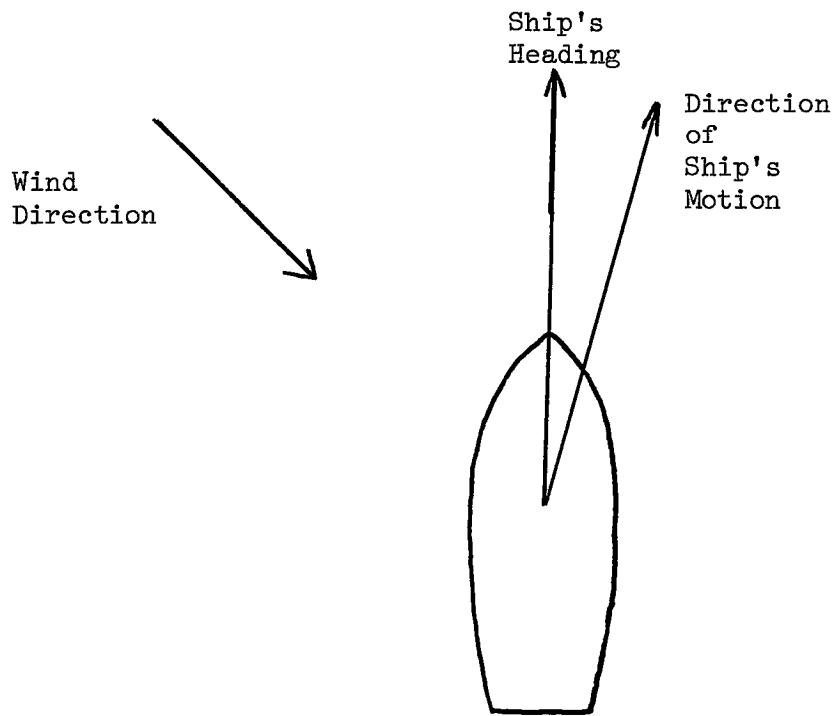


Figure 5.5

Direction of Ship's Motion due to  
Wind Forces

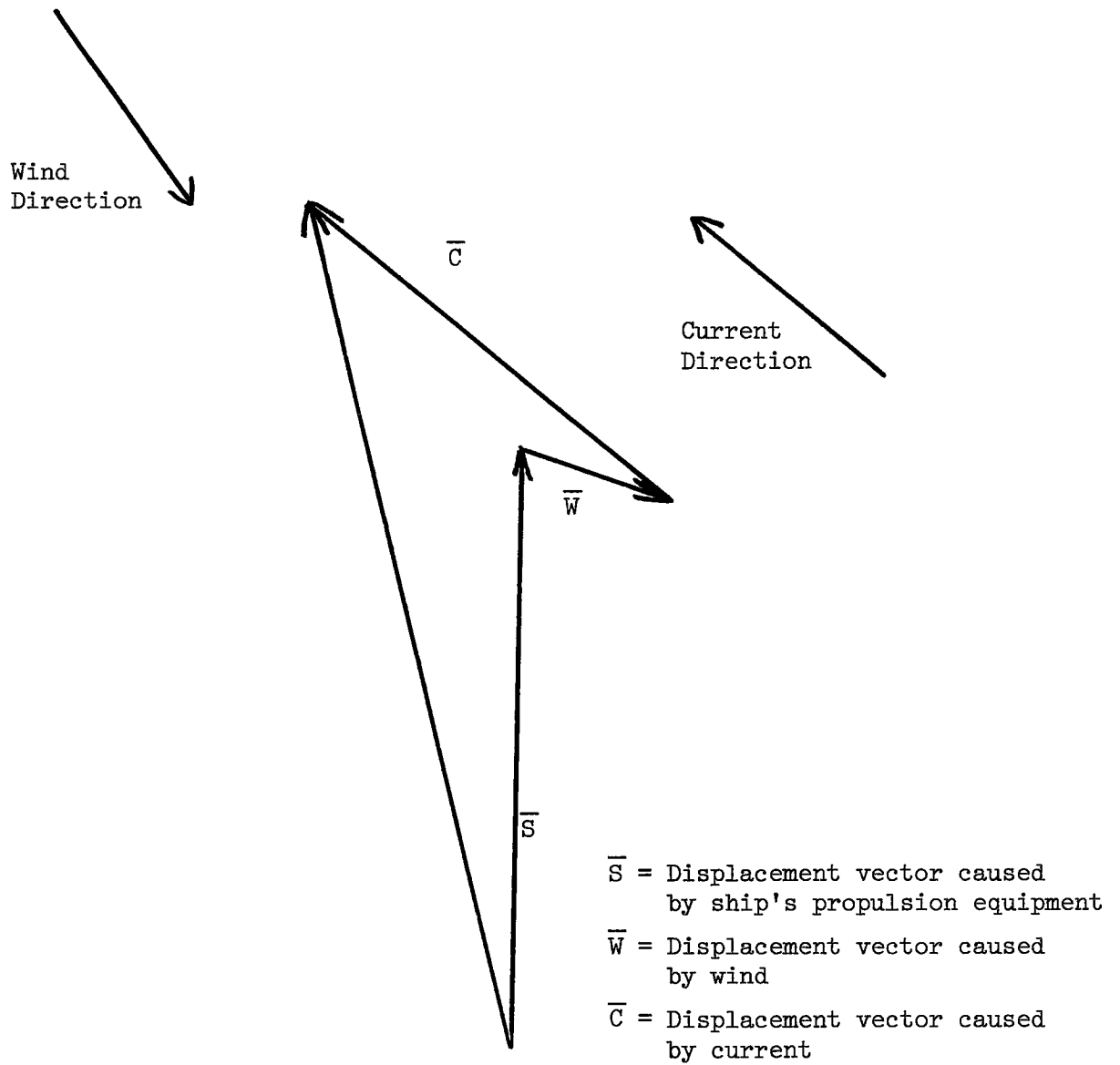


Figure 5.6. Ship's displacement vector in the presence of wind and current

Table 5.1

COMBINED WIND/CURRENT VECTOR DERIVED FROM VECTOR  
DIFFERENCE BETWEEN LORAN-C AND LOG/GYRO

Time	Loran-C		Log/Gyro		Wind/Current	
	Course (deg)	Speed (knots)	Course (deg)	Speed (knots)	Direction (deg)	Speed (knots)
1630/1730	62.64	11.0	63.22	10.99	328	0.1
1730/1830	63.46	11.12	63.04	11.06	117	0.1
1830/1930	63.63	11.15	62.91	11.06	120	0.2
1930/2030	65.08	11.32	63.09	11.09	123	0.4
2030/2130	65.69	11.19	63.11	11.10	144	0.6
2300/2400	49.37	11.18	45.28	11.14	134	0.8

In effect, with this approach, the information also flows from the sensor with good short term stability to the sensor with poor short term stability.

The complete integration of Loran-C and Transit in the sense just described for Loran-C, ship's log and gyro is not considered in this study.

### 5.2.1 Kalman Integration Filter Equations

The state vector in the Kalman Integration Filter consists of the six elements: ship's latitude  $\phi$  and longitude  $\lambda$ , north and east components of ship's velocity  $V_{NS}$  and  $V_{ES}$  and north and east components of ocean current velocity  $V_{NC}$  and  $V_{EC}$ . All velocities are relative to the earth's surface. The ocean current velocity components  $V_{NC}$  and  $V_{EC}$  are only good estimators of the true ocean current velocity in the absence of wind effects.  $\phi$  and  $\lambda$  are in radians and all velocities are in km/hr. Assuming that the ship's velocity and the ocean current do not change from time  $t_{k-1}$  to time  $t_k$  the state transition equation is

$$\hat{X}_{k/k-1} = F \cdot \hat{X}_k \quad (5.1)$$

or, written out in full,

$$\begin{bmatrix} \phi \\ \lambda \\ V_{NS} \\ V_{ES} \\ V_{NC} \\ V_{EC} \end{bmatrix}_k = \begin{bmatrix} 1 & 0 & \Delta t/a & 0 & 0 & 0 \\ 0 & 1 & 0 & \Delta t/a \cdot \cos \phi & 0 & 0 \\ 0 & 0 & 1 & 0 & 0 & 0 \\ 0 & 0 & 0 & 1 & 0 & 0 \\ 0 & 0 & 0 & 0 & 1 & 0 \\ 0 & 0 & 0 & 0 & 0 & 1 \end{bmatrix} \cdot \begin{bmatrix} \phi \\ \lambda \\ V_{NS} \\ V_{ES} \\ V_{NC} \\ V_{EC} \end{bmatrix}_{k-1}$$

where  $\Delta t = t_k - t_{k-1}$  and  $a$  is the semi-major axis of the reference ellipsoid in kilometres. The plane earth approximation used here introduces an error of less than one metre over a prediction interval of one minute.

The observations in this example consist of up to four Loran-C ranges, four rates of change of the Loran-C ranges, ship's course from gyro and ship's speed from log. The rates of change of the Loran-C ranges are obtained by computing the differences between the ranges at the last observation instant and the ranges at the current observation time and dividing the range differences by the time interval. The observation equation relating the latitude and longitude to the Loran-C range observation is given by 4.5. The equations relating the ship and current velocity components to the ship's gyro heading  $\theta$  in radians and ship's log speed  $V$  in km/hr are

$$\theta = \arctan (\Delta V_N / \Delta V_E) \quad (5.2)$$

$$V = \sqrt{\Delta V_N^2 + \Delta V_E^2} \quad (5.3)$$

$$\text{where } \Delta V_N = (V_{NS} - V_{NC}) \quad (5.4)$$

$$\Delta V_E = (V_{ES} - V_{EC}) \quad (5.5)$$

The equation relating the rates of change of the Loran-C ranges to the ship's velocity components is obtained by differentiating the spherical part of Equation 4.5 with respect to time to get

$$\frac{dV_i}{dt} = \dot{V}_i = \frac{dV_i}{d\phi} \cdot \frac{d\phi}{dt} + \frac{dV_i}{d\lambda} \cdot \frac{d\lambda}{dt} = \frac{dV_i}{d\lambda} \cdot V_{NS} + \frac{dV_i}{d\lambda} \cdot V_{ES} \quad (5.6)$$

where  $dV_i/d\phi$  and  $dV_i/d\lambda$  are given by 4.9 and 4.10.

The Jacobian matrix H needed in the Kalman filter Equations 3.21 is obtained by taking partial derivatives of the observation Equations 4.5, 5.2, 5.3, and 5.6 with respect to the state vector elements to obtain

$$\begin{aligned}
 H = & \left[ \begin{array}{cccccc}
 \frac{\partial V_1}{\partial \phi} & \frac{V_1}{\partial \lambda} & 0 & 0 & 0 & 0 \\
 \frac{\partial r_2}{\partial \phi} & \frac{\partial r_2}{\partial \lambda} & 0 & 0 & 0 & 0 \\
 \frac{\partial r_3}{\partial \phi} & \frac{\partial r_3}{\partial \lambda} & 0 & 0 & 0 & 0 \\
 \frac{\partial r_4}{\partial \phi} & \frac{\partial r_4}{\partial \lambda} & 0 & 0 & 0 & 0 \\
 0 & 0 & \frac{\partial \dot{r}_1}{\partial V_{NS}} & \frac{\partial \dot{r}_1}{\partial V_{ES}} & 0 & 0 \\
 0 & 0 & \frac{\partial \dot{r}_2}{\partial V_{NS}} & \frac{\partial \dot{r}_2}{\partial V_{ES}} & 0 & 0 \\
 0 & 0 & \frac{\partial \dot{r}_3}{\partial V_{NS}} & \frac{\partial \dot{r}_3}{\partial V_{ES}} & 0 & 0 \\
 0 & 0 & \frac{\partial \dot{r}_4}{\partial V_{NS}} & \frac{\partial \dot{r}_4}{\partial V_{ES}} & 0 & 0 \\
 0 & 0 & \frac{\partial \theta}{\partial V_{NS}} & \frac{\partial \theta}{\partial V_{ES}} & \frac{\partial \theta}{\partial V_{NC}} & \frac{\partial \theta}{\partial V_{EC}} \\
 0 & 0 & \frac{\partial V}{\partial V_{NS}} & \frac{\partial V}{\partial V_{ES}} & \frac{\partial V}{\partial V_{NC}} & \frac{\partial V}{\partial V_{EC}}
 \end{array} \right] \quad (5.7)
 \end{aligned}$$

$\partial r_i / \partial \phi$  and  $\partial r_i / \partial \lambda$  are given by 4.9 and 4.10.  $\partial \dot{r}_i / \partial V_{NS}$  and  $\partial \dot{r}_i / \partial V_{ES}$  are obtained by differentiating 5.6 with respect to  $V_{NS}$  and  $V_{ES}$  respectively to obtain

$$\frac{\partial \dot{r}_i}{\partial V_{NS}} = \frac{\partial r_i}{\partial \phi} \quad (5.8)$$

$$\frac{\partial \dot{r}_i}{\partial V_{ES}} = \frac{\partial r_i}{\partial \lambda} \quad (5.9)$$

The remaining terms in H are

$$\frac{\partial \theta}{\partial V_{NS}} = \Delta V_E / (\Delta V_N^2 + \Delta V_E^2) \quad (5.10)$$

$$\frac{\partial V}{\partial V_{NS}} = \Delta V_N / \sqrt{\Delta V_N^2 + \Delta V_E^2} \quad (5.11)$$

$$\frac{\partial \theta}{\partial V_{ES}} = -\Delta V_N / (\Delta V_N^2 + \Delta V_E^2) \quad (5.12)$$

$$\frac{\partial V}{\partial V_{ES}} = \Delta V_E / \sqrt{\Delta V_N^2 + \Delta V_E^2} \quad (5.13)$$

and

$$\frac{\partial \theta}{\partial V_{NC}} = -\frac{\partial \theta}{\partial V_{NS}}, \quad \frac{\partial V}{\partial V_{NC}} = -\frac{\partial V}{\partial V_{NS}}$$

$$\frac{\partial \theta}{\partial V_{EC}} = -\frac{\partial \theta}{\partial V_{ES}}, \quad \frac{\partial V}{\partial V_{EC}} = -\frac{\partial V}{\partial V_{ES}}$$

Except for starting estimates for the state vector elements and the three covariance matrices R, Q, and P all the components of the Kalman filter equations are completely specified.

## CHAPTER 6

DISCUSSION AND CONCLUSIONS

In Section 6.1 the results presented in Chapters 4 and 5 are summarized and discussed. Several suggestions for future work are given in Section 6.2.

6.1 Discussion of Results

The first task in applying a Kalman filter is designing the system dynamics model and the observation model and deciding what are to be the state vector elements. It is then necessary to determine:

- (a) the initial estimate of the state vector,  $\hat{X}_0$
- (b) the initial state covariance matrix,  $P_0$
- (c) the model for the observation covariance matrix,  $R$
- (d) the model for the state transition covariance matrix,  $Q$

In Chapter 4 a procedure for integrating Transit and Loran-C, called the Kalman Range Correction Filter, is described and tested. The Kalman Range Correction Filter estimates the corrections to the Loran-C ranges to compensate for the errors that result from the lack of synchronization between the transmitter and receiver atomic clocks. The observations consist of the differences between the observed Loran-C ranges and the theoretical ranges computed from Transit fixes. Ship's positions are computed from the corrected Loran-C ranges by a least squares estimation technique. Ship's velocities are determined from the displacement vector and time interval between two Loran-C fixes.

Section 4.4.4 deals with the problem of determining initial estimates of the state vector and state covariance matrix. Essentially, the procedure consists of recording the Loran-C ranges for a few days at a known point. Estimates of the rate of change of the ranges with time and a synchronization correction are computed by the method of least squares. An estimated state covariance matrix is also determined. The importance of using a large variance in the initial state covariance matrix corresponding to elements of the state vector that are not accurately known is demonstrated.

In Section 4.4.2 the model for determining the observation covariance matrix  $R$  is described. Since the observation vector consists of a single element,  $R$  is a single variance element.  $R$  is determined from the sum of the variances due to Loran-C and Transit. The Loran-C range variance is assumed to be a function of range and is computed by means of a polynomial in range. This approach is simple and reliable but neglects disturbances (e.g. meteorological) that are not range dependent. An improved approach might be to use the receiver gain or the signal-to-noise ratio in addition to the range in a more sophisticated model.

The contribution to the observation variance from Transit is determined from the Transit fix covariance matrix by the covariance law. The Transit fix covariance matrix is determined by a table look-up procedure. This approach is necessary because the Transit fix software is inaccessible and does not compute a fix covariance matrix. The Kalman Range Correction Filter would be improved if an estimated

Transit fix covariance matrix was computed with each fix.

The state transition covariance matrix  $Q$  is described in Section 4.4.3 and again in Section 4.4.5. For simplicity, it is assumed to be a time-dependent diagonal matrix although in Section 4.4.5 it is mentioned that it would be better if it could be changed by the operator. The influence of  $Q$  on the output of the Kalman Range Correction Filter was shown in Section 4.4.5 to be quite small.

In Chapter 5 the accuracies of ship's velocities determined by log and gyro and Loran-C are analyzed and a proposed model to fully integrate Loran-C, log and gyro is described. The velocity analysis shows that:

- (a) log and gyro velocities are smoother than unfiltered Loran-C velocities,
- (b) filtered Loran-C velocities approach the smoothness of log and gyro velocities but exhibit large errors during changes of course or speed,
- (c) log and gyro velocities have biases due to the combined effect of winds and currents,
- (d) Loran-C velocities are independent of the effects of winds or currents.

The proposed Kalman Integration Filter is designed to use the smoothness of the log and gyro velocities and the absolute accuracy of the Loran-C velocities.

## 6.2 Suggestions for Future Work

It is recommended that:

- (a) more sophisticated models be developed for computing the observation covariance matrix and the state transition covariance matrix in the Kalman Range Correction Filter;
- (b) more accurate long line formulae be used in the Loran-C Least Squares Fix routine, when computer memory permits;
- (c) a Transit fix covariance be computed routinely with each fix;
- (d) the Transit fix and the fix covariance matrix be presented automatically to the Kalman Range Correction Filter obviating the need for operator intervention;
- (e) work continue on developing the Kalman Integration Filter.

REFERENCES

- Admiralty Manual of Seamanship, Vol. 3, 1964.
- Anderson, F.W. (1966), "The Principles of Navigation," Hollis and Carter, London.
- Beukers, J.M. (1974), "A Review and Applications of VLF and LF Transmissions for Navigation and Tracking," Journal of the Institute of Navigation, Vol. 21, No. 2.
- Bigelow, H.W. (1965), "Electronic Surveying: Accuracy of Electronic Positioning Systems." Supplement to the International Hydrographic Review, Vol. 6.
- Black, H.D., R.E. Jenkins and L.L. Pryor (1975), "The Transit System, 1975." The Johns Hopkins University, Applied Physics Laboratory, Laurel, Maryland, U.S.A.
- Bomford, G. (1971), "Geodesy," Oxford University Press, London.
- Bowditch (1962), "American Practical Navigator." U.S. Navy Hydrographic Office Special Publication No. 9.
- Brown, R.G. (1973), "Integrated Navigation Systems and Kalman Filtering: A Perspective," Navigation, Vol. 19, No. 1.
- Brunavs, P. and D.E. Wells (1971), "Accurate Phase Lag Measurements over Seawater using Decca Lambda," A.O.L. Report 1971-2, Bedford Institute of Oceanography, Dartmouth, Nova Scotia.
- Bryant, R.S. (1973), "Great Lakes Loran-C," Technical Report, Canadian Hydrographic Service, Canada Centre for Inland Waters, Burlington, Ontario.
- Bryant, R., R.M. Eaton and S. Grant (1974), "Rho-rho Loran-C for Precise Long-Range Positioning Inland and At Sea," International Congress of Surveying, Washington, D.C.

- Digital Equipment Corporation (1972), "Programming Languages,"  
PDP-8 Handbook Series.
- Doherty, R.H. (1974), "Spatial and Temporal Electrical Properties  
Dervied from LF Pulse Ground WAVE Propagation Measurements,"  
Presented at the Technical Meeting of the Electromagnetic Wave  
Propagation Panel of AGARD-NATO, Netherlands.
- Eaton, R.M. and S.T. Grant (1972), "Rho-rho Loran-C for Offshore Surveys,"  
The Canadian Surveyor, Vol. 26, No. 2.
- Eaton, R.M. (1974), "Cruise Report, CSS Maxwell 74-010," Bedford  
Institute of Oceanography, Dartmouth, Nova Scotia.
- Eaton, R.M. (1975), "Tests of Loran-C Performance," Canadian  
Aeronautics and Space Journal, Vol. 21, No. 4.
- Eaton, R.M. (1975), "Loran-C Compared with Other Navigation Aids in  
Meeting Future Canadian Needs," Canadian Aeronautics and Space  
Journal, Vol. 21, No. 4.
- Eaton, R.M., D.E. Wells and N. Stuijbergen (1976), "Satellite Naviga-  
tion in Hydrography," Paper submitted for publication in  
International Hydrographic Review.
- Gill, T.P. (1965), "The Doppler Effect," Academic Press, London.
- Gold, B. and C.M. Rader (1969), "Digital Processing of Signals,"  
McGraw-Hill Book Co., Toronto, Ontario.
- Grant, S.T. (1973), "Rho-rho Loran-C Combined with Satellite Naviga-  
tion for Offshore Surveys," International Hydrographic  
Review, Vol. L, No. 2.
- Grant, S.T. and C. Chamberlain (1974), "Sequential Smoothing and  
Prediction." Unpublished Report, University of New Brunswick,  
Department of Surveying Engineering.

- Griswold, L.W. (1968), "Underwater Logs," Navigation, Vol. 15, No. 2.
- Hagglund, J. (1973), "Investigation of Additional Secondary Phase Lag at 100 kHz Due to Overland Path," Unpublished Report, Bedford Institute of Oceanography, Dartmouth, Nova Scotia.
- Halamandaris, H. and D. Ozdes (1970), "A Kalman Filter Augmented Marine Navigation System," AGARD 139 'Theory and Applications of Kalman Filtering.'
- Hamilton, W.C. (1964), "Statistics in Physical Science," The Ronald Press Co., New York, N.Y.
- Hatch, R.R. and J.J. Winterhalter (1974), "Differential Loran-C in Integrated Marine Navigation Systems," Presented at the International Symposium on Marine Geodesy, Columbus, Ohio.
- Heiskanen, W.A. and H. Mortiz (1967), "Physical Geodesy," W.H. Freeman and Co., San Francisco, Calif.
- Huber, P.J. (1972), "Robust Statistics: A Review," The 1972 Wald Lecture, The Annals of Mathematical Statistics, Vol. 43, No. 4, 1041-1067.
- International Hydrographic Bureau (1965), "Radio Aids to Marine Navigation and Hydrography," Special Publication No. 39 (2nd edition), Monaco.
- Johler, J.R., W.J. Keller and L.C. Walters (1946), "Phase of the Low Radiofrequency Ground Wave," National Bureau of Standards Circular 573.
- Johler, J.R. (1962), "Propagation of the Low-Frequency Radio Signal," Proceedings of the I.R.E., Vol. 50, 404.
- Kalman, R.E. (1960), "A New Approach to Linear Filtering and Prediction Problems," Journal of Basic Engineering, Vol. 82N, No. 1.

- Kalman, R.E. and R.S. Bucy (1961), "New Results in Linear Filtering and Prediction Theory," Journal of Basic Engineering, Vol. 83D.
- Krakiwsky, E.J. and D.E. Wells (1971), "Mathematical Models for Positioning by Satellite," University of New Brunswick, Dept. of Surveying Engineering Lecture Notes No. 17.
- Krakiwsky, E.J. and D.E. Wells (1971), "Coordinate Systems in Geodesy," University of New Brunswick, Dept. of Surveying Engineering Lecture Notes No. 16.
- Krakiwsky, E.J., D.E. Wells and P. Kirkham (1972), "Geodetic Control from Doppler Satellite Observations," (The Canadian Surveyor, Vol. 26, No. 2.
- Krakiwsky, E.J. and D.B. Thomson (1974), "Geodetic Position Computations," University of New Brunswick, Dept. of Surveying Engineering Lecture Notes No. 39.
- Krakiwsky, E.J. (1975), "A Synthesis of Recent Advances in the Method of Least Squares," University of New Brunswick, Dept. of Surveying Engineering, Lecture Notes No. 42.
- Liebelt, P.B. (1967), "An Introduction to Optimal Estimation," Addison-Wesley Publishing Company Inc., Don Mills, Ontario.
- Marchal, A.W. (1971), "Loran-C in the Rho-Rho Mode," Undersea Technology, April.
- Millington, G. (1949), "Ground Wave Propagation Over an Inhomogeneous Smooth Earth," Proc. Inst. Elec. Eng., Vol. 96, Pt. III.
- Morrison, N. (1969), "Introduction to Sequential Smoothing and Prediction," McGraw-Hill Book Co., Toronto, Ontario.

- Pakos, P.E. (1969), "Use of the Loran-C System for Time and Frequency Dissemination," *Frequency Technology*, July.
- Potts, C.E. and B. Wieder (1972), "Precise Time and Frequency Dissemination via the Loran-C System," *Proceedings of the IEEE*, Vol. 60, No. 5.
- Powell, C. and A.R. Woods (1967), "Loran-C, A Practical Introduction to the Operation and Performance of the System," Supplement to the *International Hydrographic Review*, Vol. 7.
- Reid, D.B. and R.K. Harman (1974), "Optimal Filtering and Smoothing of Navigation Sensor Data for Resource Exploration and Development," Presented at the Canadian Aeronautics and Space Institute First Canadian Symposium on Navigation and Resources Management.
- Roland, W.F. (1973), "Loran-C - A Decade to Maturity: 1963-1973." Presented at I.O.N. National Radio Navigation Symposium, Washington, D.C.
- Savet, P.H. (1961), "Gyroscopes: Theory and Design," McGraw-Hill Book Co., Toronto, Ontario.
- Sluiter, P.G. (1969), "Relative Weighting of Satellite Fixes," *Proceedings Second Symposium on Marine Geodesy 1969*.
- Sorenson, H.W. (1966), "Kalman Filtering Techniques," *Control and Dynamic Systems, Advances in Theory and Applications*, Vol. 3, Academic Press, New York, N.Y.
- Sorenson, H.W. and A.R. Stubberud (1970), "Linear Estimation Theory," AGARD 139 "Theory and Applications of Kalman Filtering."
- Stansell, T.A. (1968), "The Navy Navigation Satellite System: Description and Status," *Navigation*, Vol. 15, No. 3.

- Stuifbergen, N. (1974), "Satellite Navigation with Doppler Sonar,"  
 Technical Report, Canadian Hydrographic Service, Bedford  
 Institute of Oceanography, Dartmouth, Nova Scotia.
- Thomas, P.D. (1965), "Mathematical Models for Navigation Systems,"  
 Technical Report No. 185, U.S. Naval Oceanographic Office.
- Tucker, M.J., N.D. Smith, E.E. Pierce and E.P. Collins (1970), "A  
 Two-Component Electromagnetic Ship's Log," Journal of the  
 Institute of Navigation (Brit.), Vol. 23, No. 3.
- U.S. Department of Transportation (1970), "National Plan for Navigation."
- Vaníček, P. and D.E. Wells (1972), "The Least-Squares Approximation  
 and Related Topics," University of New Brunswick, Dept. of  
 Surveying Engineering Lecture Notes No. 22.
- Vaníček, P. (1973), "Introduction to Adjustment Calculus (second  
 edition)," University of New Brunswick, Dept. of Surveying  
 Engineering Lecture Notes No. 35.
- Walker, A.S. (1974), "Introductory Review of Time Series Analysis,  
 with Emphasis on Simple Digital Filters," Unpublished Report,  
 University of New Brunswick, Dept. of Surveying Engineering.
- Wells, D.E. and D.I. Ross (1969), "Experience with Satellite Naviga-  
 tion Equipment During Summer 1968," AOL Report 1969- $\phi$ , Bedford  
 Institute of Oceanography, Dartmouth, Nova Scotia.
- Wells, D.E. and E.J. Krakiwsky (1971), "The Method of Least Squares,"  
 University of New Brunswick, Dept. of Surveying Engineering.

## APPENDIX I

TRANSIT COVARIANCE MATRIX

In this appendix a computer program is described that computes a Transit fix covariance matrix. The results produced by this program agree with those found by Sluiter (1969) and confirm (a) the Transit accuracy estimates in Table 4.1 and (b) the statements about Transit accuracy in Section 2.4.

The model used in this program is illustrated in Figure I-1. The satellite is assumed to move parallel to the plane earth's surface at an altitude of 1000 km in either the positive (north) or negative (south) x direction at a velocity of 440 km/min. It is also assumed that there are no missing Doppler measurements during the pass (i.e., no 'holes'). The parameters needed by the program are:

1. number of 30 s Dopplers before pass centre,
2. number of 30 s Dopplers after pass centre,
3. maximum elevation,
4. satellite direction of travel (north or south),
5. satellite track relative to observer (east or west),
6. velocity north/velocity east covariance matrix.

The model relating the doppler counts  $N_i$  with the unknowns  $\Delta f$ ,  $x$ ,  $y$  is

$$\Delta f \cdot \Delta t + \frac{f_0}{c} \Delta S_i - N_i = 0 \quad (\text{I.1})$$

$\Delta t$  is the integration time interval which in this case is 30 s,

$\Delta S_i$  is the difference in distance from the observer to two consecutive

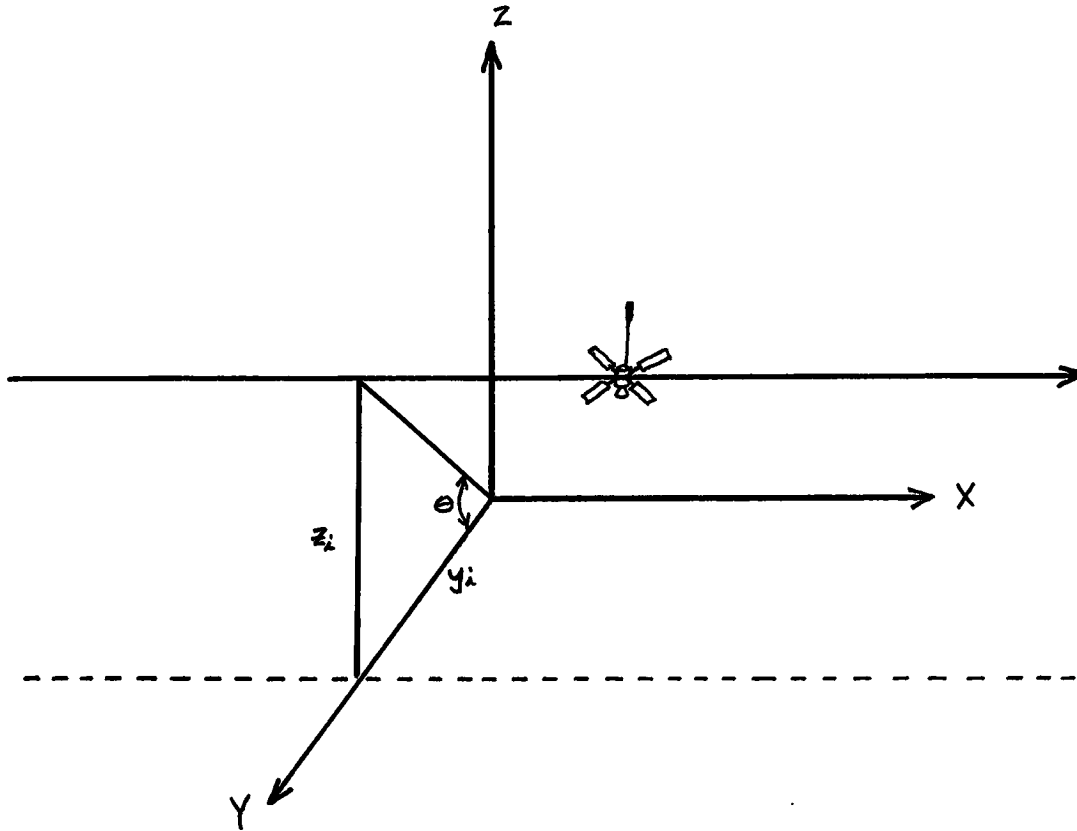


Figure I-1. Model for Transit Covariance Program

satellite positions  $i$  and  $i+1$

$$\Delta S_i = \sqrt{(x-x_i)^2 + (y-y_i)^2 + (z-z_i)^2} - \sqrt{(x-x_{i-1})^2 + (y-y_{i+1})^2 + (z-z_{i+1})^2} \quad (I.2)$$

The observer is assumed to be stationary at the origin so that

$x = y = z = 0$  and by assumption  $z_i = 1000$  km for all  $i$ .

From Figure I.1

$$y_i = 1000/\tan\theta \quad (I.3)$$

for a satellite to the east of the observer and

$$y_i = -1000/\tan\theta \quad (I.4)$$

if the satellite is to the west of the observer where  $\theta$  is the maximum elevation the satellite reaches during the pass.  $x_i$  are determined by

$$x_i = 220 \cdot i \quad (I.5)$$

where  $i$  ranges from  $-N_1$  to  $N_2$  where  $N_1$  and  $N_2$  are the number of doppler counts before and after pass centre respectively. For a south-going satellite,  $i$  goes from  $-N_2$  to  $N_1$ .

The usual least squares pre-analysis technique is used [Wells and Krakisky, 1971]. This is, if there is a linearized relationship

between the observations  $L$  (Doppler counts) and the unknowns  $X$  (observer coordinates and frequency offset), of the form

$$L = A \cdot X \quad (\text{I.6})$$

then the relationship between the observation covariance matrix  $\Sigma_L$  and the unknown covariance matrix  $\Sigma_X$  is

$$\Sigma_X = (A \Sigma_L^{-1} A^T)^{-1} \quad (\text{I.7})$$

where  $A_i = (a_{i1} \ a_{i2} \ a_{i3})$  (I.8)

$$a_{i1} = \Delta t \quad (\text{I.9})$$

$$a_{i2} = - \frac{f_0}{c} \frac{x_{i-1} - x_i}{v_{i-1} - v_i} \quad (\text{I.10})$$

$$a_{i3} = - \frac{f_0}{c} \frac{y_{i-1} - y_i}{v_{i-1} - v_i} \quad (\text{I.11})$$

For this program the observation covariance matrix is assumed to be diagonal with each diagonal element being found from

$$\sigma_{N_i}^2 = \sigma_{N_0}^2 + \sigma_{N_v}^2 \quad (\text{I.12})$$

where  $\sigma_{N_0}^2$  is a constant Doppler measurement noise term and  $\sigma_{N_v}^2$  is the additional noise in the Doppler measurement contributed by the errors in the vessel's estimated velocity. The covariance law is used to find  $\sigma_{N_v}^2$  from the velocity north/velocity east covariance matrix  $\Sigma_v$

$$\sigma_{N_v}^2 = B \Sigma_v B^T = b_{11}^2 \sigma_{VN}^2 + b_{12}^2 \sigma_{VE}^2 \quad (I.13)$$

where

$$b_{11} = \frac{x_{i-1} + x_i}{v_{i-1} + v_i} \quad (I.14)$$

$$b_{12} = \frac{y_{i-1} + y_i}{v_{i-1} + v_i} \quad (I.15)$$

and  $\sigma_{VN}$  and  $\sigma_{VE}$  are the standard deviations of the north and east components of the vessel's estimated velocity.

The value of  $\sigma_{N_0}$  of eight Doppler counts was found by trial and error to give results close to those given by Sluiter [1969] and shown in part in Figure 2.8.

A program listing in FOCAL [D.E.C., 1972] and a sample output follows. The results are tabulated in Tables I-1 and I-2.

Table I-1

## PREDICTED 95% TRANSIT ERROR ELLIPSES

(A = semi-major axis, B = semi-minor axis,

= orientation of semi-major axis)

 $\sigma_{VN} = 1$  knot,  $\sigma_{VE} = 1$  knot

Maximum Elevation	Ellipse Elements	15 Dopplers before Pass Centre 15 Dopplers after Pass Centre	5 Dopplers before Pass Centre 20 Dopplers after Pass Centre
15°	A	705 m	1277 m
	B	434 m	480 m
	$\theta$	0°	54°
30°	A	237 m	423 m
	B	215 m	195 m
	$\theta$	90°	70°
45°	A	212 m	295 m
	B	128 m	126 m
	$\theta$	90°	79°
60°	A	241 m	294 m
	B	91 m	93 m
	$\theta$	90°	84°
75°	A	396 m	451 m
	B	71 m	74 m
	$\theta$	90°	88°



## SAMPLE OUTPUT FROM TRANSIT COVARIANCE PROGRAM

```

# DOPS BEFORE :15
# DOPS AFTER  :15
MAX. ELEV.    :15
NORTH GOING(0) OR SOUTH GOING(1) :0
SAT. EAST(0) OR WEST(1) OF OBSERVER :0
CO/SP COV.   :1 :0 :1
S/N COV = = 0.082843844    = -0.000000000    = 0.031358125
ERROR ELLIPSE
A   = 705.1738585    B   = 433.8515232    TH   = -0.000000014

```

```

# DOPS BEFORE :15
# DOPS AFTER  :15
MAX. ELEV.    :15
NORTH GOING(0) OR SOUTH GOING(1) :0
SAT. EAST(0) OR WEST(1) OF OBSERVER :0
CO/SP COV.   :.3 :0 :.3
S/N COV = = 0.017827948    = -0.000000000    = 0.006738285
ERROR ELLIPSE
A   = 327.1272802    B   = 201.1132825    TH   = -0.000000033

```

```

# DOPS BEFORE :5
# DOPS AFTER  :20
MAX. ELEV.    :15
NORTH GOING(0) OR SOUTH GOING(1) :0
SAT. EAST(0) OR WEST(1) OF OBSERVER :0
CO/SP COV.   :1 :0 :1
S/N COV = = 0.120727572    = 0.111546215    = 0.189299197
ERROR ELLIPSE
A   = 1277.082076    B   = 479.5800771    TH   = 53.54289416

```

```

# DOPS BEFORE :5
# DOPS AFTER  :20
MAX. ELEV.    :15
NORTH GOING(0) OR SOUTH GOING(1) :0
SAT. EAST(0) OR WEST(1) OF OBSERVER :0
CO/SP COV.   :.3 :0 :.3
S/N COV = = 0.025914384    = 0.024011144    = 0.040853915
ERROR ELLIPSE
A   = 592.7297387    B   = 222.3694377    TH   = 53.64034870

```

## TRANSIT COVARIANCE PROGRAM

```

01.10 E
01.20 S PI=3.141592654; S RD=PI/180.0; S GO=400000000.0
01.22 S C=299792.5000; S DZ=1000.0; S SN=8
01.30 T "# DOPS BEFORE "; A N1
01.31 T !,"# DOPS AFTER "; A N2
01.32 T !,"MAX. ELEV. "; A AL
01.33 D 3
01.35 T !"CO/SP COV. "; A CS(1),CS(2),CS(3); D 4
01.36 S DY=-1000.0/(FSIN(AL*RD)/FCOS(AL*RD))
01.40 S I=-N1
01.50 S I=I+1
01.52 S D1=220.0*(I-1); S D2=220.0*I
01.54 S R1=FSQRT(D1^2+DY^2+DZ^2); S R2=FSQRT(D2^2+DY^2+DZ^2)
01.58 S A1=30.0; S A2=-GO*((D1/R1)-(D2/R2))/C
01.60 S A3=-GO*DY*((1/R1)-(1/R2))/C
01.61 S C1=(D1+D2)/(R1+R2); S C2=2*DY/(R1+R2)
01.62 S F=1/(C1^2*CS(1)+2*C1*C2*CS(2)+C2^2*CS(3)+SN^2)
01.64 S B1=B1+F*A1^2; S B2=B2+F*A1*A2; S B3=B3+F*A1*A3
01.68 S B4=B4+F*A2^2; S B5=B5+F*A2*A3; S B6=B6+F*A3^2
01.70 I (1-N2)1.50,1.72,1.72
01.72 S B7=B4-B2^2/B1; S B8=B5-B2*B3/B1
01.77 S B9=B6-B3^2/B1; S DD=B7*B9-B8^2
01.80 S CO(1)=B9/DD; S CO(2)=-B8/DD; S CO(3)=B7/DD
01.90 T %10.5,!,"S/N COV = ",CO(1)," ",CO(2)," ",CO(3),!
01.92 D 2
01.95 G 1.10

02.10 S DD=CO(1)*CO(3)-CO(2)^2; S DS=CO(1)+CO(3)
02.15 S A=2.45*1000.0*FSQRT(0.5*(DS+FSQRT((DS^2)-4*(DD))))
02.20 S B=2.45*1000.0*FSQRT(0.5*(DS-FSQRT((DS^2)-4*(DD))))
02.22 S DY=CO(1)-CO(3); S DX=2*CO(2); D 6
02.25 S TH=0.5*(AZ+180*FATN(DX/DY)/PI)
02.30 T %10.5,"ERROR ELLIPSE",!,"A ",A," B ",B," TH

03.10 T !,"NORTH GOING(0) OR SOUTH GOING(1) "; A Z
03.15 I (Z-1)3.25; S HO=N1; S N1=N2; S N2=HO
03.25 T !,"SAT. EAST(0) OR WEST(1) OF OBSERVER "; A Z
03.30 I (Z-1)3.35; S AL=-AL
03.35 R

04.10 F I=1,3; S CS(I)=((GO/C)*CS(I)*1.852/120)^2

06.10 I (DY)6.15,6.15; S AZ=0; R
06.15 I (DX)6.20,6.30,6.40
06.20 S AZ=-180; R
06.30 S AZ=0; R
06.40 S AZ=180; R
*
```

**APPENDIX II**

**PROGRAM LORSG**

## SAMPLE DIALOGUE FOR STARTING LORSG

```

:PR,LORSG
TYPE DE FOR PROGRAM DESCRIPTION ON LINE PRINTER
:
DE
:
ST
  STATION NO.:
1
  LAT:
46 46.5313
  LONG:
53 10.4860
  EDLY:
36389.56
  STATION NO.:
2
  LAT:
41 15.2048
  LONG:
69 58.6517
  EDLY:
52541.27
  STATION NO.:
3
  LAT:
59 59.2865
  LONG:
45 10.4578
  EDLY:
0.0
  STATION NO.:
4
  LAT:
46 46.5313
  LONG:
53 10.4860
  EDLY:
48212.24
  STATION NO.:
0
      1      46 46.5312      53 10.4860      36389.56
      2      41 15.2046      69 58.6514      52541.27
      3      59 59.2868      45 10.4576      .00
      4      46 46.5312      53 10.4860      48212.26
:
WF
WF =      .00      .00      .00      .00
NEW WF:
1.0 1.0 0.5 1.0

```

## DIALOGUE (CONTINUED)

:  
 IN  
 DAY:  
 185  
 LAT:  
 45 00  
 LONG:  
 63 00  
 COURSE AND SPEED:  
 63 11  
 ENTER STN #'S OF CAPE RACE:  
 1 4

:  
 DR  
 START TIME:  
 185 00 00  
 RANGE NO.:  
 1  
 ENTER SYNC, SYNC STD, SLOPE, SLOPE STD:  
 0.0 0.1 0.0 0.05  
 RANGE NO.:  
 2  
 ENTER SYNC, SYNC STD, SLOPE, SLOPE STD:  
 0.0 0.2 0.0 0.04  
 RANGE NO.:  
 3  
 ENTER SYNC, SYNC STD, SLOPE, SLOPE STD:  
 0.0 0.15 0.0 0.02  
 RANGE NO.:  
 4  
 ENTER SYNC, SYNC STD, SLOPE, SLOPE STD:  
 0.0 0.2 0.0 0.05  
 RANGE NO.:  
 0

RANGE NO.	START TIME =	185	0	0	SLOPE	SLOPE STD
1	SYNC	.0000	.1000	.0000	.0500	
2	SYNC	.0000	.2000	.0000	.0400	
3	SYNC	.0000	.1500	.0000	.0200	
4	SYNC	.0000	.2000	.0000	.0500	

:  
 D  
 D CORR'N'S = .00 .00 .00 .00  
 NEW D CORR'N'S:  
 1.0 1.0 -9.0 1.0

:  
 SA  
 LAT:  
 45 00  
 LONG:  
 63 45  
 39205.65 54729.41 6930.70 51028.33

:

## PROGRAM LORSG DESCRIPTION PRODUCED BY DESCRIBE COMMAND

PROGRAM NAME: LORSG  
 FUNCTION: OFF-LINE RHO-RHO LORAN-C/SATNAV INTEGRATION PROGRAM  
 AUTHOR: S. GRANT, BIO NAV. GROUP  
 DATE: 20 FEB. 1976

THIS PROGRAM READS TIME, LORAN-C AND LOG/GYRO DATA FROM A CLEANED UP BIODAL MAGNETIC TAPE (UNIT 0) AND SATNAV DATA FROM PUNCHED PAPER TAPE (MSR) AND OUTPUTS RESULTS TO A SECOND MAGNETIC TAPE (UNIT 1), THE LINE PRINTER AND THE TTY. COMMANDS ST, IN AND WF MUST BE EXECUTED BEFORE DATA PROCESSING CAN BEGIN. INTERRUPT DATA PROCESSING AT ANY TIME BY SETTING SWITCH REGISTER BIT 0 = 1.

STATION(ST)  
 ENTER STATION NUMBER, STATION COORDINATES(DEG. & MIN.) AND EMISSION DELAY(MICROSEC.)  
 ENTER STN # = 0 TO GET PRINT OUT OF DATA.  
 ENTER STN # NEG. OR GREATER THAN 4 TO EXIT.

INITIALIZE(IN)  
 ENTER DAY, INITIAL LAT. AND LONG.(DEG. & MIN.) AND APPROX. COURSE AND SPEED(DEG. & KTS.)

0  
 ENTER ONE CORRECTION(MICROSEC.) TO EACH RANGE.

WEIGHT FACTORS(WF)  
 WEIGHT FACTORS ARE NORMALLY SET EQUAL TO ONE.  
 IF A RANGE IS NOT USED SET ITS WF EQUAL TO ZERO.  
 IF THERE IS LAND ALONG THE PROPAGATION PATH SET THAT WF BETWEEN 0.3 AND 1.0. SET WF = 0.3 FOR ALL LAND PATH.

DRIFT(DR)  
 ENTER START TIME FOR CLOCK DRIFT CORRECTION FOLLOWED BY THE RANGE NO., THE SLOPE, SYNC AND STANDARD DEVIATIONS.  
 ENTER RNG # = 0 TO GET PRINT OUT OF DATA.  
 ENTER RNG # NEG. OR GREATER THAN 4 TO EXIT.

SATNAV(SA)  
 ENTER SATNAV FIX AND GET COMPUTED LORAN-C RANGES ON TTY.  
 (RANGES ARE CORRECTED FOR LAND AND WATER PHASE LAG.)

FIX(FI)  
 COMMENCE PROCESSING DATA.

DESCRIBE(DE)  
 PRINT THIS PROGRAM DESCRIPTION ON THE LINE PRINTER.

## LORSG SWITCH REGISTER OPTIONS

BIT #	FUNCTION(WHEN ON)
0	INTERRUPT DATA PROCESSING AND RETURN TO EXEC.
2	DO NOT OUTPUT TO LINE PRINTER.
3	DO NOT OUTPUT TO MAG. TAPE(UNIT 1).

## PROGRAM LORSG LISTING

```

0001 FTN4
0002 PROGRAM LORSG
0003 REAL LAT,LON,LATS(4),LONS(4),M,ED(4),D(4),LM,P(4,4)
0004 #,A(4,2),R(4),W(4),DIST(4),V(4),WF(4),X(2,4)
0005 #,UZ(4),LATO,LONO,MIN1,MIN2
0006 #,MIN
0007 DIMENSION ICR(3)
0008 COMMON AE,FL,PI,RD,RLS,P,X,LATS,LONS,ED
0009 #,IPD,PM,ILO,LM,A,DIST
0010 C LOGICAL UNITS
0011 ITTY=1
0012 ILPK=6
0013 IHSR=5
0014 C SOME CONSTANTS
0015 PI=3.1415926535
0016 RD=PI/180.0
0017 AE=6378144.0
0018 FL=1/298.23
0019 Ab=AE*(2.0-FL)/2.0
0020 C=299.7925
0021 C OVER WATER PHASE LAG POLYNOMIAL CONSTANTS
0022 C1=0.85347
0023 C2=-0.13511
0024 C3=0.0008687
0025 C4=1.265E-8
0026 C STO LORAN-C RANGE POLYNOMIAL CONSTANTS
0027 D1=135.0
0028 D2=-0.17E-3
0029 D3=0.86E-10
0030 C Q MATRIX ELEMENTS
0031 Q11=0.02
0032 Q22=0.021
0033 IFIRST=1
0034 IFLAG=0
0035 WRITE(ITYY,20)
0036 20 FORMAT("TYPE DE FOR PROGRAM DESCRIPTION ON LINE PRINTER")
0037 WRITE(ILPR,29)
0038 29 FORMAT(1H1)
0039 DO 30 I=1,4
0040 P(1,I)=0.01
0041 P(2,I)=0.0
0042 P(3,I)=0.0
0043 P(4,I)=0.0025
0044 X(1,I)=0.0
0045 X(2,I)=0.0
0046 D(I)=0.0
0047 30 CONTINUE
0048 ICR(1)=0
0049 ICR(2)=0
0050 ICR(3)=0
0051 TLN=0.0
0052 TLS=0.0
0053 C
0054 C EXECUTIVE ROUTINE
0055 C
0056 49 WRITE(ITYY,50)
0057 50 FORMAT(2H 1)
0058 READ(ITYY,55)ICOM
0059 55 FORMAT(A2)
0060 CALL DECOD(ICOM,I)

```

```

0061      GO TO(100,200,400,500,600,850,700,3000,4000),I
0062      C
0063      C      ENTER LORAN-C STATION COORDINATES AND EMISSION DELAYS
0064      C
0065      C      AN ALTERNATIVE TO THIS APPROACH IS TO HAVE ALL
0066      C      THE LORAN-C STATION COORDS. PERM. STORED IN MEMORY.
0067      100      CONTINUE
0068      WRITE(ITTY,105)
0069      105      FORMAT(13H STATION NO.!)
0070      READ(ITTY,*)I
0071      C
0072      C      IF 0<I<4 INPUT DATA
0073      C      IF I=0 OUTPUT ALL STATION COORD. DATA
0074      C      IF 0>I>4 RETURN TO EXEC
0075      C
0076      IF(I.LT.0.OR.I.GT.4)GO TO 49
0077      IF(I.EQ.0)GO TO 150
0078      CALL GETCO(LATS(I),LONS(I))
0079      WRITE(ITTY,130)
0080      130      FORMAT(6H EDLY!)
0081      READ(ITTY,*)ED(I)
0082      GO TO 100
0083      C
0084      C      OUTPUT STATION COORDINATE INFO
0085      C
0086      150      CALL STNIO(ITTY)
0087      GO TO 49
0088      C
0089      C      ENTER INITIAL LATITUDE AND LONGITUDE
0090      C
0091      200      CONTINUE
0092      WRITE(ITTY,205)
0093      205      FORMAT(5H DAY:)
0094      READ(ITTY,*)TEMP1
0095      IF(TEMP1.EQ.0,0)GO TO 208
0096      TLN=TEMP1
0097      TLS=TEMP1
0098      208      CALL GETCO(LAT,LON)
0099      WRITE(ITTY,209)
0100      209      FORMAT("COURSE AND SPEED:")
0101      READ(ITTY,*)CORSE,SPEED
0102      WRITE(ITTY,210)
0103      210      FORMAT("ENTER STN #'S OF CAPE RACE:")
0104      READ(ITTY,*)(ICR(I),I=1,2)
0105      WRITE(ITTY,225)
0106      225      FORMAT(/)
0107      GO TO 49
0108      C
0109      C      ENTER DIFFERENTIAL SYNCHRONIZATION CORRECTIONS
0110      C
0111      400      CONTINUE
0112      WRITE(ITTY,405)(D(I),I=1,4)
0113      405      FORMAT(14H D CORR'N'S = ,4X,4F8.2)
0114      WRITE(ITTY,410)
0115      410      FORMAT(16H NEW D CORR'N'S:)
0116      READ(ITTY,*)(D(I),I=1,4)
0117      GO TO 49
0118      C
0119      C      ENTER WEIGHT FACTORS
0120      C

```

```

0121 500 CONTINUE
0122 WRITE(ITY,505)(WF(I),I=1,4)
0123 505 FORMAT(6H WF = ,4X,4F6.2)
0124 WRITE(ITY,510)
0125 510 FORMAT(6H NEW WF:)
0126 READ(ITY,*)WF(1),WF(2),WF(3),WF(4)
0127 GO TO 49
0128 C
0129 C ENTER INITIAL CLOCK DRIFT CONSTANTS
0130 C
0131 600 WRITE(ITY,590)
0132 590 FORMAT(12H START TIME:)
0133 READ(ITY,*)DAY,HR,MIN
0134 IF(DAY.EQ.0)GO TO 650
0135 TLS=DAY+(HR+MIN/60.0)/24.0
0136 609 WRITE(ITY,610)
0137 610 FORMAT(11H RANGE NO.!)
0138 READ(ITY,*)I
0139 IF(I.LT.0.OR.I.GT.4)GO TO 49
0140 C
0141 C IF 0<I<4 READ DATA
0142 C IF I=0 OUTPUT CLOCK DRIFT DATA
0143 C IF 0>I>4 RETURN TO EXEC
0144 C
0145 IF(I.EQ.0)GO TO 650
0146 WRITE(ITY,620)
0147 620 FORMAT("ENTER SYNC, SYNC STD, SLOPE, SLOPE STD:")
0148 READ(ITY,*)X(1,I),P(1,I),X(2,I),P(4,I)
0149 P(1,I)=P(1,I)*P(1,I)
0150 P(4,I)=P(4,I)*P(4,I)
0151 GO TO 609
0152 C
0153 C CLOCK DRIFT CONSTANTS OUTPUT ROUTINE
0154 C
0155 650 CALL CLKIO(ITY)
0156 GO TO 49
0157 700 CONTINUE
0158 IF(TLS.GT.TLN)GO TO 1000
0159 C
0160 C SATNAV INPUT AND CLOCK DRIFT UPDATE ROUTINE
0161 C
0162 READ(INSK,*)DAY,HR1,M,DEG1,MIN1,DEG2,MIN2,COV1,COV2
0163 SLAT=(DEG1+MIN1/60.0)*RD
0164 SLON=- (DEG2+MIN2/60.0)*RD
0165 C SAVE TIME OF LAST SATNAV FIX
0166 TLS0=TLS
0167 TLS=DAY+(HR1+M/60.0)/24.0
0168 DTSS=TLS-TLS0
0169 C TLS0 IS TIME OF OLD SATNAV FIX
0170 C TLS IS TIME OF NEW SATNAV FIX
0171 C DTSS IS TIME INTERVAL FROM LAST TO CURRENT SATNAV FIX
0172 C
0173 COV1=COV1/AE
0174 COV1=COV1*COV1
0175 COV2=COV2/AE
0176 COV2=COV2*COV2
0177 IF(TLS.LT.TLN)GO TO 700
0178 IF(IFLAG.EQ.1)GO TO 1030
0179 GO TO 1000
0180 C

```

```

0181 C COMPUTE LORAN-C RANGES FROM SATNAV FIX
0182 C AND VARIANCE OF RANGE DIFFERENCE CALCULATION.
0183 C
0184 729 CALL ANDL(SLAT,SLON)
0185 DO 730 I=1,4
0186 W(I)=D1+D2*DIST(I)+D3*DIST(I)*DIST(I)
0187 W(I)=W(I)*W(I)+A(I,1)*A(I,1)*COV1+A(I,2)*A(I,2)*COV2
0188 W(I)=W(I)/(C*C)
0189 DZ(I)=(DIST(I)/C)-R(I)
0190 730 CONTINUE
0191 WRITE(ITTY,753)(DZ(I),I=1,4)
0192 753 FORMAT("OBSERVED CORR'N'S ",4F6.2)
0193 C
0194 C ENTER KALMAN FILTER ROUTINE
0195 C
0196 C (NOTE: THE ASSUMPTION IS MADE HERE THAT
0197 C EACH RANGE IS INDIPENDENT OF ALL OTHER RANGES
0198 C (IE. NO CORRELATION). THIS IS OBVIOUSLY NOT
0199 C CORRECT BUT IS MADE TO CUT DOWN ON THE SIZE
0200 C OF THE ARRAYS.)
0201 C
0202 DO 800 I=1,4
0203 C
0204 C PREDICT STATE VECTOR
0205 C (ONLY THE FIRST ELEMENT CHANGES)
0206 C
0207 X(1,I)=X(1,I)+X(2,I)*DTSS
0208 C
0209 C PREDICT STATE COVARIANCE MATRIX
0210 C
0211 P(1,I)=P(1,I)+2.0*DTSS*P(2,I)
0212 * +DTSS*DTSS*P(4,I)+Q11*DTSS
0213 P(2,I)=P(2,I)+DTSS*P(4,I)
0214 P(3,I)=P(3,I)+DTSS*P(4,I)
0215 P(4,I)=P(4,I)+Q22*DTSS
0216 C
0217 C COMPUTE GAIN MATRIX
0218 C
0219 G1=P(1,I)/(W(I)+P(1,I))
0220 G2=P(3,I)/(W(I)+P(1,I))
0221 C
0222 C UPDATE STATE VECTOR
0223 C
0224 C IF DIFFERENCE IS > 3 MICROSEC. DON'T UPDATE.
0225 IF (ABS(X(1,I)-DZ(I)).GT.3.0)GO TO 790
0226 X(1,I)=X(1,I)+G1*(DZ(I)-X(1,I))
0227 X(2,I)=X(2,I)+G2*(DZ(I)-X(1,I))
0228 C
0229 C
0230 C UPDATE COVARIANCE MATRIX
0231 C
0232 P(4,I)=P(4,I)-G2*P(2,I)
0233 P(2,I)=P(2,I)*(1.0-G1)
0234 P(3,I)=P(3,I)-P(1,I)*G2
0235 P(1,I)=(1.0-G1)*P(1,I)
0236 C
0237 C CHECK TO SEE IF ANY PII'S ARE NEG. AND IF SO TELL
0238 C OPERATOR AND SET IT TO A POS. VALUE.
0239 C
0240 J=1

```

```

0241 765 IF(P(J,I).GT.0.0)GO TO 775
0242 WRITE(ITTY,770)J,I,P(J,I)
0243 770 FORMAT(3H P(,I2,1H,,I2,6H) WAS ,F10.8)
0244 P(J,I)=0.00
0245 775 J=J+3
0246 IF(J.LE.4)GO TO 765
0247 GO TO 800
0248 790 CONTINUE
0249 C OUTPUT MESSAGE IF DIFFERENCE IS > 2 MICROSEC.
0250 WRITE(ITTY,795)I
0251 795 FORMAT(17H REJECT ON RANGE ,I3)
0252 800 CONTINUE
0253 C
0254 C OUTPUT DATA FROM SAT AND CLOCK DRIFT UPDATE ROUTINE.
0255 C
0256 CALL CLKID(ITTY)
0257 GO TO 700
0258 850 CALL GETCO(SLAT,SLON)
0259 CALL ANDL(SLAT,SLON)
0260 JCR=1
0261 C COMPUTE OVERLAND PHASE LAG CORR'N FOR CAPE RACE
0262 CALL CRCRN(SLAT,SLON,CRN)
0263 DO 880 I=1,4
0264 DIST(I)=DIST(I)/C
0265 IF(I.NE.ICR(JCR))GO TO 870
0266 DIST(I)=DIST(I)+CRN
0267 JCR=JCR+1
0268 870 DIST(I)=DIST(I)+C1/DIST(I)+C2+C3*DIST(I)+C4*DIST(I)**2
0269 880 DIST(I)=DIST(I)+FD(I)
0270 WRITE(ITTY,885)(DIST(I),I=1,4)
0271 885 FORMAT(1H ,4F12.2)
0272 GO TO 49
0273 C
0274 C
0275 C LORAN-C FIX ROUTINE
0276 C
0277 1000 IF(ISSW(0).LT.0)GO TO 49
0278 CALL FIXDT(DAY,HR,MIN,R,COR,SPD)
0279 IF(DAY.LE.0,0,OR,DAY.GT.366,0)GO TO 1000
0280 C SAVE OLD LAT & LONG
0281 LAT0=LAT
0282 LONG0=LON
0283 TL0=TLN
0284 TLN=DAY+(HR+MIN/60.0)/24.0
0285 DTL=TLN-TL0
0286 DTS=TLN-TLS
0287 C TL0 IS TIME OF OLD LORAN FIX
0288 C TLN IS TIME OF NEW LORAN FIX
0289 C TLS IS TIME OF LAST SATNAV FIX
0290 C DTL IS TIME INTERVAL FROM LAST TO CURRENT LORAN FIX
0291 C DTS IS TIME INTERVAL FROM LAST SATNAV FIX TO NEW LORAN FIX
0292 C
0293 C READ LORAN RANGES
0294 C
0295 C
0296 C CORRECT RANGES FOR SYNC,CLOCK DRIFT,DIFFERENTIAL SYNC AND
0297 C SUBTRACT EMISSION DELAYS. CORRECT FOR OVER-WATER PHASELAG
0298 C AND OVERLAND PHASE LAG FOR CAPE RACE
0299 C AND CONVERT TO UNITS OF METRES.
0300 C

```

```

0301      JCR=1
0302 C      COMPUTE OVERLAND PHASE LAG CORRIN FOR CAPE RACE
0303      CALL CRCRN(LAT,LON,CRN)
0304      DO 1020 I=1,4
0305 1008    IF(I.NE.ICR(JCR))GO TO 1015
0306      R(I)=R(I)-CRN
0307      JCR=JCR+1
0308 1015    R(I)=R(I)+D(I)-ED(I)
0309 1020    R(I)=R(I)-(C1/R(I)+C2+C3*R(I)+C4*R(I)*R(I))
0310      C
0311      IFLAG=1
0312      IF(TLS.EQ.TLN)GO TO 729
0313 C      CORRECT FOR CLOCK DRIFT AND CONVERT TO METRES
0314 1030    IFLAG=0
0315      DO 1045 I=1,4
0316      R(I)=(R(I)+X(1,I)+DTS*X(2,I))*C
0317      C
0318 C      COMPUTE RANGE STANDARD DEVIATIONS
0319      C
0320 1045    W(I)=D1+D2*R(I)+D3*R(I)*R(I)
0321      C      START FIX CALCULATION
0322      C
0323      J=0
0324 1050    B11=0.0
0325      B22=0.0
0326      B21=0.0
0327      D11=0.0
0328      D22=0.0
0329      CALL ANDL(LAT,LON)
0330      DO 1100 I=1,4
0331      IF(IFIRST.EQ.1)GO TO 1075
0332      IF(ABS(DIST(I)-R(I)).GT.10000.0)GO TO 2200
0333 1075    PT=W(I)/(W(I)*W(I)+P(1,I)*C*C)
0334      B11=B11+PT*A(1,1)*A(I,1)
0335      B22=B22+PT*A(1,2)*A(I,2)
0336      B21=B21+A(I,1)*A(I,2)*PT
0337      D11=D11+A(I,1)*PT*(DIST(I)-R(I))
0338      D22=D22+A(I,2)*PT*(DIST(I)-R(I))
0339 1100    CONTINUE
0340      DD=B11*B22-B21*B21
0341      DLA=(B22*D11-B21*D22)/DD
0342      DLO=(B11*D22-B21*D11)/DD
0343      LAT=LAT-DLA
0344      LON=LON-DLO
0345      CK=SQRT(DLA*DLA+DLO*DLO)
0346      J=J+1
0347      IF(J.GE.21)GO TO 1250
0348      IF(CK.GT.5.E-7)GO TO 1050
0349      C
0350 C      COMPUTE RESIDUALS AND VARIANCE FACTOR.
0351      C
0352      VAR=0.0
0353      DO 1200 I=1,4
0354      V(I)=A(I,1)*DLA+A(I,2)*DLO+(DIST(I)-R(I))
0355      PT=W(I)/(W(I)*W(I)+P(1,I))
0356      VAR=VAR+V(I)*V(I)*PT
0357 1200    CONTINUE
0358      C
0359 C      COMPUTE ERROR ELLIPSE PARAMETERS.
0360      C

```

```

0361      B21=(B21/DD)*AE*AE*COS(LAT)
0362      D11=B22
0363      B22=(B11/DD)*AE*AE*COS(LAT)**2
0364      B11=(D11/DD)*AE**2
0365      DD=B11*B22-B21**2
0366      AEL=2.45*SQRT(0.5*(B22+B11+SQRT((B22+B11)**2-4.0*DD)))
0367      BEL=2.45*SQRT(0.5*(B22+B11-SQRT((B22+B11)**2-4.0*DD)))
0368      THEL=ATAN2((2.0*B21),(B11-B22))/RD
0369      GU TO 1500
0370      C
0371      C      TYPE MESSAGE WHEN MORE THAN 20 ITERS
0372      C
0373      1250  WRITE(ITTY,1260)
0374      1260  FORMAT(29H 20 ITERATIONS, REINITIALIZE!,/)
0375      GO TO 49
0376      1500  CONTINUE
0377      IF(IFIRST.EQ.1)GO TO 1600
0378      C
0379      C      COMPUTE COURSE AND SPEED FROM PREVIOUS FIX.
0380      C      PLANE EARTH APPROX.
0381      C
0382      C      SAVE OLD COURSE AND SPEED.
0383      C
0384      CORSO=COURSE
0385      SPEED=SPEED
0386      DLAT=LAT-LATO
0387      DLON=(LON-LONO)*COS((LAT+LATO)/2.0)
0388      SPEED=SQRT(DLAT*DLAT+DLON*DLON)*AB/1852.0
0389      SPEED=SPEED/(DTL*24.0)
0390      C
0391      CURSE=ATAN2(DLON,DLAT)/RD
0392      IF(CURSE.GT.0.0)GO TO 1550
0393      CORSE=COURSE+360.0
0394      C      FILTER COURSE AND SPEED.
0395      C
0396      1550  CURSH=COURSE
0397      SPEEH=SPEED
0398      CONST=1.0-EXP(-144.0*DTL)
0399      C      144 GIVES AN AVERAGING TIME OF 10 MIN.
0400      SPEED=CONST*SPEED-(CONST-1.0)*SPEED
0401      DCURS=COURSE-CORSO
0402      IF(ABS(DCURS).LT.180.0)GO TO 1590
0403      IF(DCURS.LT.0.0)GO TO 1580
0404      DCURS=DLURS-360.0
0405      GU TO 1590
0406      1580  DCURS=DCURS+360.0
0407      1590  CURSE=COURSE+CONST*DCURS
0408      IF(CURSE.LT.360.0)GO TO 1600
0409      CURSE=COURSE-360.0
0410      1600  GU TO 2000
0411      C
0412      C      LURAN-C FIX OUTPUT ROUTINE
0413      C
0414      C
0415      2000  CONTINUE
0416      IFIRST=0
0417      C
0418      CALL RADN(LAT,IPD,PM)
0419      CALL RADM(-LON,ILD,LM)
0420      IF(ISSW(2).LT.0)GO TO 2060

```

```

0421      WRITE(ILPR,2020)DAY,HR,MIN,IPD,PM,ILD,LM,CORSE,SPEED
0422      #,CORSH,SPEEDH,COR,SPD
0423 2020  FORMAT(1H ,3I3,2(I4,F7.3),8F5.1)
0424      WRITE(ILPR,2040)J,(V(I),I=1,4),AEL,BEL,THEL
0425 2040  FORMAT(1H ,4X,I2,9F7.1)
0426 2060  IF(ISSW(3).LT.0)GO TO 2100
0427      WRITE(8,2020)DAY,HR,MIN,IPO,PM,ILD,LM,CORSE,SPEED
0428      #,CORSH,SPEEDH,COR,SPD
0429      WRITE(8,2040)J,(V(I),I=1,4),AEL,BEL,THEL
0430 2100  IF(TLS.LT.TLN)GO TO 700
0431      GO TO 1000
0432 2200  CONTINUE
0433      LAT=LATO
0434      LON=LONO
0435      TLN=TLO
0436      WRITE(ITTY,2210)HR,MIN
0437 2210  FURMAT(9H BAD DATA,2I3)
0438      GO TO 1000
0439 3000  CONTINUE
0440      WRITE(ITTY,3010)
0441 3010  FORMAT(6H ERROR)
0442      GO TO 49
0443 4000  CALL DESCR(ILPR)
0444      GO TO 49
0445      END
0446      SUBROUTINE RADM(RAD,IO,FM)
0447  C
0448  C      CONVERT RADS. TO DEG. AND MIN.
0449  C
0450      COMMON AE,FL,PI,RD
0451      D=RAD/RD
0452      FM=(D-FLOAT(IFIX(D)))*60.0
0453      IO=IFIX(D)
0454      RETURN
0455      END
0456      SUBROUTINE ANDL(PHP,FLP)
0457  L
0458  C      INVERSE DISTANCE BY ANDOYER-LAMBERT FORMULA.
0459  C
0460      REAL P(4,4),X(2,4),LATS(4),LONS(4),ED(4),A(4,2),DIST(4),LM
0461      COMMON AE,FL,PI,RD,TLN,P,X,LATS,LONS,ED,IPD,PM,ILD,LM,A,DIST
0462      DO 100 I=1,4
0463      DLON=FLP-LONS(I)
0464      SL=SIN(DLON)
0465      CL=COS(DLON)
0466  C
0467  C      SHIP POSITION
0468  C
0469      SP=SIN(PHP)
0470      CP=COS(PHP)
0471  C
0472  C      SHORE POSITION
0473  C
0474      SS=SIN(LATS(I))
0475      CS=COS(LATS(I))
0476  C
0477  C      SPHERICAL TRIANGLE BY X,Y,Z COORDINATES.
0478  C
0479      DX=CS*CL-CP
0480      DY=CS*SL

```

```

0481      DZ=SS-SP
0482 C     CHORD DIST SQ.
0483      CH=DX*DX+DY*DY+DZ*DZ
0484      S=SQRT(0.25*CH)
0485      C=SQRT(1.0-0.25*CH)
0486 C     ARC LENGTH
0487      U=ATAN(S/C)
0488      D=2.0*U
0489      SD=SIN(D)
0490 C     ELLIPSOIDAL CORRECTION FOR DISTANCE
0491      DV=(SS-SP)/S
0492      DV=(D+3.0*SD)*DV*DV*0.5
0493      DW=SS+SP
0494      DW=DW*DW/(1.0-S*S)
0495      DW=DW*0.5*(D-3.0*SD)
0496      DIST(I)=AE*(U-0.25*FL*(DV+DW))
0497 C     COMPUTE DERIVATIVES
0498      A(I,1)=(SP*CS*CL-CP*SS)*AE/SD
0499 100   A(I,2)=AE*CP*CS*SL/SD
0500      RETURN
0501      END
0502      SUBROUTINE DECOD(ICOM,I)
0503 C     COMMAND DECODER ROUTINE
0504      I=0
0505      IF(ICOM.NE.2HST)GO TO 10
0506      I=1
0507      GO TO 100
0508 10     IF(ICOM.NE.2HIN)GO TO 30
0509      I=2
0510      GO TO 100
0511 30     IF(ICOM.NE.2HD )GO TO 40
0512      I=3
0513      GO TO 100
0514 40     IF(ICOM.NE.2HWF)GO TO 50
0515      I=4
0516      GO TO 100
0517 50     IF(ICOM.NE.2HDR)GO TO 60
0518      I=5
0519      GO TO 100
0520 60     IF(ICOM.NE.2HSA)GO TO 70
0521      I=6
0522      GO TO 100
0523 70     IF(ICOM.NE.2HFI)GO TO 80
0524      I=7
0525      GO TO 100
0526 80     IF(ICOM.NE.2HDE)GO TO 90
0527      I=9
0528      GO TO 100
0529 90     I=8
0530 100   RETURN
0531      END
0532      SUBROUTINE GETCO(LAT,LON)
0533      COMMON AE,FL,PI,RD
0534      REAL LAT,LON,MIN
0535      ITTY=1
0536      WRITE(ITTY,10)
0537 10     FORMAT(5H LAT:)
0538      READ(ITTY,*)DEG,MIN
0539      LAT=(DEG+MIN/60.0)*RD
0540      WRITE(ITTY,20)

```

```

0541 20  FORMAT(6H LONG:)
0542      READ(ITTY,*)DEG,MIN
0543      LON=- (DEG+MIN/60.0)*RD
0544      RETURN
0545      END
0546      SUBROUTINE CLKIO(IO)
0547      REAL P(4,4),X(2,4),LATS(4),LONS(4),ED(4)
0548      COMMON AE,FL,PI,RD,TLS,P,X,LATS,LONS,ED
0549      IDAY=INT(TLS)
0550      HR=(TLS-IDAY)*24.0
0551      IHR=INT(HR)
0552      MIN=INT((HR-IHR)*60.0)
0553      WRITE(IO,655)IDAY,IHR,MIN
0554 655   FORMAT(14H START TIME = ,3I4)
0555      WRITE(IO,660)
0556 660   FORMAT(10H RANGE NO.,5X,4HSYNC,5X,8HSYNC STD,5X
0557      #,5HSLOPE,5X,9HSLOPE STD)
0558      DO 680 I=1,4
0559      TEMP1=SGRT(P(1,I))
0560      TEMP2=SGRT(P(4,I))
0561      WRITE(IO,670)I,X(1,I),TEMP1,X(2,I),TEMP2
0562 670   FORMAT(1H ,I3,4X,2(3X,F8.4,3X,F8.4))
0563 680   CONTINUE
0564      RETURN
0565      END
0566      SUBROUTINE STNIO(IO)
0567      REAL P(4,4),X(2,4),LATS(4),LONS(4),ED(4),LM
0568      COMMON AE,FL,PI,RD,TLS,P,X,LATS,LONS,ED
0569      #,IPD,PM,ILD,LM,A,DIST
0570      DO 170 I=1,4
0571      CALL RADM(LATS(I),IPD,PM)
0572      CALL RADM(-LONS(I),ILD,LM)
0573      WRITE(IO,160)I,IPD,PM,ILD,LM,ED(I)
0574 160   FORMAT(1H ,5X,I3,5X,I4,F8.4,3X,I4,F8.4,5X,F9.2)
0575 170   CONTINUE
0576      RETURN
0577      END
0578      SUBROUTINE FIXDT(DAY,HR,MIN,R,COR,SPD)
0579      DIMENSION IA(41),IGT1(164),R(4)
0580      REAL MIN
0581      INT=7
0582      IGT1=-164
0583      CALL EXEC(1,INT,IGT1,IGT1)
0584      CALL CODE
0585      READ(IGT1,205)(IA(I),I=1,41)
0586 205   FORMAT(41I4)
0587      DAY=IA(1)
0588      HR=AINT(IA(2)/100.0)
0589      MIN=(((IA(2)/100.0)-HR)*100.0)
0590      J=32
0591      DO 20 I=1,4
0592      J=J+2
0593      K=J+1
0594      R(I)=IA(J)*10.0+IA(K)/1000.0
0595 20    CONTINUE
0596      SPD=IA(7)/10.0
0597      CUR=IA(8)/10.0
0598      RETURN
0599      END
0600      SUBROUTINE DESCR(IO)

```

```

0601      WRITE(IO,10)
0602 10    FORMAT(1H1,"PROGRAM NAME: LORSG")
0603      WRITE(IO,20)
0604 20    FORMAT("FUNCTION: OFF-LINE RHO-RHO LORAN-C/SATNAV ",
0605      # "INTEGRATION PROGRAM")
0606      WRITE(IO,30)
0607 30    FORMAT("AUTHOR: S. GRANT, BIO NAV. GROUP")
0608      WRITE(IO,40)
0609 40    FORMAT("DATE: 20 FEB. 1976",//)
0610      WRITE(IO,50)
0611 50    FORMAT("      THIS PROGRAM READS TIME, LORAN-C AND ",
0612      # "LOG/GYRO DATA",//,"FROM A CLEANED UP BIODAL MAGNETIC TAPE ",
0613      # "(UNIT 0) AND SATNAV DATA",//,"FROM PUNCHED PAPER TAPE ",
0614      # "(MSR) AND OUTPUTS RESULTS TO A SECOND",//,"MAGNETIC TAPE",
0615      # "(UNIT 1), THE LINE PRINTER AND THE TTY. COMMANDS",/
0616      # ",ST,IN AND WF MUST BE EXECUTED BEFORE DATA PROCESSING CAN ",
0617      # "BEGIN.",//,"INTERRUPT DATA PROCESSING AT ANY TIME BY",
0618      # " SETTING SWITCH REGISTER BIT 0 = 1.",//)
0619      WRITE(IO,60)
0620 60    FORMAT("STATION(ST)",//,"ENTER STATION NUMBER, STATION ",
0621      # "COORDINATES(DEG. & MIN.)",//,"AND EMISSION DELAY(MICROSEC.)",
0622      # ",",//,"ENTER STN # = 0 TO GET PRINT OUT OF DATA.",/
0623      # ",",//,"ENTER STN # NEG. OR GREATER THAN 4 TO EXIT."/)
0624      WRITE(IO,70)
0625 70    FORMAT("INITIALIZE(IN)",//,"ENTER DAY, INITIAL LAT. AND ",
0626      # "LONG.(DEG. & MIN.)",//,"AND APPROX. COURSE AND SPEED",
0627      # "(DEG. & KTS.)",//)
0628      WRITE(IO,80)
0629 80    FORMAT("0",//,"ENTER ONE CORRECTION(MICROSEC.) TO EACH RANGE.",//)
0630      WRITE(IO,90)
0631 90    FORMAT("WEIGHT FACTORS(WF)",//,"WEIGHT FACTORS ARE NORMALLY ",
0632      # "SET EQUAL TO ONE.",//,"IF A RANGE IS NOT USED SET ITS",
0633      # " WF EQUAL TO ZERO."/,"IF THERE IS LAND ALONG THE PROPAGATION",
0634      # " PATH",//,"SET THAT WF BETWEEN 0.3 AND 1.0. SET WF = 0.3",
0635      # " FOR ALL LAND PATH."/)
0636      WRITE(IO,100)
0637 100   FORMAT("DRIFT(DR)",//,"ENTER START TIME FOR CLOCK DRIFT ",
0638      # "CORRECTION FOLLOWED BY THE",//,"RANGE NO., THE SLOPE, ",
0639      # "SYNC AND STANDARD DEVIATIONS.",//,"ENTER RNG # = 0 TO GET ",
0640      # "PRINT OUT OF DATA.",//,"ENTER RNG # NEG. OR GREATER ",
0641      # "THAN 4 TO EXIT.",//)
0642      WRITE(IO,110)
0643 110   FORMAT("SATNAV(SA)",//,"ENTER SATNAV FIX AND GET COMPUTED ",
0644      # "LORAN-C RANGES ON TTY.",//,"(RANGES ARE CORRECTED FOR ",
0645      # "LAND AND WATER PHASE LAG.)",//)
0646      WRITE(IO,120)
0647 120   FORMAT("FIX(FI)",//,"COMMENCE PROCESSING DATA.",//)
0648      WRITE(IO,130)
0649 130   FORMAT("DESCRIBE(DE)",//,"PRINT THIS PROGRAM DESCRIPTION ",
0650      # "ON THE LINE PRINTER.",//)
0651      WRITE(IO,140)
0652 140   FORMAT("LORSG SWITCH REGISTER OPTIONS",//,5X,"BIT #",
0653      # 10X,"FUNCTION(WHEN ON)",//,7X,"0",13X,"INTERRUPT DATA ",
0654      # "PROCESSING AND RETURN TO EXEC.",//,7X,"2",13X,
0655      # "DO NOT OUTPUT TO LINE PRINTER.",//,7X,"3",13X,
0656      # "DO NOT OUTPUT TO MAG. TAPE(UNIT 1).",//)
0657      RETURN
0658      END
0659      SUBROUTINE CRCRN(LAT,LON,CRN)
0660 C      THIS SUBROUTINE COMPUTES THE OVERLAND PHASE LAG

```

```

0661 C      ERROR (CRN) TO THE CAPE RACE RANGE AS A FIN OF LAT,LON.
0662      REAL LA1,LON,LATCR,LONCR
0663      LATCR=0.81658686
0664      LONCR=-0.92807476
0665      R50=0.8726646
0666      R30=0.5235987
0667      R347=-0.2268928
0668      R280=-1.3962634
0669      R285=-1.3089969
0670      R336=-0.418879
0671      C1=1.3
0672      C2=-0.92
0673      C3=8.0
0674      C4=-17.1
0675      DLON=LON-LONCR
0676      IF (DLON.EQ.0.0)GO TO 100
0677      SL=SIN(DLON)
0678      CL=COS(DLON)
0679      SP=SIN(LAT)
0680      CP=COS(LAT)
0681      SS=SIN(LATCR)
0682      CS=COS(LATCR)
0683      CU=SP*SS+CP*CS*CL
0684      SU=SQRT(1.0-CU*CU)
0685      U=ATAN(SU/CU)
0686      DIST=6378206.0*U
0687      SAA=SL*CP/SU
0688      CAA=SQRT(1.0-SAA*SAA)
0689      IF (LAT.GT.LATCR)GO TO 90
0690      CAA=-CAA
0691 90      AZ=ATAN2(SAA,CAA)
0692      GO TO 130
0693 100     IF (LAT.LT.LATCR)GO TO 120
0694      AZ=0.0
0695      GO TO 130
0696 120     AZ=3.1415926536
0697 130     CONTINUE
0698      CRN=0.0
0699      IF (AZ.GT.R50.OR.AZ.LT.R280)RETURN
0700      IF (AZ.LT.R30.AND.AZ.GT.R336)GO TO 200
0701      IF (AZ.GT.R285.AND.AZ.LT.R336)GO TO 170
0702      CRN=0.25
0703      RETURN
0704 170     CRN=1.0+(AZ-R285)*1.5/(R336-R285)
0705      RETURN
0706 200     IF (AZ.LT.R347.AND.DIST.LT.777840.0)GO TO 300
0707      CRN=C1+C2*AZ+C3*AZ*AZ+C4*AZ*AZ*AZ
0708      RETURN
0709 300     CRN=2.5
0710      RETURN
0711      END
0712      ENDS
**** LIST END ****

```



Environment  
Canada

Department of Energy,  
Mines and Resources

Environnement  
Canada

Ministère de l'Énergie,  
des Mines et des Ressources